

Einfluss von Glycolaldehyd und Glyoxal auf die  
Maillard-Reaktion *in vitro* und *in vivo*

Dissertation

zur Erlangung des Doktorgrades der Naturwissenschaften  
(Dr. rer. nat.)

der

Naturwissenschaftlichen Fakultät II  
Chemie, Physik und Mathematik

der Martin-Luther-Universität  
Halle-Wittenberg

vorgelegt von

Herrn Diplom-Lebensmittelchemiker Alexander Klaus  
geb. am 23. März 1989 in Gera

erster Gutachter: Prof. Dr. M. Glomb  
zweiter Gutachter: Prof. Dr. M. Pischetsrieder

Verteidigungsdatum: 17.04.2019

## Danksagung

An erster Stelle möchte ich mich bei Herrn Prof. Dr. Marcus A. Glomb für die Bereitstellung dieses interessanten und vielseitigen Themas bedanken. Ich danke für die stetige Diskussionsbereitschaft, wertvolle und kritische Hinweise sowie der Ermöglichung einer fachübergreifenden Zusammenarbeit. Durch die Arbeit habe ich mich fachlich und handwerklich weiterentwickelt.

Mein Dank geht außerdem an Prof. Dr. G. Sprenger, Dr. R. Golbik und Prof. Dr. K. Tittmann für die Bereitstellung der Plasmide für Transketolase A von *Escherichia coli* und humane Transketolase. Herrn Dr. T. Pfirrmann und seinem Arbeitskreis danke ich für die Möglichkeit der rekombinanten Expression der Transketolase. Für die Studien an humanem Blut möchte ich mich bei Herrn Prof. Dr. M. Girndt, Dr. R. Fiedler, dem Blutspendedienst des Universitätsklinikums Halle für die Blutentnahmen und natürlich auch bei den vielen Freiwilligen bedanken. Ohne diese Kooperationen wäre diese Arbeit nicht zustande gekommen.

Außerdem gilt dem NMR-Team um Dr. D. Ströhl und dem HR-MS-Team um Dr. A. Frolov und A. Laub ein großer Dank für die Messung der Spektren.

Großer Dank an meine Diplomanden Wilhelmine Feller, Tim Baldensperger, Elisabeth Koch, Lukas Blaschke und Robert Rau für die entspannte Stimmung und Hilfsbereitschaft. Ohne euch wäre die vorliegende Arbeit nicht in diesem Umfang zustande gekommen.

Ein Dankeschön auch an den gesamten Arbeitskreis Glomb für die fachliche Kompetenz und angenehme Atmosphäre. Ein gesonderter Dank gilt Tobias Jost und Thomas Heymann, die stets für gute Laune und Spaß gesorgt haben.

Schließlich gilt mein Dank allen, die an der Entstehung dieser Arbeit beteiligt waren. Vor allem meiner Familie danke ich für die ermutigenden Worte und Unterstützung.

## **Vorwort**

Diese Arbeit entstand im Arbeitskreis für Lebensmittelchemie von Prof. Dr. Marcus A. Glomb am Institut für Chemie der Martin-Luther-Universität Halle-Wittenberg im Zeitraum von Juni 2014 bis Mai 2018 im Rahmen einer Beschäftigung als wissenschaftlicher Mitarbeiter. Die vorliegende Dissertation wurde in kumulativer Form angefertigt. Die enthaltenen Forschungsergebnisse wurden vollständig in international anerkannten Fachzeitschriften publiziert, denen die experimentellen Daten, Einzelergebnisse sowie deren Diskussion zu entnehmen sind. Der Fokus dieser Dissertation liegt in der Einordnung der Forschungsergebnisse in den wissenschaftlichen Kontext.

# Inhaltsverzeichnis

<b>Abkürzungsverzeichnis</b> .....	<b>V</b>
<b>1 Einleitung</b> .....	<b>1</b>
<b>2 Aktueller Stand der Forschung</b> .....	<b>2</b>
2.1 Die Maillard-Reaktion .....	2
2.1.1 Initialphase .....	3
2.1.2 Bildung reaktiver Intermediate .....	3
2.1.3 Folgeprodukte und deren Bedeutung <i>in vivo</i> .....	7
2.2 Rolle der Transketolase-Reaktion .....	10
2.2.1 Stoffwechselfunktion .....	10
2.2.2 Cofaktoren & Substratspezifität .....	12
2.2.3 Reaktionsmechanismus der Transketolase.....	13
<b>3 Zielstellung</b> .....	<b>15</b>
<b>4 Diskussion und Einordnung der Ergebnisse</b> .....	<b>16</b>
4.1 Modellsysteme zur Untersuchung der Transketolase-Reaktion und ihren Einfluss auf die Bildung von Proteinmodifikationen.....	16
4.2 Einfluss der Transketolase-Reaktion <i>in vivo</i> .....	23
4.3 Einfluss von Glycolaldehyd und Glyoxal auf die physikochemischen Eigenschaften von Proteinen.....	26
<b>5 Zusammenfassung</b> .....	<b>31</b>
<b>6 Summary</b> .....	<b>33</b>
<b>7 Abbildungsverzeichnis</b> .....	<b>35</b>
<b>8 Tabellenverzeichnis</b> .....	<b>37</b>
<b>9 Literaturverzeichnis</b> .....	<b>38</b>
<b>10 Publikationen</b> .....	<b>53</b>
10.1 <i>Journal of Agricultural and Food Chemistry</i> , 2017, 65, 8196-8202.....	53
10.2 <i>Journal of Agricultural and Food Chemistry</i> , 2018, 66, 1498-1508.....	60
10.3 <i>Journal of Agricultural and Food Chemistry</i> , 2018, 66, 10835–10843 .....	71

<b>11</b>	<b>Anhang</b> .....	<b>80</b>
11.1	<i>Supporting Information zu Journal of Agricultural and Food Chemistry, 2018, 66, 1598-1508</i> .....	80
11.2	<i>Supporting Information zu Journal of Agricultural and Food Chemistry, 2018, 66, 10835–10843</i> ....	83
<b>13</b>	<b>Publikationsliste</b> .....	<b>95</b>
<b>14</b>	<b>Lebenslauf</b> .....	<b>97</b>
<b>15</b>	<b>Eigenständigkeitserklärung</b> .....	<b>98</b>

## Abkürzungsverzeichnis

2D-PAGE	2D-Gelelektrophorese
AGEs	Advanced Glycation Endproducts
ALEs	Advanced Lipoxidation Endproducts
BSA	<i>Bovines</i> Serum Albumin, Rinderserumalbumin
CMA	<i>N</i> <sup>7</sup> -Carboxymethylarginin
CML	<i>N</i> <sup>6</sup> -Carboxymethyllysin
DHETHDP	1,2-Dihydroxyethylthiamindiphosphat
DLP	Dilysinopyridin, 1-(5-amino-5-carboxypentyl)-4-(5-amino-5-carboxypentyl-amino)pyridiniumsalz
<i>E. coli</i>	<i>Escherichia coli</i>
E4P	Erythrose-4-phosphat
G3P	Glycerinaldehyd-3-phosphat
G6P	Glucose-6-phosphat
GALA	<i>N</i> <sup>6</sup> -Glycoloyllysin
GPC	Gelpermeationschromatographie
GODIC	Glyoxal-Lysin-Arginin-Crosslink
GOLA	Glyoxal-Lysin-Amid
GOLD	Glyoxal-Lysin-Dimer
HEL	<i>N</i> <sup>6</sup> -(2-Hydroxyethyl)lysin
HSA	Humanes Serum Albumin
Imidazolinon, GH-3	5-(2-Amino-4-hydro-5-imidazolon-1-yl)-norvalin
IEF	Isoelektrische Fokussierung
IEX	Ionenaustauschchromatographie
LC-MS <sup>2</sup>	Flüssigchromatographie Tandem-Massenpektrometrie
MW	Molekulargewicht
NADPH	Nicotinamidadenindinucleotidphosphat
P	Phosphat
pI	Isoelektrischer Punkt
R5P	Ribose-5-phosphat
RBC	Rote Blutkörperchen/ Erythrozyten
RNase A	<i>Bovine</i> Ribonuclease A
Ru5P	Ribulose-5-phosphat

S7P	Sedoheptulose-7-phosphat
<i>S. cerevisiae</i>	<i>Saccharomyces cerevisiae</i>
SDS-PAGE	Natriumdodecylsulfat-Polyacrylamid-Gelelektrophorese
ThDP	Thiamindiphosphat
TKA	Transketolaseaktivität
X5P	Xylulose-5-phosphat

# 1 Einleitung

Der fortschreitende demografische Wandel in der Altersstruktur der Bevölkerung stellt eine der herausforderndsten Fragen der heutigen Zeit dar. Im Jahr 2017 betrug der Anteil an Personen über 65 Jahren 21,4% der Gesamtbevölkerung Deutschlands und ist damit um 36,6% innerhalb der letzten 20 Jahre gestiegen.<sup>1</sup> Altern ist ein komplexer physiologischer Vorgang bei dem bereits über 300 verschiedene beteiligte Mechanismen auf zellulärer und makromolekularer Ebene vorgeschlagen wurden.<sup>2</sup> Die meisten Theorien über molekulare Veränderungen basieren auf spontanen chemischen Reaktionen, welche die Funktion von Proteinen und anderen biologischen Makromolekülen beeinträchtigen.<sup>3</sup> Eine der wichtigsten Ursachen für die irreversible, nicht-enzymatische Modifikation von Proteinen besteht in ihrer Interaktion mit Kohlenhydraten, der sogenannten Maillard-Reaktion.

Der wohl schwierigste Aspekt der Maillard-Reaktion besteht dabei in der Fülle der gebildeten Reaktionsprodukte.<sup>4</sup> Unter physiologischen Bedingungen wird die Komplexität der auftretenden Mechanismen durch weitere Einflussfaktoren wie dem Redoxzustand und den zahlreichen parallel ablaufenden enzymatischen Vorgängen *in vivo* erhöht. Nach unserem heutigen Verständnis stellen Enzyme bemerkenswert spezifische Katalysatoren dar und die Vorstellung, dass „ein Enzym – ein Substrat – eine Reaktion“ bestimmt, ist weit verbreitet.<sup>5</sup> Durch alternative Cofaktoren, konformativer Diversität und einem breiten Substratspektrum können jedoch Abweichungen von der eigentlich vorgesehenen physiologischen Reaktion entstehen.<sup>6</sup> Abweichungen dieser Art treten vor allem in diversen Pathologien auf, die eine Störung des chemischen und biochemischen Gleichgewichts bedingen.

Die Vereinigung von verschiedenen chemischen und biochemischen Mechanismen in Verbindung mit klinischen Studien kann so einen einheitlichen konzeptionellen Rahmen für die zukünftige Forschung und dem Verständnis der zugrunde liegenden Mechanismen in der Modifikation von Proteinen bilden.

## 2 Aktueller Stand der Forschung

### 2.1 Die Maillard-Reaktion

Die nach dem französischen Chemiker Louis Camille Maillard benannte Reaktion ist vor allem durch ihren Einfluss auf Lebensmittel bekannt geworden. Sie ist maßgeblich an der Ausbildung von Farbe und der Entwicklung eines charakteristischen Aromaprofils beteiligt. Zusätzlich wird die Relevanz dieser Reaktion bei pathologischen Prozessen immer häufiger diskutiert.<sup>7</sup>

Generell beschreibt die Maillard-Reaktion die Reaktion zwischen freien Aminogruppen von Aminosäuren, Peptiden und Proteinen mit reduzierenden Zuckern. Im weiteren Verlauf der Reaktion entstehen reaktive Verbindungen, welche weiteren Enolisierungen, Dehydratationen, Cyclisierungen, Fragmentierungen und Redoxreaktionen unterliegen. Diese Verbindungen sind maßgeblich an der Reaktion beteiligt und tragen zur Bildung von posttranslationalen Aminosäure- und Proteinmodifikationen (Advanced Glycation Endproducts, AGEs), aromaaktiven Stoffen und braunen Pigmenten, den Melanoidinen, bei (Abb. 1).<sup>8</sup> Die Reaktion wird insbesondere von der Temperatur, dem pH-Wert und dem Redoxpotential der Umgebung beeinflusst.<sup>9-11</sup> Ebenso sind reduzierende Zucker in der Lage, auch ohne Zusatz von Aminosäuren zu reagieren. Dieser Vorgang wird als Karamellisierung zusammengefasst.<sup>12</sup>

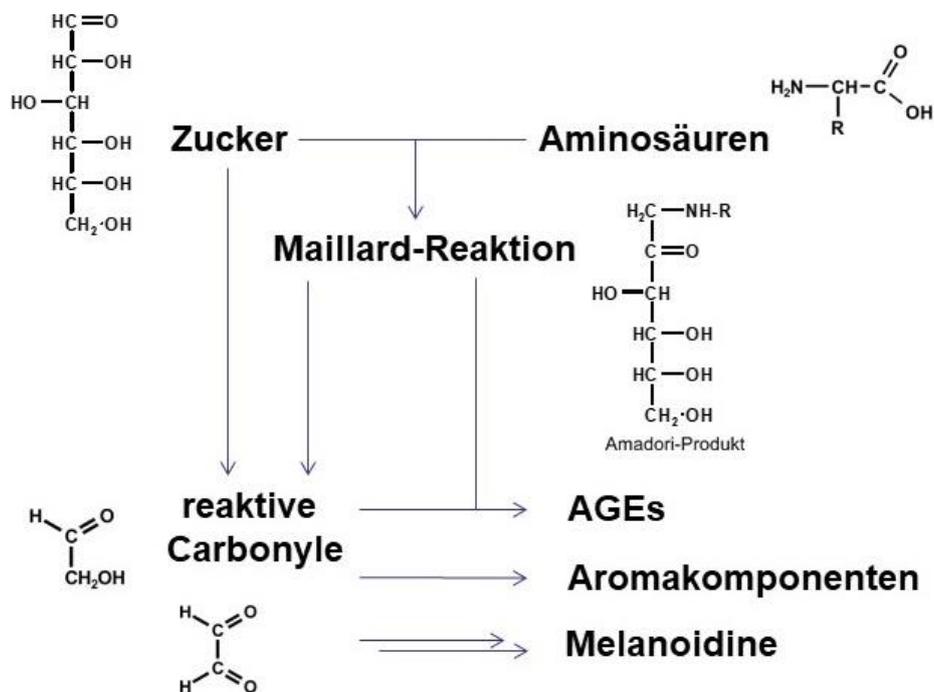


Abb. 1: Grundzüge der Maillard-Reaktion<sup>13</sup>

### 2.1.1 Initialphase

Die Maillard-Reaktion kann in drei Phasen unterteilt werden. In der Anfangsphase der Reaktion greift die freie Aminogruppe der Aminosäure nucleophil an die Carbonylfunktion des Zuckers an (Abb. 2). Diese Reaktion führt zum Halbaminal, das in einer Folgereaktion unter der Abspaltung von Wasser zum Imin, der so genannten Schiff'schen Base, übergeht. Über Enolisierungen verlaufende Folgereaktionen führen über das 1,2-Enaminol zu der 1-Amino-1-Desoxyketose (Amadori-Produkt).<sup>14</sup> Dabei korreliert die Reaktivität verschiedener Zucker und Zuckerphosphate mit der Verfügbarkeit der offenkettigen Carbonylform.<sup>15,16</sup>

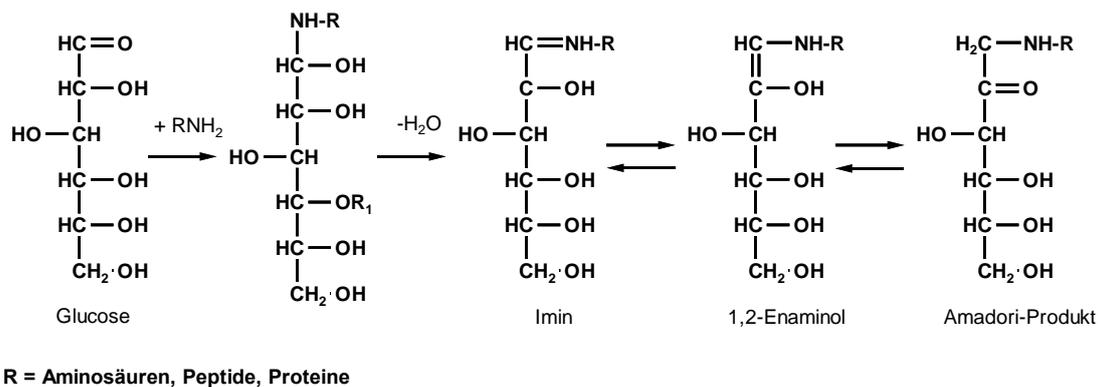


Abb. 2: Bildung des Amadori-Produktes am Beispiel der Glucose

Das Amadori-Produkt stellt die zunächst quantitativ bedeutendste Verbindung dar, da es, gemäß einer intramolekularen Halbacetalbildung zwischen dem Carbonylkohlenstoff und einer Hydroxylgruppe, für gewöhnlich als verhältnismäßig stabile Pyranose vorliegt. Die analog verlaufende Reaktion mit Ketosen führt zu den instabileren Aminoaldosen (Heyns-Produkt).<sup>17</sup> Infolge des Gleichgewichts zwischen offenkettiger und cyclischer Form finden weitere Umlagerungs- und Abbaureaktionen statt.

### 2.1.2 Bildung reaktiver Intermediate

Die fortgeschrittene Phase der Maillard-Reaktion beschreibt die Umwandlung und den Abbau des Amadori-Produkts unter Bildung von reaktiven Carbonylverbindungen. Darunter befindet sich eine Gruppe von  $\alpha$ -Dicarbonylen mit zwei vicinal angeordneten Carbonylfunktionen.

Ihre Bildung kann auf verschiedenen Wegen erfolgen (Abb. 3). Die Säure-Basen-katalysierte Enolisierung des Amadori-Produkts kann zum 1,2-Enaminol oder dem 2,3-Endiol führen. Ausgehend vom 1,2-Enaminol bildet sich nach  $\beta$ -Eliminierung der Hydroxylgruppe am C<sub>3</sub>-Atom und anschließender hydrolytischer Abspaltung der Aminosäure das 3-Desoxyglucoson. Das 1-Desoxyglucoson repräsentiert ein zentrales Folgeprodukt des 2,3-Endiols und wird durch  $\beta$ -Eliminierung der Aminosäure am C<sub>1</sub> gebildet.<sup>8,18</sup> Nach

Enolisierung entlang des kompletten Kohlenstoffgrundgerüsts bildet sich das Lederer Glucoson aus dem 5,6-Endiol. Redoxreaktionen sind ebenfalls von entscheidender Bedeutung für die Bildung von Folgeprodukten. So kann, durch Autoxidation oder der aminkatalysierten Oxidation, aus dem Amadori-Produkt das Glucoson gebildet werden.<sup>19,20</sup>

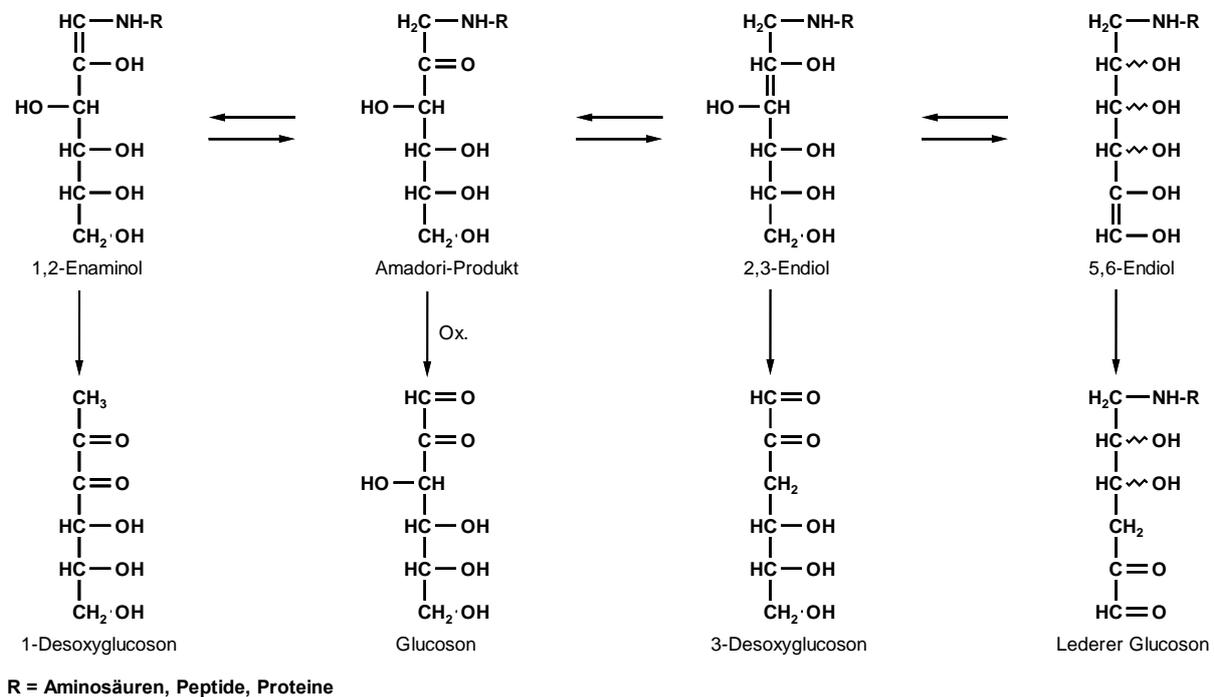


Abb. 3: Bildung von  $\alpha$ -Dicarbonylen ausgehend vom Amadori-Produkt der Glucose

Aufgrund der hohen Reaktivität von  $\alpha$ -Dicarbonylen erfolgt der weitere Abbau des Kohlenstoff-Grundgerüsts zu kurzkettigen Carbonylverbindungen ( $\alpha$ -Dicarbonyle, Reduktone, Aldehyde und Carbonsäuren), die das Produktspektrum dieser Substanzklasse weiter erhöhen. Einige wichtige Vertreter sind in Abb. 4 dargestellt.

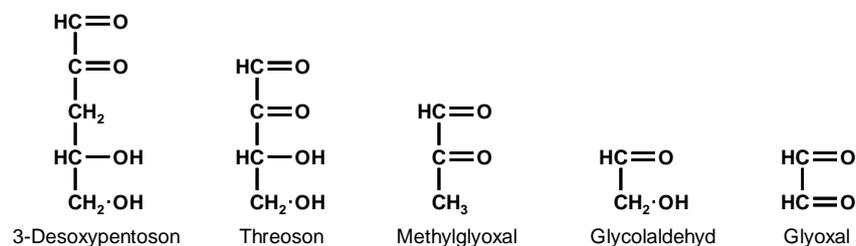


Abb. 4: Reaktive Intermediate mit C2-C5 Kohlenstoff-Grundgerüst

3-Desoxypentosen wird als charakteristisches Abbauprodukt von Di- und Oligosacchariden beschrieben. Allerdings kann seine Bildung auch aus dem Glucoson erfolgen.<sup>19,21,22</sup> Threoson konnte als Folgeprodukt von 1-Desoxyglucoson aus dem Maillard-induzierten Abbau von Glucose nachgewiesen werden.<sup>23</sup> Methylglyoxal und Glyoxal stellen die mitunter am häufigsten in Lebensmitteln identifizierten  $\alpha$ -Dicarbonyle dar. Obwohl zahlreiche Untersuchungen

durchgeführt wurden, können weder für Methylglyoxal noch Glyoxal definierte Bildungsmechanismen beschrieben werden. Experimente über den Abbau von  $^{13}\text{C}$ -markierter Glucose zeigten die Entstehung von Methylglyoxal und Glyoxal entlang des kompletten Kohlenstoffskeletts auf.<sup>19,24</sup> Ein weiteres Folgeprodukt stellt Glycolaldehyd dar. Als möglicher Vorläufer wurde unter anderem das Threoson identifiziert, welches nach einer  $\beta$ -Dicarbonylsplaltung zu Glycolaldehyd führt.<sup>25</sup>

### ***Zentrale Mechanismen der Fragmentierung und Bildung reaktiver Carbonylverbindungen***

Weenen und Tressl beschrieben drei grundlegende Fragmentierungsmechanismen für die Bildung von  $\alpha$ -Dicarbonylen während der Maillard-Reaktion: Retro-Aldol-Reaktion,  $\alpha$ -Dicarbonylsplaltung und  $\beta$ -Dicarbonylsplaltung.<sup>26,27</sup> Allerdings zeigten aktuelle Studien, dass nur die oxidative  $\alpha$ -Dicarbonylsplaltung sowie die hydrolytische und amininduzierte  $\beta$ -Dicarbonylsplaltung von Relevanz sind.<sup>28</sup>

Die Retro-Aldol-Splaltung setzt beim umzusetzenden Kohlenhydrat eine  $\beta$ -Hydroxycarbonylstruktur voraus und führt zu einem Bruch zwischen dem  $\text{C}_\alpha$  und  $\text{C}_\beta$  in Nachbarschaft zur Carbonylgruppe. Pfeifer und Kroh postulierten die Bildung von Glycolaldehyd und D-Erythrose ausgehend von Glucose.<sup>29</sup> Obwohl diesem Mechanismus eine große Bedeutung zugesprochen wird, bleibt seine Relevanz *in vivo* fraglich.<sup>28,30</sup> Zum derzeitigen Stand der Forschung konnte die Retro-Aldol-Reaktion nicht eindeutig nachgewiesen werden.<sup>18</sup> Wohingegen die Bildung von  $\alpha$ -Dicarbonylen und anderen Verbindungen durch Aldolkondensation einen festen Bestandteil der Maillard-Kaskade darstellt.<sup>29,31</sup>

Die Splaltung von  $\alpha$ -Dicarbonylen über einen oxidativen Weg wurde erstmals von Davídek et al. nachgewiesen und später anhand von Modelluntersuchungen mit Ascorbinsäure (Vitamin C) bestätigt.<sup>32,33</sup> Dabei greift aktivierter molekularer Sauerstoff an einer der beiden Carbonylverbindungen an (Abb. 5). Das entstehende Alkoxyradikal reagiert über eine Elektronenübergangsreaktion zum Hydroperoxidanion. Durch eine Bayer-Villiger Umlagerung wird ein Sauerstoffatom in das Kohlenstoffskelett eingebaut und liefert ein gemischtes Säureanhydrid. Dieses kann nun wieder nucleophil von einer Aminosäure oder einem Hydroxidion angegriffen werden, welches zu den entsprechenden Carbonsäuren beziehungsweise Amiden führt. Eine rein hydrolytisch erfolgende  $\alpha$ -Dicarbonylsplaltung kann dagegen ausgeschlossen werden.<sup>28</sup>

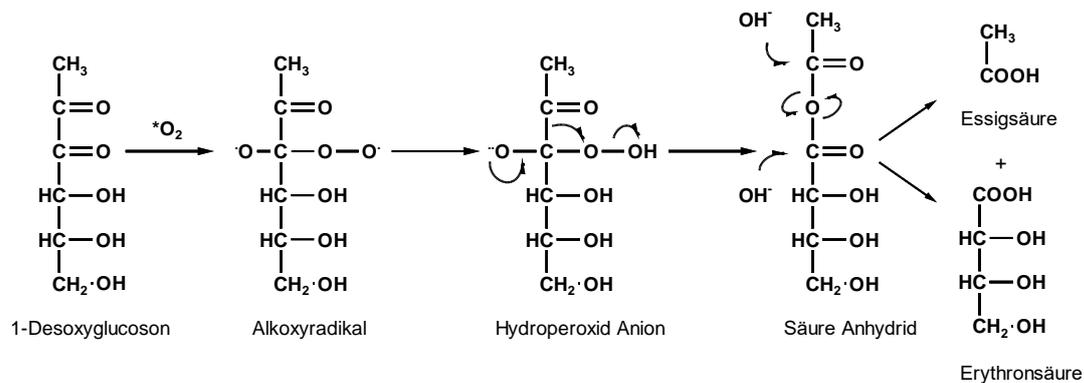


Abb. 5: Mechanismus der oxidativen  $\alpha$ -Dicarbonylsplattung am Beispiel des 1-Desoxyglucosons nach Davidek et al.<sup>32</sup>

Die hydrolytische  $\beta$ -Dicarbonylsplattung wurde bereits 1961 als alternativer Mechanismus zur Retro-Aldol-Reaktion erwähnt und gilt als Hauptweg der Zuckerfragmentierung (Abb. 6).<sup>23,25,34</sup> Generell erfolgt der Angriff nach Tautomerisierung des Dicarbonyls in seine Reduktonform, welche dann in seine korrespondierenden Fragmente gespalten wird. Die hydrolytische  $\beta$ -Dicarbonylsplattung folgt dem Prinzip einer Retro-Claisen-Kondensation, wobei ein Hydroxidion an eine der beiden Carbonylfunktionen des  $\beta$ -Diketons angreift und Carbonsäuren beziehungsweise  $\alpha$ -Hydroxycarbonylverbindungen resultieren.<sup>26,32</sup> Neben Hydroxidionen können auch andere Nucleophile in Form von Aminosäuren zum weiteren Abbau von Dicarbonylen führen. Diese amininduzierte Dicarbonylsplattung verläuft nach dem Prinzip seines hydrolytischen und oxidativen Pendantes, jedoch in deutlich geringerem Umfang.<sup>35</sup>

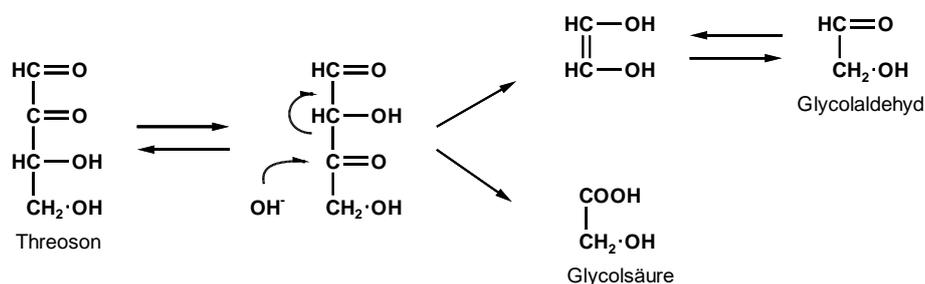


Abb. 6: Mechanismus der hydrolytischen  $\beta$ -Dicarbonylsplattung am Beispiel des Threosons nach Voigt et al.<sup>25</sup>

Des Weiteren werden die Autoxidation von Zuckern, welche allerdings quantitativ nur eine marginale Bedeutung besitzt, und radikalische Mechanismen diskutiert.<sup>36,37</sup> Der radikalische Abbau von Maillard-Intermediaten ist nach seinem Entdecker Namiki benannt und umfasst die durch freie Radikale vermittelte Bildung von Carbonylsplattungsprodukten.<sup>38</sup>

### 2.1.3 Folgeprodukte und deren Bedeutung *in vivo*

Neben aromaaktiven Stoffen und den hochpolymeren Melanoidinen bilden AGEs die stabilen Endprodukte der Maillard-Reaktion. Sie zeichnen sich durch einen breiten Bereich ihrer chemischen Stabilität und durch hohe Variation ihrer biologischen Wirkungsweise aus.<sup>39</sup> Typischerweise erfolgt die Modifikation an der  $\epsilon$ -Aminogruppe von Lysin oder der Guanidinogruppe von Arginin. Obwohl Glucose eine deutlich höhere Plasmakonzentration aufweist, sind kurzkettige Carbonylverbindungen wesentlich reaktiver und können aufgrund ihrer geringen Molekülgröße leichter und tiefer in ein Protein und dessen Kontaktregionen vordringen.<sup>40,41</sup> Daher verläuft die Bildung von AGEs häufig über freie oder proteingebundene  $\alpha$ -Dicarbonyl-Intermediate.<sup>42</sup> Es sind drei grundlegende Bildungswege für AGEs durch die Maillard-Reaktion bekannt. Die erste Möglichkeit besteht in der Umlagerung der Amadori-Produkte, gefolgt von oxidativen und nicht-oxidativen Abbauwegen. Zweitens bilden Kondensationsreaktionen von Arginin-, Lysin- und Cysteinseitenketten von Proteinen mit reaktiven Carbonylen AGEs und drittens führen amininduzierte Dicarbonylsplaltungen direkt zu Amid-AGEs.<sup>43,44</sup>

Trotz ihrer Komplexität und umfassenden pathologischen Verteilung verursachen alle bekannten AGEs das gleiche chemische Resultat. Sie modifizieren Proteine und bedingen deren kovalente Verknüpfung. Man unterscheidet hierbei in monovalente Modifikationen einzelner Aminosäuren und bivalente Modifikationen von zwei Aminosäuren und die damit verbundene Quervernetzung innerhalb eines Proteins (intramolekular) oder verschiedener Proteine (intermolekular). Die Vielfältigkeit der Reaktion wird dabei einerseits an der möglichen Fülle der gebildeten AGEs aus einem Carbonylsubstrat (Abb. 7, hier am Beispiel von Glycolaldehyd, der einfachsten Verbindung aus der Gruppe der  $\alpha$ -Hydroxyaldehyde) und andererseits an der Anzahl unterschiedlicher Ausgangssubstrate und Mechanismen deutlich, die zu einem AGE führen. So sind allein für die Bildung von  $N^6$ -Carboxymethyllysin (CML), dem ersten *in vivo* identifizierten und häufig als Biomarker verwendeten AGE, bereits mehrere Möglichkeiten bekannt.<sup>45,46</sup> Die Reaktion von Glyoxal zu CML benötigt Enolisierungs- und Cannizzaro-ähnliche Schritte, während für Glycolaldehyd ein zusätzlicher oxidativer Schritt erforderlich ist. Darüber hinaus kann Glycolaldehyd über einen oxidativ radikalisch unterstützten Mechanismus zu CML führen.<sup>47</sup> Neben der Reaktion von Glycolaldehyd und Glyoxal mit Lysin führt auch die oxidative Fragmentierung des Amadori-Produkts verschiedener Zucker, die Peroxidation von Lipiden und die Autoxidation von Ascorbinsäure zu CML.<sup>37,48-51</sup> Die Bildung von bivalenten, quervernetzenden AGEs (Crosslinks) ist, neben dem mechanistischen Aspekt ihrer Bildung, zusätzlich stark von der Verfügbarkeit der Aminogruppen in Proteinen abhängig.

Bisher sind nur Crosslinks zwischen Lysin-Lysin (z.B. Glyoxal-Lysin-Dimer, GOLD) und Arginin-Lysin (z.B. Glyoxal-Lysin-Arginin-Crosslink, GODIC) bekannt. Die Aufklärung dieser Verbindungen und der zugehörigen Reaktionsmechanismen ist daher von entscheidender Bedeutung für ein umfassendes Verständnis der Maillard-Reaktion *in vitro* und *in vivo*.

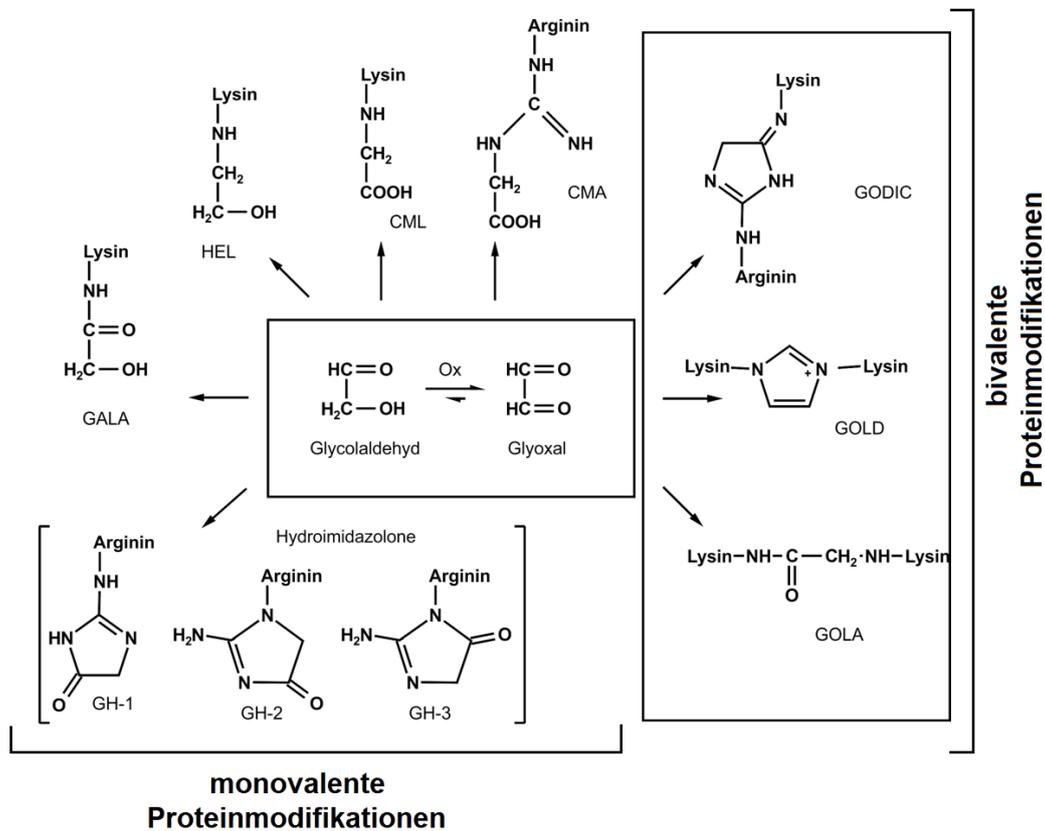


Abb. 7: Übersicht von mono- und bivalenten AGEs ausgehend von Glycolaldehyd und Glyoxal

*In vivo* wird die endogene Akkumulation von AGEs durch oxidativen und Carbonyl-induzierten Stress gefördert, was zu veränderten Strukturen und Funktionen von Proteinen führt und so einen wichtigen Marker für Gewebeschäden bei der Alterung und diversen Krankheitsbildern wie Diabetes, Herz-Kreislauf-Erkrankungen, Nierenbeschwerden und neurodegenerativen Erkrankungen darstellt.<sup>52-56</sup> Die Akkumulation wird dabei durch verschiedene biologische Faktoren beeinflusst. Die wichtigsten sind der Umsatz von Proteinen (*protein turnover*) und die Konzentration der reagierenden Carbonylsubstrate.<sup>57</sup> Unter den bekannten biologischen Parametern sind ebenfalls die Art der reagierenden Carbonylsubstrate, Position und Reaktivität der basischen Aminosäure, der Einfluss von reaktiven Sauerstoffspezies, der chemische oder enzymatische Abbau von AGEs und ihren Vorläuferstrukturen und deren Ausscheidung (renale Eliminierung) von Bedeutung.<sup>58-60</sup> Vor allem langlebige Proteine der extrazellulären Matrix wie Augenlinsen oder Kollagen, mit einer Lebensdauer von mehreren Jahren, sind äußerst anfällig für Strukturveränderungen.<sup>61-63</sup> Die zunehmende Versteifung und Dysfunktion

des Gewebes korreliert dabei mit steigender Konzentration an mono- und bivalenten AGEs.<sup>64</sup> Es ist allerdings hervorzuheben, dass auch kurzlebige Proteine modifiziert werden. Während eine anhaltende, exzessive Modifikation von Enzymen sich negativ auf die Substratbindung und enzymatische Aktivität auswirkt, kann eine minimale Glykierung auch eine aktivitätssteigernde Wirkung, z. B. durch die Verbesserung der Löslichkeit, auslösen.<sup>65,66</sup>

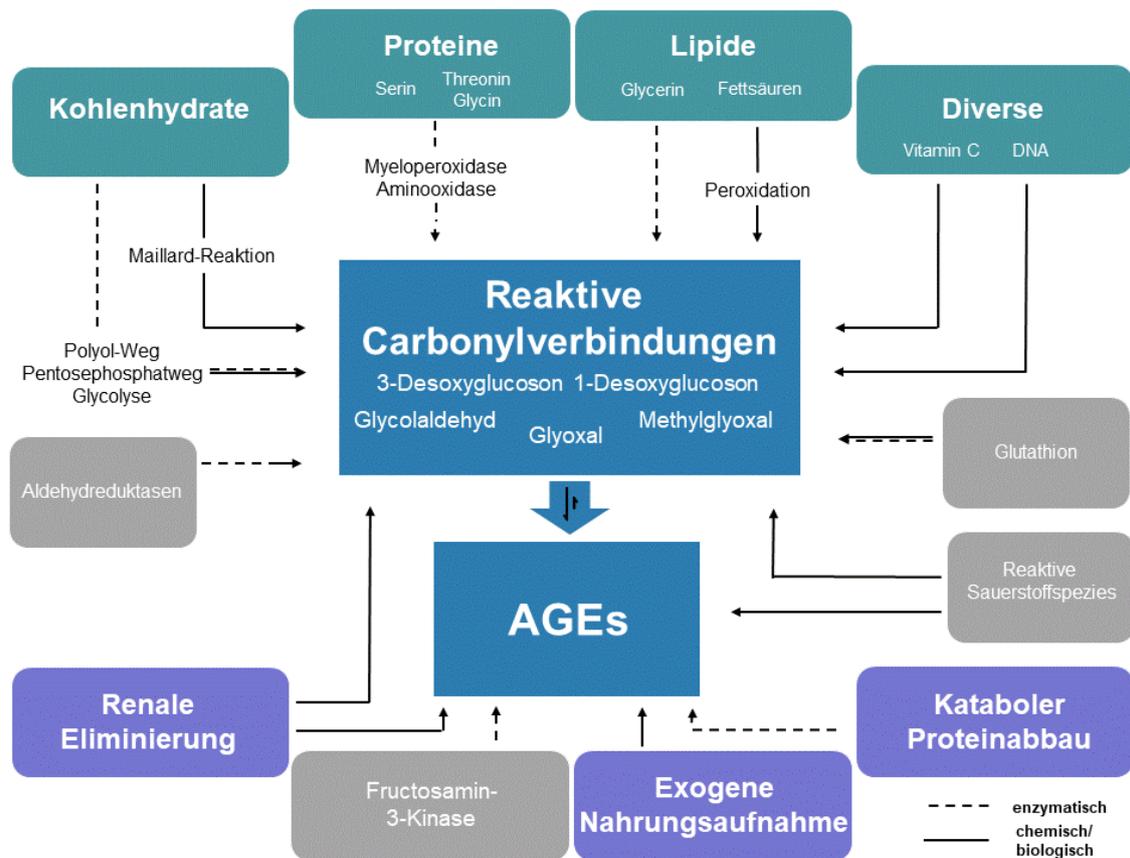


Abb. 8: Übersicht über chemische, enzymatische und biologische Einflussfaktoren auf die Bildung von AGEs *in vivo*

Zusätzlich zur Maillard-induzierten AGE-Bildung durch die Reaktion mit Kohlenhydraten und deren Degradationsprodukten, werden auch andere physiologische Wege, wie der chemische Abbau von DNA und Lipiden diskutiert. Dabei werden diese durch den enzymatischen beziehungsweise oxidativen Abbau von Glycerin und Fettsäuren gebildeten Proteinmodifikationen in der Literatur auch als Advanced Lipoxidation Endproducts (ALEs) bezeichnet. Neben diesen rein nicht-enzymatischen Reaktionen erfolgt parallel auch eine enzymatische Bildung und Entgiftung ihrer Vorläuferstrukturen und Endprodukte. Dabei spielen vor allem der Polyol- und Pentosephosphatweg, die Glycolyse, das Glutathion-Redoxsystem und der direkte Abbau von Aminosäuren und reaktiven Carbonylspezies durch Enzyme (z.B. Aldehydreduktasen) eine entscheidende Rolle.<sup>67-76</sup> Abgesehen von den endogenen Bildungswegen werden AGEs auch exogen über die Nahrung aufgenommen.<sup>77,78</sup>

Abb. 8 fasst die postulierten Einflussfaktoren auf die Bildung reaktiver Carbonyle und folgender AGEs zusammen. Die direkte Modulierung von AGEs und reaktiven Carbonylverbindungen durch biologische und spontane chemische Reaktionen der Maillard-Reaktion wurde bereits intensiv untersucht. Allerdings sind auch die enzymkatalysierte Beeinflussung und die ineinander übergreifende Wechselwirkung dieser Mechanismen von entscheidender Bedeutung.

## 2.2 Rolle der Transketolase-Reaktion

Da dem Einfluss der Transketolase-Reaktion und des Pentosephosphatwegs auf die Modifikation von Proteinen eine besondere Bedeutung in dieser Dissertation zufällt, werden an dieser Stelle spezifische Details dieser essentiellen Stoffwechselreaktion beleuchtet.

Transketolase (Glycolaldehydtransferase, EC 2.2.1.1) ist das geschwindigkeitsbestimmende Enzym im nicht-oxidativen Teil des Pentosephosphatweges, einem der Hauptstoffwechselwege für Kohlenhydrate. Eine gestörte metabolische Funktion wurde bereits mit einer Reihe von Krankheiten wie Diabetes, Alzheimer, Krebs und dem Wernicke-Korsakoff-Syndrom in Verbindung gebracht.<sup>79-81</sup>

### 2.2.1 Stoffwechselfunktion

An der Schnittstelle zwischen den Hexose- und Pentosephosphaten steht der Pentosephosphatweg mit seinen spezifischen Enzymen Transketolase und Transaldolase. Der Pentosephosphatweg dient der Gewinnung von Nicotinamidadenindinucleotidphosphat (NADPH) für anabole Reaktionen, Erythrose-4-phosphat (E4P) für die Synthese aromatischer Aminosäuren und der Bildung und Umwandlung von Pentosephosphaten, die wichtige Vorstufen für die Biosynthese von Nucleinsäuren, Vitaminen und Coenzymen darstellen.<sup>82</sup> Darüber hinaus hilft NADPH den Redoxzustand einer Zelle aufrecht zu erhalten, indem Reduktionsäquivalente für die Glutathion-Produktion bereitgestellt werden. Glutathion ist ein essentielles Molekül zum Ausgleich des Redoxzustands und der Biotransformation von Schadstoffen in einer Zelle.<sup>83,84</sup>

Der Pentosephosphatweg (Abb. 9) ist ein von Glucose ausgehender teilweise parallel zur Glycolyse geschalteter Stoffwechselweg. Zuerst wird die aufgenommene Glucose durch das Enzym Hexokinase phosphoryliert. Das gebildete Glucose-6-phosphat (G6P) wird danach hauptsächlich für die Energiegewinnung durch die Glycolyse und anschließender Oxidation der Produkte im Citratcyclus genutzt oder über den Pentosephosphatweg umgewandelt.<sup>83,84</sup>

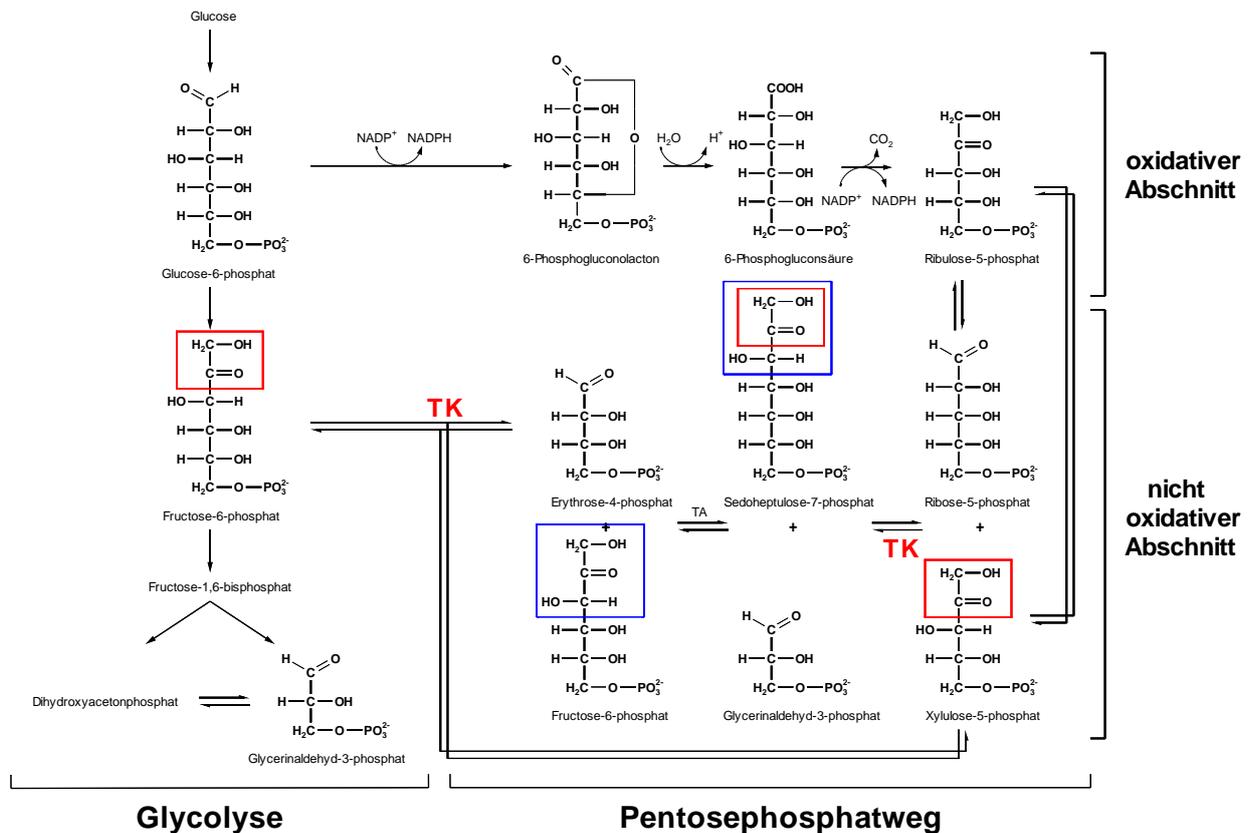


Abb. 9: Glycolyse und Pentosephosphatweg

Der Pentosephosphatweg kann in zwei Phasen unterteilt werden, die oxidative, irreversible Phase und die sich anschließende nicht-oxidative, reversible Phase. Dabei wird G6P durch Glucose-6-phosphat-Dehydrogenase und Lactonase in Gluconat-6-phosphat überführt und NADPH gebildet. Durch Dehydrierung und Decarboxylierung wird unter Katalyse der 6-Phosphogluconat-Dehydrogenase NADPH, CO<sub>2</sub> und Ribulose-5-phosphat (Ru5P) gebildet. Im weiteren Verlauf der Reaktion wird im reversiblen nicht-oxidativen Abschnitt Ru5P in Xylulose-5-phosphat (X5P) oder Ribose-5-phosphat (R5P) isomerisiert. Dabei kann das gebildete R5P einerseits für die Zellproliferation verwendet oder zusammen mit X5P über eine Transketolase- und Transaldolase-katalysierte Transferreaktion wieder in die Glycolyse eingeschleust werden. Dafür wird durch Transketolase die obere C2-Einheit (Abb. 9, roter Rahmen) von X5P auf R5P übertragen, sodass aus zwei C5-Zuckern ein C3-Zucker (Glycerinaldehyd-3-phosphat, G3P) und ein C7-Zucker (Sedoheptulose-7-phosphat, S7P) entsteht. Anschließend erfolgt die Transaldolase-katalysierte Übertragung einer C3-Einheit (Abb. 9, blauer Rahmen) von S7P auf G3P zu Fructose-6-phosphat (F6P) und E4P. Ein weiteres im oxidativen Abschnitt entstandenes X5P wird zusammen mit E4P erneut als Substrat der Transketolase genutzt. Die Reaktionskaskade des nicht-oxidativen Teils liefert so zwei Moleküle F6P und ein Molekül G3P, die Zwischenstufen der Glycolyse darstellen. S7P stellt

das einzige Intermediat des Pentosephosphatwegs dar, das nicht an anderen Stoffwechselwegen beteiligt ist. Je nach Stoffwechsellage erfolgt der weitere glycolytische Abbau aller anderen Metaboliten oder durch einige Enzyme der Gluconeogenese ein erneuter Zyklus für die Generierung von NADPH.<sup>83-86</sup>

### 2.2.2 Cofaktoren & Substratspezifität

Transketolase benötigt Thiamindiphosphat (ThDP, Abb. 10), die biologisch aktive Form des Vitamin B1 und ein bivalentes Metallkation wie  $Mg^{2+}$ ,  $Mn^{2+}$  oder  $Ca^{2+}$  als Cofaktoren. Thiamin setzt sich aus einem aromatischen Methyl-Aminopyrimidinring und einem Methyl-Thiazoliumring zusammen, die über eine Methylengruppe verknüpft sind. Die physiologisch aktive Form trägt zusätzlich eine Pyrophosphatgruppe an der Hydroxyethylseitenkette des Thiazoliumrings. ThDP bestimmt trotz seiner Vielseitigkeit weder die Richtung noch das jeweilig umzusetzende Substrat der Transketolase-Reaktion. Dies wird ausschließlich von der Struktur des Apoproteins bestimmt.<sup>82,87</sup>



Abb. 10: Strukturformel von Thiamindiphosphat

Das Enzym kommt ubiquitär in der Natur vor und weist eine 45-50% Homologie der Aminosäuresequenz in Bakterien, Hefen und Pflanzen auf. Humane Transketolase hingegen zeigt, verglichen mit Hefe und *Escherichia coli* (*E. coli*), lediglich eine Überschneidung von ca. 27%.<sup>88</sup> Bevorzugt werden Donorsubstrate mit D-threo-Konfiguration und  $\alpha$ -hydroxylierte C<sub>2</sub>-D-Akzeptorsubstrate umgesetzt, da diese Konfigurationen zu optimal ausgebildeten Wasserstoffbrückenbindungen zwischen Enzym und Substrat führen.<sup>89,90</sup> Während humane Transketolase ausschließlich phosphorylierte Donorketosen (X5P, F6P und S7P) und Akzeptoralosen (R5P, G3P und E4P) mit Kettenlängen zwischen drei und sieben C-Atomen umsetzen kann, verfügt Transketolase aus *E. coli*, *Saccharomyces cerevisiae* (*S. cerevisiae*) und Spinat über ein breites Spektrum an phosphorylierten und nicht-phosphorylierten Substraten (Tab. 1).<sup>82,91</sup> Das geringere Substratspektrum von humaner Transketolase kann, neben einem kleineren Durchmesser des Substratkanals, in einer abweichenden Aminosäuresequenz begründet sein. Ein zusätzlicher Lysinrest (Lysin 260) soll so zu einer höheren Affinität von phosphorylierten Substraten führen.<sup>88</sup> Eine Sonderform stellt die Dihydroxyaceton-Synthase

beziehungsweise Formaldehydtransketolase aus den Organismen *Hansenula polymorpha*, *Candida boidinii* und *Acetivobacter sp.* dar, welche zusätzlich Formaldehyd und Acetaldehyd als Akzeptoren nutzen kann.<sup>92-94</sup>

Tab. 1: Substrate verschiedener Transketolasen

	Human <sup>88,95-98</sup>	<i>S. cerevisiae</i> <sup>99</sup>	<i>E. coli</i> <sup>89,91</sup>	Spinat <sup>89,100</sup>
<b>Donorketosene</b>				
D-Xylulose-5-phosphat	X	X	X	X
D-Fructose-6-phosphat	X	X	X	X
D-Sedoheptulose-7-phosphat	X	X	X	X
Dihydroxyacetonphosphat		X	X	X
Dihydroxyaceton		X	X	X
$\beta$ -Hydroxypyruvat		X	X	X
<b>Akzeptoraldozen</b>				
D-Ribose-5-phosphat	X	X	X	X
D-Erythrose-4-phosphat	X	X	X	X
D-Glycerinaldehyd-3-phosphat	X	X	X	X
Glycolaldehyd	X	X	X	X
unphosphorylierte Aldosen				X

### 2.2.3 Reaktionsmechanismus der Transketolase

Transketolase ist ein aus zwei identischen Untereinheiten aufgebautes, rotationssymmetrisches Homodimer mit zwei aktiven Zentren.<sup>101,102</sup> Pro Untereinheit sind jeweils ein Molekül ThDP und ein bivalentes Metallion für eine katalytische Aktivität notwendig.<sup>103</sup>

Die Wirkungsweise der Transketolase beruht auf der Übertragung eines C<sub>2</sub>-Fragments („aktivierter Glycolaldehyd“) von einer Donorketose (X5P) auf eine Akzeptoraldose (R5P) (Abb. 11). Die Reaktion kann dabei in zwei Abschnitte unterteilt werden. Zunächst erfolgt die Deprotonierung des Cofaktors am C<sub>2</sub>-Atom des Thiazoliumrings zum Carbanion (Ylid). Nach nucleophilem Angriff an die Carbonylfunktion der Donorketose entsteht das kovalent gebundene Donor-ThDP-Addukt. Die enzymvermittelte Deprotonierung der C<sub>3</sub>-OH-Gruppe führt zur Spaltung der Bindung zwischen C<sub>2</sub> und C<sub>3</sub> der Donorketose und zur Bildung einer um zwei C-Atome verkürzten Aldose (G3P) und 1,2-Dihydroxyethylthiamindiphosphat (DHETHDP).<sup>90,104</sup> Im zweiten Teil der Reaktion erfolgt der nucleophile Angriff des Carbanion-DHETHDP-Intermediats am C<sub>1</sub> einer Akzeptoraldose (R5P) wodurch der am Cofaktor gebundene Glycolaldehydrest übertragen wird. Als Produkt entsteht eine um zwei Kohlenstoffeinheiten verlängerte Ketose (S7P) und ThDP in seiner ursprünglichen Form.<sup>105,106</sup>

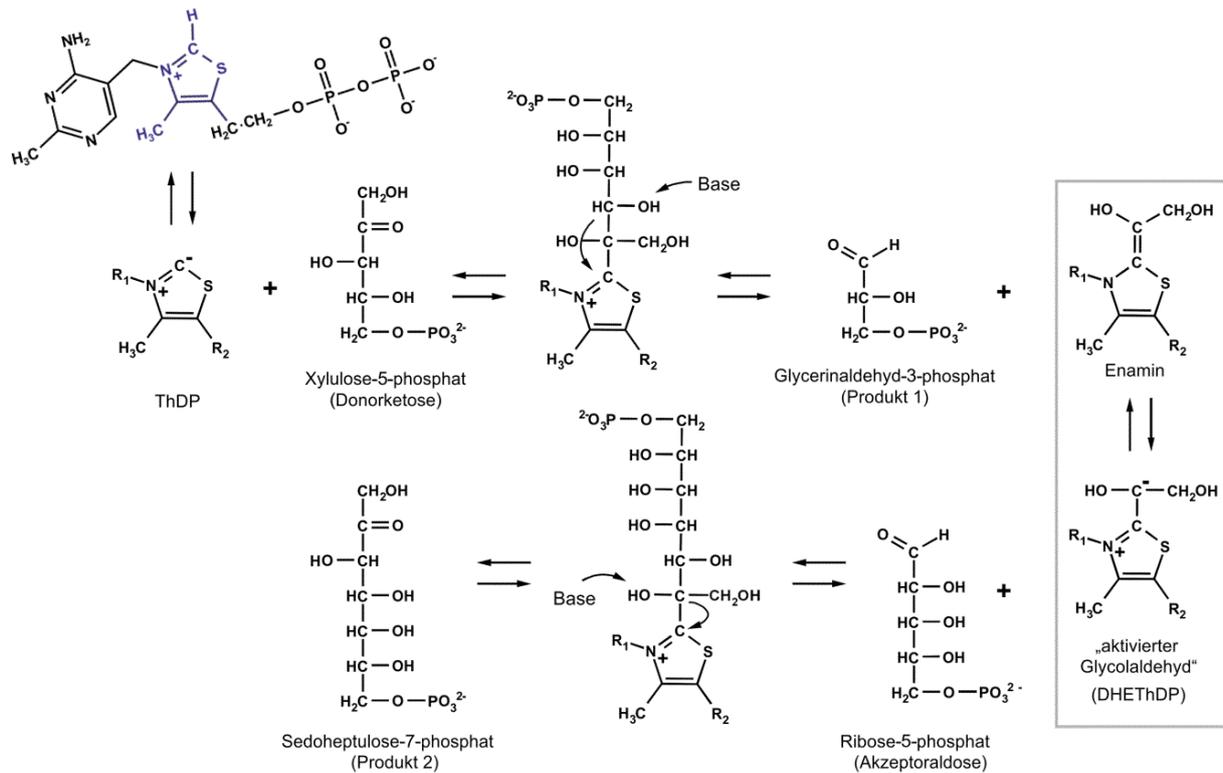


Abb. 11: Reaktionsmechanismus der Katalyse am Beispiel von Xylulose-5-phosphat und Ribose-5-phosphat

Neben der Zweisubstratreaktion, bei der eine Donorketose mit einer Akzeptoraldose umgesetzt wird, kann das Enzym auch Einsubstratreaktionen unter Ausschluss der Akzeptoraldose ausführen.<sup>88,96</sup> Dabei wird lediglich eine Hälfte des Homodimers genutzt.<sup>107</sup> Die katalytische Umsetzung der Donorketose verläuft dabei zunächst analog zur Zweisubstrat-katalysierten Umsetzung und führt zu der entsprechenden Aldose und DHEThDP. Der Zerfall des DHEThDP-Intermediats in ThDP und Glycolaldehyd, welches nun als Akzeptoraldose dienen kann, stellt den geschwindigkeitsbestimmenden Schritt der Katalyse dar und kann nur enzymatisch erfolgen.<sup>108–110</sup>

### 3 Zielstellung

Die Bildung von Maillard-abgeleiteten posttranslationalen Proteinmodifikationen ist ein wichtiger Forschungsbereich sowohl in der Lebensmittelchemie als auch *in vivo*. Nicht-enzymatische Carbonyl-Amin-Reaktionen führen dabei zu Veränderungen in der biologischen Funktion und Struktur von Proteinen. Besonders reaktive kurzkettige Aldehyde wie Glycolaldehyd und sein oxidatives Pendant Glyoxal sind zentrale Vorläufer für die Bildung von Proteinmodifikationen (Advanced Glycation Endproducts, AGEs). Dabei werden diese Carbonylverbindungen und ihre Folgeprodukte durch verschiedene Pathologien, dem Redoxzustand und multiple enzymatische Reaktionen beeinflusst. Die in dieser Dissertation präsentierten Ergebnisse sollen zu einem tieferen Verständnis der Reaktionen von Glycolaldehyd und Glyoxal *in vitro* und *in vivo* beitragen.

Ein Ziel der Arbeit war es, die Bedeutung der Transketolase-Reaktion in der Bildung und Reduktion reaktiver Carbonylspezies und deren Beteiligung an der Glykierung von Proteinen im Detail zu untersuchen. Zur Etablierung eines aussagekräftigen Modellsystems wurde zunächst rekombinante Transketolase A von *Escherichia coli* mit dem artifiziellen Substrat  $\beta$ -Hydroxypyruvat umgesetzt. Für mechanistische Aussagen wurden die Inkubationen in Gegenwart von *Bovinem* Serum Albumin mit und ohne Zusatz von Glycolaldehyd durchgeführt. Um die Relevanz dieser Reaktion *in vivo* zu beurteilen, wurden Folgeuntersuchungen mit humaner Transketolase und  $^{13}\text{C}$ -markierten Standards durchgeführt. Durch die Implementierung neuer Methoden zur Quantifizierung von Glycolaldehyd und anderen Zuckern sowie Zuckerphosphaten wurde darüber hinaus die Rolle zentraler Stoffwechselintermediate der Transketolase im Krankheitsbild der Urämie untersucht.

Ein weiterer Aspekt der vorliegenden Arbeit bezog sich auf die Veränderung der physikochemischen Eigenschaften von Proteinen durch die Modifikation mit Glycolaldehyd und Glyoxal. Die Bildung von AGEs durch beide Aldehyde ist eng miteinander verknüpft. Allerdings wurden *in vitro* grundlegend unterschiedliche Reaktionsmechanismen und Arten von Proteinspezies für beide Aldehyde beobachtet. Um die Veränderung der physikochemischen Eigenschaften von Proteinen auf molekularer Ebene zu verstehen, wurden einzelne Proteinspezies charakterisiert, isoliert und anschließend auf ihren Gehalt an spezifischen AGEs untersucht.

## 4 Diskussion und Einordnung der Ergebnisse

### 4.1 Modellsysteme zur Untersuchung der Transketolase-Reaktion und ihren Einfluss auf die Bildung von Proteinmodifikationen

Zahlreiche Studien belegen einen direkten Zusammenhang zwischen oxidativem und Carbonyl-induziertem Stress und der Bildung von Proteinmodifikationen *in vivo*.<sup>111–116</sup> Im Zentrum dieser Reaktion befinden sich vor allem kurzkettige Aldehyde wie Glycolaldehyd und Glyoxal, welche direkte Vorläuferstrukturen für die Bildung von Advanced Glycation Endproducts (AGEs) darstellen. Dabei wird die Glykierung von Proteinen durch zahlreiche enzymatische Vorgänge beeinflusst, die den metabolischen Fluss und den Redoxzustand *in vivo* regulieren.<sup>13</sup> Neben dem Glyoxalase-System wird auch der Transketolase-Reaktion eine zentrale Rolle in der Unterdrückung von Carbonylstress zugesprochen.<sup>117</sup> So wurde bereits die indirekte Unterdrückung von Methylglyoxal infolge der Reduktion von Glycerinaldehyd-3-phosphat (G3P) nach Aktivierung der Transketolaseaktivität (TKA) durch Thornalley et al. beschrieben.<sup>118</sup> Gleichzeitig postulierten die Arbeitsgruppen um Fiedler et al. und Bykova et al. erstmals die enzymkatalysierte Freisetzung des Cofaktor-gebundenen Glycolaldehyds im aktiven Zentrum der Transketolase als einen möglichen Nebenweg der C2-Transferreaktion.<sup>108,109</sup> Im Gegensatz zu dieser Annahme konnte bis jetzt kein freier Glycolaldehyd sondern lediglich das Kondensationsprodukt Erythrulose nachgewiesen werden.

Anhand der Literatur können drei mögliche Szenarien für die Transketolase-katalysierte Modulation von Glycolaldehyd in Gegenwart von Proteinen postuliert werden (Abb. 12). So kann (I) die Einsubstrat-katalysierte Freisetzung von Glycolaldehyd aus dem 1,2-Dihydroxyethylthiamindiphosphat-Intermediat (DHETHDP) erfolgen und zur Erhöhung von posttranslationalen Proteinmodifikationen führen. Zum anderen (II) bedingt die enzymkatalysierte Umwandlung von Glycolaldehyd in die stabilere Erythrulose die Senkung von Proteinmodifikationen oder (III) durch die Bindung von Glycolaldehyd an das Modellprotein erfolgt keine Interaktion mit dem aktiven Zentrum der Transketolase.

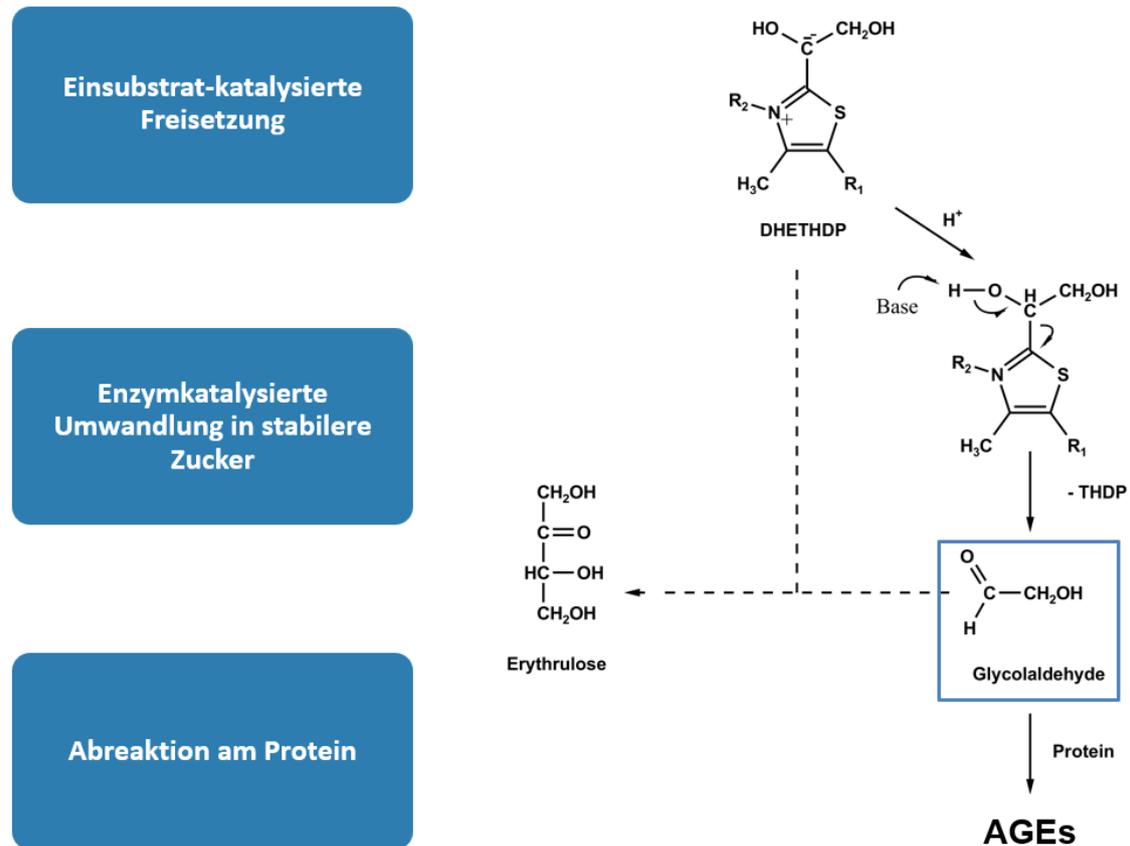


Abb. 12: Rolle von Glycolaldehyd während der Transketolase-Reaktion

Daher war es das Ziel, das Verständnis um die Transketolase-Reaktion zu erweitern und ihren Einfluss auf die Bildung von posttranslationalen Proteinmodifikationen zu untersuchen. Eine detaillierte Beschreibung des experimentellen Aufbaus sowie die Diskussion der Ergebnisse können den Veröffentlichungen „Transketolase A From *E. Coli* Significantly Suppresses Protein Glycation By Glycolaldehyde And Glyoxal *in Vitro*“ (Journal of Agricultural and Food Chemistry, 2017, 65, 8196-8202) und „Influence of Transketolase-Catalyzed Reactions on the Formation of Glycolaldehyde and Glyoxal Specific Posttranslational Modifications under Physiological Conditions“ (Journal of Agricultural and Food Chemistry, 2018, 66, 1498-1508) entnommen werden.<sup>119,120</sup>

### **Modellsystem A: Untersuchungen mit rekombinanter Transketolase A von *E. coli***

Um mechanistische Aussagen über die Rolle von Glycolaldehyd während der Transketolase-Reaktion zu treffen, wurden zunächst Umsetzungen mit rekombinant synthetisierter Transketolase A aus *Escherichia coli* (*E. coli*) untersucht. Dazu wurden äquimolare Anteile an  $\beta$ -Hydroxypyruvat und Ribose-5-phosphat (R5P) mit und ohne Zusatz von 10 mol% Glycolaldehyd in Gegenwart von *Bovinem* Serum Albumin (BSA) inkubiert (pH = 7,4 und 25°C). Um die Quelle von enzymatisch und nicht-enzymatisch gebildeten Glycolaldehyd zu

unterscheiden, wurden zusätzlich Inkubationen mit inaktivierter Transketolase durchgeführt. Die Umwandlung der Zucker und die Bildung von posttranslationalen Proteinmodifikationen wurden dabei über verschiedene Methoden der instrumentellen Analytik verfolgt.

Da die Reaktion mit dem Einsatz von  $\beta$ -Hydroxypyruvat als artifizielle Donorketose unter Freisetzung von  $\text{CO}_2$  irreversibel verläuft, konnte das Modellsystem ausreichend vereinfacht werden, um mechanistische Zusammenhänge herzustellen (Abb. 13). Die Thiamindiphosphat-vermittelte (ThDP) Katalyse führt dabei zuerst zum DHETHDP. Das Carbanion-Enamin-Intermediat überträgt den gebundenen Glycolaldehyd auf R5P, wobei als Hauptprodukt der Reaktion Sedoheptulose-7-phosphat (S7P) entsteht. Bei der Zugabe von Glycolaldehyd als konkurrierender Akzeptor erfolgt zusätzlich die Bildung von Erythulose.

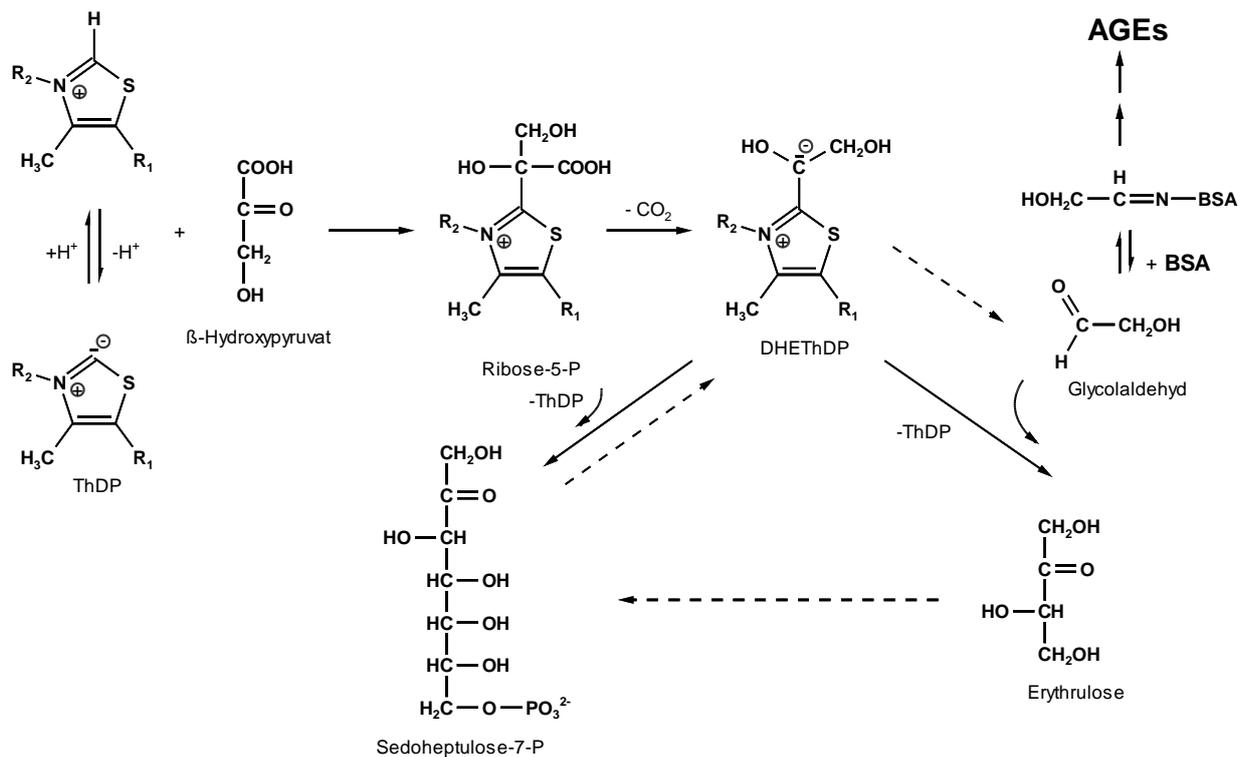


Abb. 13: Modellsystem A: Mechanismus der Transketolase-katalysierten Umsetzung von Glycolaldehyd in Gegenwart von BSA (übernommen von Klaus et al. 2017)<sup>119</sup>

Ein entscheidender Faktor bei der Umsetzung von Multi-Komponenten-Systemen durch Enzyme stellt die Substrataffinität der einzelnen Verbindungen gegenüber dem Enzym dar. Glycolaldehyd stellt, gemessen an seiner Affinität ( $K_M = 14 \text{ mM}$ )<sup>91</sup>, das beste nicht-phosphorylierte Akzeptorsubstrat für nicht-tierische Transketolasen dar und wurde bereits für die enzymatische Synthese von Erythulose verwendet.<sup>121–123</sup> Tatsächlich konnte neben einer signifikanten Abnahme der Glycolaldehydkonzentration die verstärkte Bildung von Erythulose in Inkubationen mit Glycolaldehyd beobachtet werden (Tab. 2). Die mögliche enzymatische Bildung von Erythulose aus der Kondensation von zwei

Glycolaldehydmolekülen kann aufgrund der sehr geringen Affinität von Glycolaldehyd als Donorsubstrat ( $K_M = 140 \text{ mM}$ , gemessen mit Transketolase aus *Saccharomyces cerevisiae*) ausgeschlossen werden.<sup>124</sup> Inkubationen ohne den Zusatz von Glycolaldehyd zeigten ebenfalls die Bildung geringer Mengen an Erythrose. Allerdings muss diese auf die nicht-enzymatische Bildung von Glycolaldehyd durch den Maillard-katalysierten Abbau der Substrate und die anschließende Umwandlung in Erythrose durch Transketolase zurückgeführt werden. Vor allem  $\beta$ -Hydroxypyruvat ist anfällig für nicht-enzymatische Abbaureaktionen die zu Glycolaldehyd, Glyoxylsäure und Spuren von Erythrose durch Aldolkondensation führen.<sup>89,125,126</sup> Die signifikanten Unterschiede zwischen den Inkubationen mit und ohne Glycolaldehyd beweisen, dass im Verlauf der Reaktion ebenfalls S7P ( $K_M = 4 \text{ mM}$ )<sup>91</sup> neben  $\beta$ -Hydroxypyruvat ( $K_M = 18 \text{ mM}$ )<sup>91</sup> als Donorketose für die Bildung von Erythrose agiert. Die dabei gebildete Erythrose, kann nun in einem weiteren Reaktionszyklus (*futile Cycle*) als Donorketose fungieren. Ob sich dabei ein Gleichgewichtszustand (*Steady-State*) zwischen Erythrose, R5P, S7P und ungebundenem Glycolaldehyd ausbildet oder die Reaktion zum Erliegen kommt, wurde nicht abschließend geklärt.<sup>127</sup>

Tab. 2: Gehalte an Zucker [mol%, Ribose-5-phosphat] und Proteinmodifikationen [mmol/mol L-Leu] in Gegenwart von Transketolase A (TK) oder inaktivierter Transketolase A (ITK) nach 8 h mit und ohne Zusatz von 10 mol% Glycolaldehyd (GA).<sup>119</sup>

	TK ohne GA	ITK ohne GA	TK mit GA	ITK mit GA
Sedoheptulose-7-P	87.3 ± 1.6	< NG <sup>a</sup>	82.0 ± 1.9*	< NG
Ribose-5-P	11.5 ± 0.6	89.2 ± 0.7	13.5 ± 0.5*	88.5 ± 0.8
Glycolaldehyd	0.108 ± 0.006	0.536 ± 0.009	1.23 ± 0.03 <sup>#</sup>	3.7 ± 0.1 <sup>#</sup>
Erythrose	0.58 ± 0.05	< BG <sup>b</sup>	5.3 ± 0.3*	< BG
HEL	3.4 ± 0.2	4.1 ± 0.3*	6.2 ± 0.2	18 ± 1 <sup>#</sup>
CML	0.62 ± 0.05	0.64 ± 0.03	0.85 ± 0.02	1.6 ± 0.1 <sup>#</sup>
Imidazolinon	0.034 ± 0.002	0.033 ± 0.002	0.049 ± 0.002	0.09 ± 0.01*

<sup>a</sup>NG: Nachweisgrenze, <sup>b</sup>BG: Bestimmungsgrenze, \*signifikanter Unterschied im Vergleich zu Inkubationen ohne GA mit t-Test ( $\alpha = 0.05$ ), <sup>#</sup> signifikanter Unterschied im Vergleich zu Inkubationen ohne GA mit WELCH-Test ( $\alpha = 0.05$ )

Alle Inkubationen wurden in Gegenwart von BSA durchgeführt. Dabei sollte das Modellprotein als eine Art Abfangreagenz für möglicherweise aus dem Intermediat freigesetztes Glycolaldehyd dienen. Zur Überprüfung dieser Hypothese wurde BSA auf glycolaldehyd- und glyoxalspezifische Proteinmodifikationen untersucht. Die Ergebnisse sind in Tab. 2 zusammengefasst. In Inkubationen ohne zugesetzten Glycolaldehyd konnten analog zu der ungebundenen Glycolaldehydkonzentration signifikant niedrigere Gehalte an

$N^6$ -(2-Hydroxyethyl)lysin (HEL) bestimmt werden. Dieser Unterschied muss dabei dem nicht-enzymatischen Abbau von  $\beta$ -Hydroxypyruvat und anderen Zuckern zugeordnet werden. Während die Maillard-Reaktion von Glycolaldehyd mit der  $\epsilon$ -Aminofunktion von Lysin direkt zur instabilen Schiff'schen Base führt, welche mit Hilfe von  $\text{NaBH}_4$  zu HEL reduziert wird, erfolgt die Bildung von  $N^6$ -Carboxymethyllysin (CML) und 5-(2-Amino-4-hydro-5-imidazol-1-yl)-norvalin (Imidazolinon) verzögert.<sup>37,40,47</sup> So konnten erwartungsgemäß bei CML und Imidazolinon keine signifikanten Unterschiede ermittelt werden. Inkubationen unter Zugabe von Glycolaldehyd hingegen zeigten eine signifikante Verringerung der HEL-Konzentration von über 60% und jeweils rund 50% bei CML und Imidazolinon durch die Transketolase-Reaktion.

Zusammenfassend konnte eine mögliche Freisetzung von Glycolaldehyd aus dem DHETHDP-Intermediat in Gegenwart einer Akzeptoraldose eindeutig widerlegt werden. Vor kurzem wurden diese Ergebnisse durch Solovjeva et al. bestätigt. Eine massenspektrometrische Analyse des katalytischen Intermediats zeigte, dass der Rest des „aktivierten Glycolaldehyds“ während der Umsetzung zu Erythrose in der Einsubstratreaktion gleichermaßen an den Thiazolring von ThDP und an der Aminogruppe seines Aminopyrimidinrings gebunden bleibt.<sup>128</sup> Zusätzlich ist die Geschwindigkeit der Bildung von DHETHDP beträchtlich höher als seine Spaltungsrate. Die gebildeten Mengen in Gegenwart einer Akzeptoraldose bleiben vernachlässigbar klein.<sup>129</sup> Weder Glycolaldehyd noch die detektierten Proteinmodifikationen stiegen während der Transketolase-Reaktion. Das Enzym ist damit in der Lage Glycolaldehyd zu metabolisieren und trägt so zu einer Reduktion von AGEs bei.

### **Modellsystem B: Untersuchungen mit rekombinanter humaner Transketolase**

Um die Relevanz der Reaktion *in vivo* beurteilen zu können, wurden weiterführende Untersuchungen mit rekombinant synthetisierter humaner Transketolase durchgeführt. Im Gegensatz zum irreversibel ablaufendem Modellsystem A ist das Transketolase-System *in vivo* aufgrund der Gleichgewichtseinstellung zwischen den Edukten und Produkten der Reaktion deutlich komplexer. Dazu wurde Fructose-6-phosphat (F6P) und R5P unter Zusatz von Glycolaldehyd in Gegenwart von humanem Serum Albumin (HSA) unter physiologischen Bedingungen (pH = 7.4, 37°C) inkubiert und mit Inkubationen mit inaktivierter humaner Transketolase verglichen. Basierend auf den hier ermittelten Ergebnissen (Vergleich 4.2, Tab. 3) und den Daten in der Literatur wurde das Verhältnis der Edukte an die Konzentrationen *in vivo* angepasst.<sup>130</sup> Zucker und Zuckerphosphate wurden durch Nachinkubation mit 1-Naphthylamin und Natriumcyanoborhydrid abgefangen und mittels LC-MS<sup>2</sup> analysiert.<sup>131</sup>

Durch die Verwendung  $^{13}\text{C}$ -markierter Standards (1- $^{13}\text{C}$ -F6P und 1- $^{13}\text{C}$ -Glycolaldehyd) in mehreren Modellsystemen war es so möglich (I) die Metabolisierung der einzelnen Substrate genau zu verfolgen und (II) die Quelle der gebildeten AGEs durch die Interaktion von Glycolaldehyd und den Substraten mit HSA genau zu bestimmen. Der katalytische Umsatz ist schematisch in Abb. 14 dargestellt.

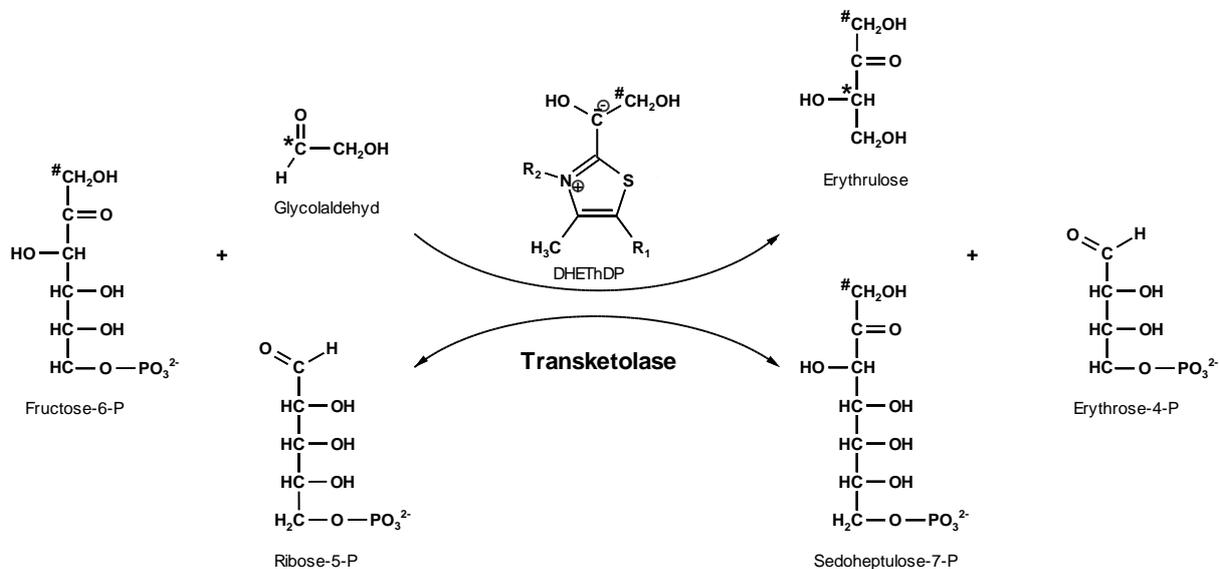


Abb. 14: Modellsystem B: Umsetzung von Glycolaldehyd durch humane Transketolase, \* und # markieren dabei  $^{13}\text{C}$ -markierte Positionen (übernommen von Klaus et al. 2018)<sup>120</sup>

Als Donorketose überträgt F6P eine C2-Einheit auf R5P oder Glycolaldehyd unter Bildung von S7P, Erythrulose und der Freisetzung von Erythrose-4-phosphat (E4P). Wie in Abb. 15 dargestellt, führt die Reaktion zu einem Edukt zu Produkt-Verhältnis von etwa 80:20, welche zunehmend durch den parallel ablaufenden, nicht-enzymatischen Abbau von E4P in Richtung der Produkte verschoben wird. Im Vergleich zu Modellsystem A wurde bei 50 mol% zugesetztem Glycolaldehyd in Modellsystem B nur ein relativ geringer Anteil in Erythrulose (50% des eingesetzten Glycolaldehyds mit Transketolase A vs. 7% des eingesetzten Glycolaldehyds mit humaner Transketolase) umgewandelt. Da das aktive Zentrum von humaner Transketolase durch die ständige Konkurrenzreaktion mehrerer Akzeptoraldosen stärker belegt ist als in Modellsystem A, spielt die mutmaßlich niedrigere Affinität von Glycolaldehyd zu humaner Transketolase eine tragende Rolle. Nach aktuellem Kenntnisstand wurde die Verwendung von Glycolaldehyd als Akzeptorsubstrat für humane Transketolase bisher nur von Meshalkina et al. beschrieben, die jedoch keine greifbaren Substrateigenschaften bestimmten.<sup>96</sup> Allerdings wird die stetige Bildung von Erythrulose durch die fehlende Substrataffinität von humaner Transketolase gegenüber dem C4-Zucker begünstigt.

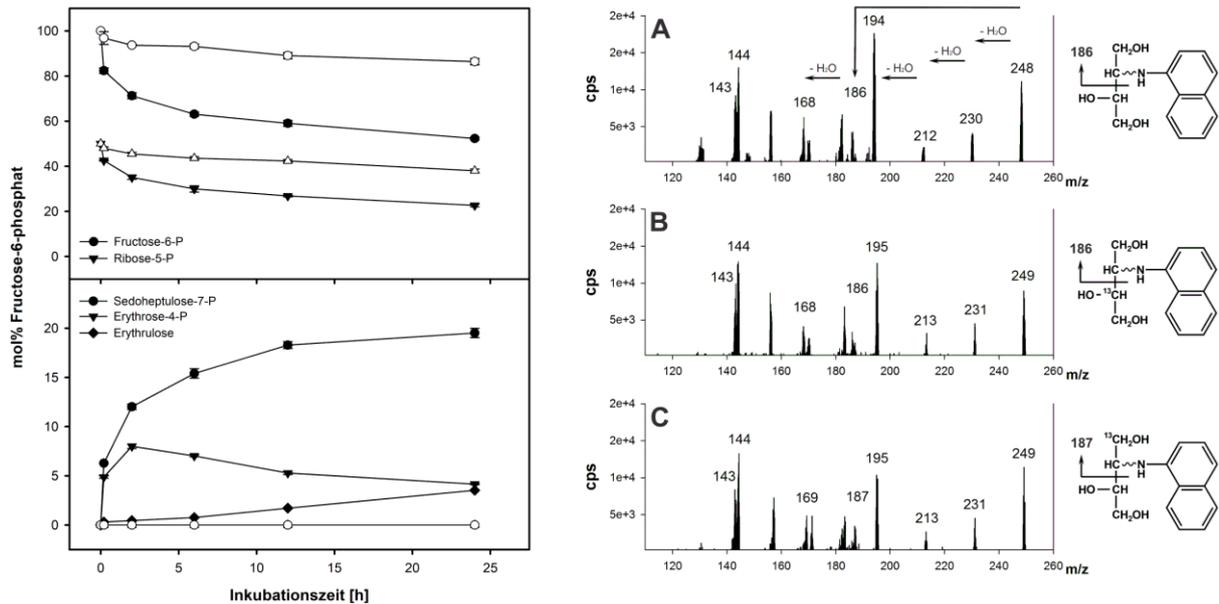


Abb. 15: Umsatzkurven von Modellsystem B in Gegenwart von Transketolase (geschlossene Symbole) und inaktivierter Transketolase (offene Symbole), sowie massenspektrometrischer Nachweis der Metabolisierung von Glycolaldehyd durch humane Transketolase nach reduktiver Aminierung A) Standard, B) 1-<sup>13</sup>C-Glycolaldehyd, C) 1-<sup>13</sup>C-Fructose-6-phosphat<sup>120</sup>

Die Bildung von Erythrose durch die Reaktion von DHETHDP mit Glycolaldehyd konnte durch ein kollisionsinduziertes Dissoziationsexperiment und den Vergleich der Fragmentierungsspektren von Erythrose eindeutig bewiesen werden (Abb. 15). Modellinkubationen von F6P in Gegenwart von 1-<sup>13</sup>C-Glycolaldehyd (Abb. 15B) und von 1-<sup>13</sup>C-F6P in Gegenwart von Glycolaldehyd (Abb. 15C) führten zum Einbau einer <sup>13</sup>C-Markierung in das Erythroselerückgrat und erhöhten das  $m/z$  des Moleküls und seiner Dehydratisierungsprodukte um 1 amu. Da die Reaktion von F6P mit 1-<sup>13</sup>C-Glycolaldehyd zu 3-<sup>13</sup>C-Erythrose führt, folgt mit der Eliminierung der 1,2-Dihydroxyethylgruppe und Dehydratisierung der Verlust der markierten Position und resultiert in den  $m/z$  186 und 168 (siehe A und B). Demgegenüber bleibt im Inkubationssystem mit 1-<sup>13</sup>C-F6P und Glycolaldehyd die markierte Position in 1-<sup>13</sup>C-Erythrose erhalten ( $m/z$  187 und 169, C).

Um den Einfluss auf die Bildung von Proteinmodifikationen zu untersuchen, wurden alle Reaktionen in Gegenwart von HSA durchgeführt. Die Ergebnisse aus Inkubationen mit 1-<sup>13</sup>C-Glycolaldehyd sind in Abb. 16 dargestellt. Wie in Modellsystem A konnte dabei der signifikanten Reduktion von HEL um 30% folgend auch eine Reduktion der glyoxalspezifischen AGEs, des Imidazolinons um 50% und des bivalenten Glyoxal-Lysin-Dimer (GOLD) um 70% durch humane Transketolase bestimmt werden. Nicht-enzymatische Maillard-Prozesse oxidieren Glycolaldehyd leicht zu Glyoxal.<sup>37</sup> Da Glyoxal nicht durch Transketolasen metabolisiert wird, können diese Unterschiede nur durch den

enzymatischen Entzug der Vorläuferverbindung Glycolaldehyd aus dem Inkubationssystem erklärt werden. Entgegen den Erwartungen wurden signifikant erhöhte Gehalte an CML während der Transketolase-Reaktion beobachtet. Während HEL, GH-3 und GOLD ausschließlich durch die Reaktion von Glycolaldehyd und Glyoxal mit Lysin bzw. Arginin gebildet werden,<sup>132,133</sup> wurde die oxidative Fragmentierung des Amadori-Produkts als alternativer Weg für CML beschrieben.<sup>37,49</sup> Offensichtlich wird während der Transketolase-Reaktion instabiles E4P gebildet und infolge seiner offenkettigen Struktur zu mehr als 80% abgebaut. Diese Argumentation wurde weiter durch die Tatsache bestätigt, dass der signifikante Unterschied zwischen Transketolase und Blindwert auf den unmarkierten Anteil von CML zurückzuführen ist.

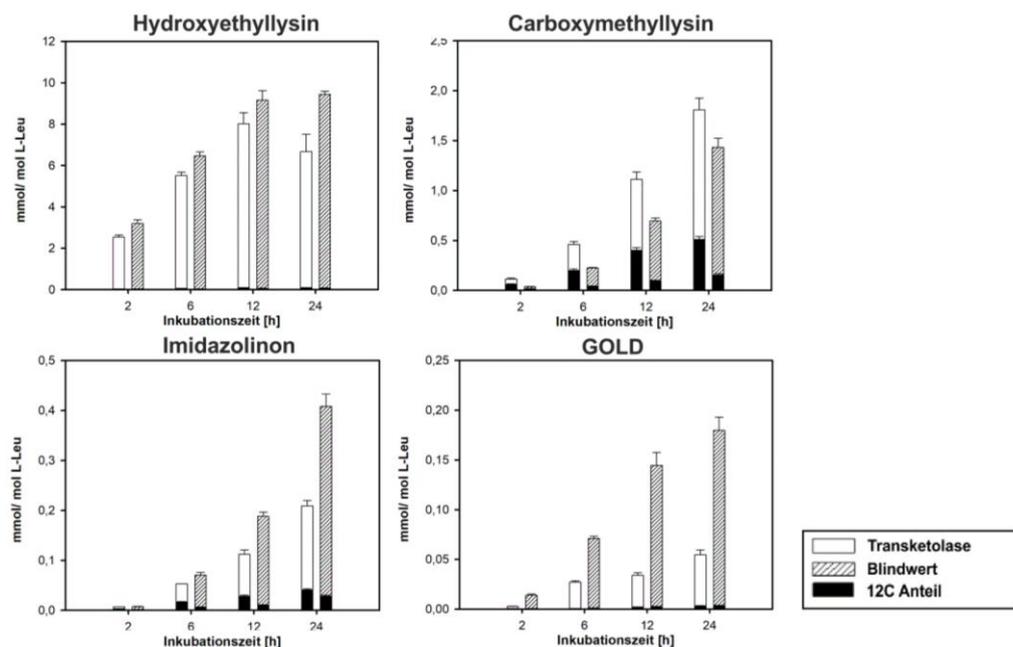


Abb. 16: Einfluss der Transketolase-Reaktion auf die Bildung glycolaldehyd- und glyoxalspezifischer Proteinmodifikationen<sup>120</sup>

Entgegen der ursprünglichen Annahme wurde eine Freisetzung von Glycolaldehyd *in vivo* widerlegt.<sup>134</sup> Dies bestätigt die hier dargestellte Reduktion von AGEs durch humane Transketolase *in vitro*.

## 4.2 Einfluss der Transketolase-Reaktion *in vivo*

Um die Bedeutung der Transketolase-Reaktion *in vivo* zu ermitteln, wurden Glycolaldehyd sowie relevante Zucker-Edukte und -Produkte in Vollblut, Plasma und Erythrozyten (RBC) mit einer neuartigen optimierten Aufarbeitung und LC-MS<sup>2</sup> bestimmt. Dadurch war es erstmals möglich, eine gesunde Kontrollgruppe mit urämischen Patienten zu vergleichen. Nierenversagen zeichnet sich durch erhöhte Mengen an harnpflichtigen Substanzen im Plasma

und ein Ungleichgewicht des Redoxzustands aus.<sup>135,136</sup> Diese Intoxikation wurde bereits mit einer gestörten metabolischen Funktion des Pentosephosphatwegs in Verbindung gebracht.<sup>137,138</sup> Daher ist die Aktivierung des Pentosephosphatwegs für die Aufrechterhaltung antioxidativer Abwehrmechanismen durch die Produktion von NADPH wünschenswert.<sup>139–141</sup> In der klinischen Anwendung wird Benfotiamin, eine fettlösliche Vorstufe von Vitamin B1, aufgrund seiner höheren Bioverfügbarkeit verwendet um die Transketolaseaktivität (TKA) zu erhöhen. Dabei wurde gleichzeitig die Reduktion von AGEs postuliert.<sup>142–145</sup> Eine detaillierte Beschreibung der Aufarbeitung und Bestimmung der Analyten in den Blutproben sowie eine ausführliche Diskussion der Ergebnisse kann der Veröffentlichung „Influence of Transketolase-Catalyzed Reactions on the Formation of Glycolaldehyde and Glyoxal Specific Posttranslational Modifications under Physiological Conditions“ (Journal of Agricultural and Food Chemistry, 2018, 66, 1498-1508) entnommen werden.<sup>120</sup>

Tab. 3: Bestimmte Gehalte an Zucker und Transketolaseaktivität (TKA) in Vollblut, Erythrozyten (RBC) und Plasma von einer gesunden Kontrollgruppe und Urämie-Patienten.<sup>120,146</sup>

[μM]	Kontrollgruppe			Urämie-Patienten			
	Vollblut	RBC	Plasma	Vollblut	RBC	Plasma	
Fructose-6-P	2.03 ± 0.82	4.7 ± 1.3	< NG <sup>a</sup>	2.2 ± 1.0	5.5 ± 2.8	< NG	
Ribose-5-P	0.69 ± 0.20	3.1 ± 1.4*	< BG <sup>b</sup>	0.99 ± 0.29	5.6 ± 1.4	< BG	
Erythrose	0.98 ± 0.37**	< BG	4.0 ± 1.2*	0.43 ± 0.26	< BG	2.4 ± 1.1	
Glycolaldehyd	1.39 ± 0.62	2.06 ± 0.65	0.58 ± 0.16*	1.48 ± 0.47	1.75 ± 0.91	0.95 ± 0.22	
Glyoxal <sup>146</sup>	-	-	0.49 ± 0.05*	-	-	1.27 ± 0.98	
TKA	- ThDP [U/g Hb]	0.87 ± 0.10	0.68 ± 0.07	< NG	0.99 ± 0.16	0.73 ± 0.12	< NG
	+ ThDP [%]	111 ± 12	116 ± 20	< NG	104 ± 13	113 ± 10	< NG

<sup>a</sup>NG: Nachweisgrenze, <sup>b</sup>BG: Bestimmungsgrenze, \* signifikanter Unterschied im Vergleich zu Urämie-Patienten mit t-Test ( $\alpha = 0.05$ ), \*\*signifikanter Unterschied im Vergleich zu Urämie-Patienten mit t-Test ( $\alpha = 0.01$ )

Die prozentuale Erhöhung der TKA in RBCs und Leukozyten durch die *in vitro* Zugabe von ThDP gilt als empfohlener funktioneller Test zur Überprüfung des Thiaminstatus, da die Sättigung des Apoenzyms mit Coenzym bestimmt wird („TPP-Effekt“). Allerdings berichten verschiedene Autoren über normale und teilweise sogar erhöhte TKA bei urämischen Patienten, während andere eine signifikant unterdrückte TKA beschreiben.<sup>97,147–149</sup> In der vorliegenden Studie konnte kein signifikanter Unterschied in der TKA mit oder ohne Zugabe von ThDP festgestellt werden (Tab. 3). *In vivo* kann Glyoxal durch den oxidativen Abbau von Zuckern, Lipiden und glykierten Proteinen gebildet, aber durch das Glyoxalase-System auch entgiftet

werden.<sup>117,150</sup> Im Gegensatz dazu ist zusätzlich zur Maillard-Reaktion lediglich der Abbau von L-Serin durch das Enzym Myeloperoxidase an chronischen Entzündungsstellen für die Bildung von Glycolaldehyd und der nicht-enzymatische Abbau von Ascorbinsäure für die Bildung von Erythrose bekannt.<sup>151,152</sup> Da die Verteilung und Metabolisierung der Analyten zwischen den Kompartimenten unterschiedlich ausfällt und signifikante Unterschiede im Zuckerprofil von Urämie-Patienten im Vergleich zur Kontrollgruppe ermittelt wurden, konnte keine abschließende Beurteilung über die Relevanz der Transketolasereaktion *in vivo* getroffen werden. Allerdings muss die aminkatalysierte Oxidation von Glycolaldehyd zu Glyoxal als ein zentraler Vorgang angesehen werden.<sup>47</sup> Aufgrund des erhöhten oxidativen Stresses bei Urämie kann Oxidation zum Entzug von Glycolaldehyd als Substrat für Transketolase führen.

Die physiologische Konzentration von Glycolaldehyd wurde bisher auf 0,1 bis 1 mM geschätzt.<sup>153–156</sup> Allerdings konnte der hier bestimmte Gehalt von  $0.58 \pm 0.16 \mu\text{M}$  erst kürzlich indirekt durch Henning et al. bestätigt werden.<sup>47,146</sup> Glycolaldehyd und Glyoxal sind über ein Redoxsystem miteinander verknüpft.<sup>157</sup> Durch den Vergleich von proteingebundenem Glycolaldehyd zu Glyoxal, welche im Gleichgewicht mit ihrer freien Form vorliegen, können direkte Aussagen über die Glycolaldehydkonzentrationen *in vivo* getroffen werden. Nach Reduktion der Plasmaproteine in Gegenwart von  $\text{NaBD}_4$  kann über das Isotopenverhältnis von HEL-1D (Glycolaldehyd) zu HEL-2D (Glyoxal) das Verhältnis von Glycolaldehyd zu Glyoxal bestimmt werden (Abb. 17). Dies liegt bei ca. 60:40 (HEL-1D vs. HEL-2D) und ist nahezu identisch zu den freien Gehalten 55:45 (Glycolaldehyd vs. Glyoxal). Glycolaldehyd stellt damit, verglichen mit anderen  $\alpha$ -Dicarbonylen<sup>146</sup>, eine der quantitativ bedeutendsten direkten Vorläuferstrukturen von AGEs *in vivo* dar. Sein genauer Ursprung bleibt jedoch unklar.

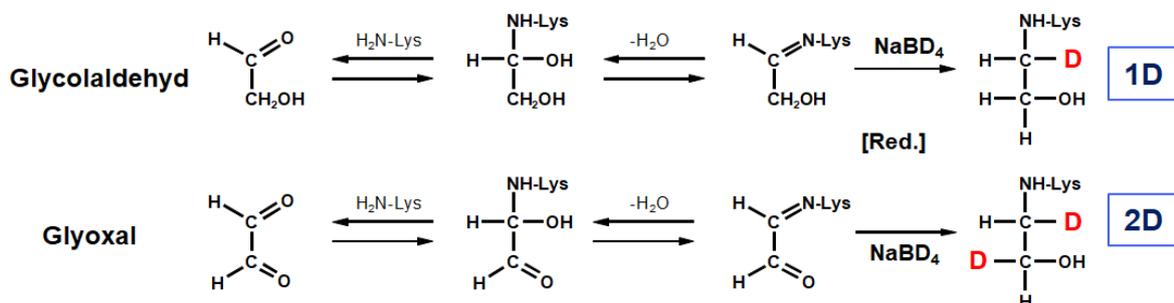


Abb. 17: Unterscheidung von proteingebundenem Glycolaldehyd und Glyoxal durch Deuterierung<sup>47</sup>

### 4.3 Einfluss von Glycolaldehyd und Glyoxal auf die physikochemischen Eigenschaften von Proteinen

Es wird angenommen, dass reaktive Sauerstoffspezies die primäre Quelle für physiologische und pathologische Schäden an Proteinen sind.<sup>158</sup> Nach heutiger Sicht der Maillard-Reaktion sind unabhängig von ihrer Herkunft, vor allem kurzkettige Aldehyde und  $\alpha$ -Dicarbonylverbindungen an der Bildung von AGEs beteiligt. Während die Reaktion von Glyoxal mit Aminosäuren und Proteinen bereits intensiv untersucht wurde, ist der Einfluss von Glycolaldehyd sowohl auf mechanistischer und makromolekularer Ebene kaum verstanden.<sup>37,40,47,159,160</sup> Obwohl hauptsächlich Crosslinks für die Versteifung und Dysfunktion von Geweben verantwortlich gemacht werden, ist in der Literatur nur wenig über die seitenspezifische Modifikation von Proteinen und das unterschiedliche intermolekulare Quervernetzungspotential von reaktiven Carbonylverbindungen bekannt.<sup>64</sup> Ob inter- oder intramolekulare Lysin-Lysin oder Lysin-Arginin Vernetzungen gebildet werden, sollte dabei von der Verfügbarkeit und Reaktivität der freien Aminogruppen abhängen. Eine Möglichkeit die Position von Aminosäuremodifikationen zu bestimmen, besteht in der seitenspezifischen Massenspektrometrie (*De-Novo*-Peptidsequenzierung).<sup>161,162</sup> Allerdings gestaltet sich die Identifikation aufgrund der hohen Variabilität und unterschiedlichen Verteilung der gebildeten Produkte als schwierig. Der gezielte Nachweis von inter- und intramolekularen Crosslinks gelang bislang nur wenigen Arbeitsgruppen.<sup>163,164</sup> Eine mögliche Alternative stellt die Kombination elektrophoretischer und chromatographischer Methoden dar.

Mit dem Ziel, die Modifikation von Proteinen durch Glycolaldehyd und Glyoxal zu untersuchen, wurden Modellinkubationen mit *Boviner* Ribonuclease A (RNase A) unter physiologischen Bedingungen (pH = 7.4, 37°C, anaerob) durchgeführt. Unter Verwendung von verschiedenen elektrophoretischen Verfahren konnten unterschiedliche Proteinspezies identifiziert und charakterisiert werden. Mithilfe von Ionenaustauschchromatographie (IEX) und Gelpermeationschromatographie (GPC) wurde ein Aufarbeitungsverfahren zur Isolation der verschiedenen Proteinspezies entwickelt und die Quantifizierung der gebildeten AGEs mit LC-MS<sup>2</sup> nach saurer und enzymatischer Hydrolyse implementiert. Eine detaillierte Beschreibung der experimentellen Vorgehensweise und die Diskussion der Ergebnisse können der Veröffentlichung „Modification and Crosslinking of Proteins by Glycolaldehyde and Glyoxal: A Model System“ (Journal of Agricultural and Food Chemistry, 2018, 66, 10835–10843) entnommen werden.<sup>165</sup>

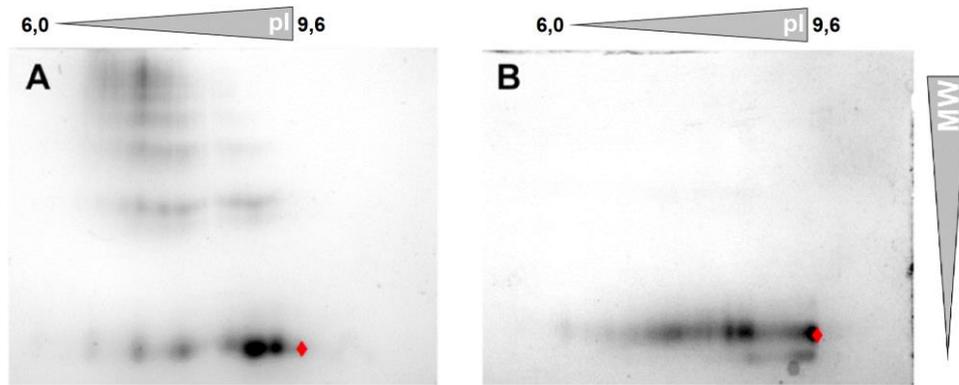


Abb. 18: 2D-Gelelektrophorese nach Inkubation von RNase A mit Glycolaldehyd (A) und Glyoxal (B), die Position nativer RNase A wurde durch  $\blacklozenge$  markiert<sup>165</sup>

RNase A stellt mit einem Molekulargewicht (MW) von 13,7 kDa und einem isoelektrischen Punkt (pI) von 9,6 (aufgrund von vier Arginin- und 10 Lysinseitenketten) das ideale Modellprotein für die chemische Modifikation dar.<sup>166,167</sup> Mithilfe der 2D-Gelelektrophorese (2D-PAGE, Abb. 18) konnten unterschiedliche Polymerisationsgrade und isoelektrische Punkte (pI) zwischen Glycolaldehyd- und Glyoxal-Inkubationen mit RNase A nachgewiesen werden. Während die Modifikation von RNase A durch Glyoxal überwiegend zu monomeren Proteinspezies führt und nur geringe Mengen an Dimer und Trimer nachgewiesen wurden (detektiert nach Aufreinigung mittels GPC), führten Inkubationen mit Glycolaldehyd zu einer deutlich stärkeren Vernetzung des Proteins. Darüber hinaus findet eine Verschiebung des pI der Proteinspezies vom alkalischen Bereich (9,6) in den sauren Bereich (6,0) statt.

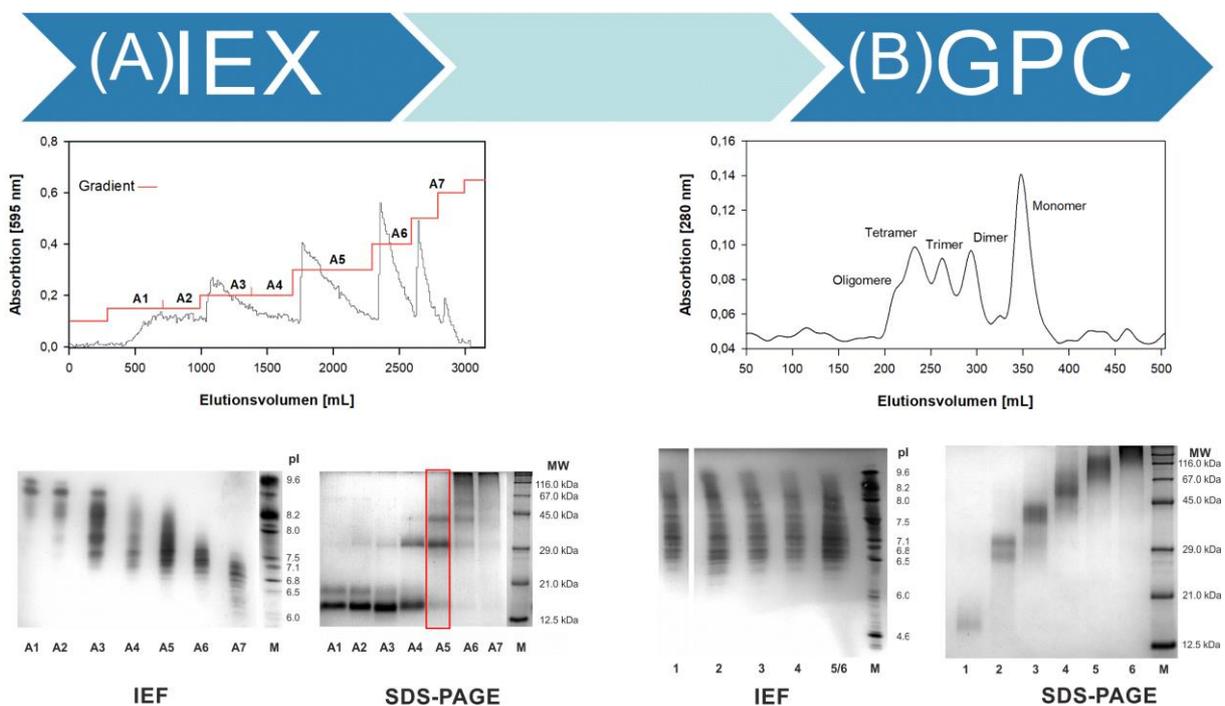


Abb. 19: Isolation und Charakterisierung der gebildeten Proteinspezies nach Inkubation von RNase A mit Glycolaldehyd mithilfe von Ionenaustausch- (IEX) und Gelpermeationschromatographie (GPC)<sup>165</sup>

Um die gebildeten Proteinspezies aufzutrennen, wurde zuerst eine Anionenaustauschchromatographie (Abb. 19A) unter Verwendung abnehmender pH-Werte und steigender NaCl-Konzentrationen durchgeführt. Die erhaltenen Fraktionen wurden mittels isoelektrischer Fokussierung (IEF) und Natriumdodecylsulfat-Polyacrylamid-Gelelektrophorese (SDS-PAGE) auf ihre physikochemischen Eigenschaften untersucht. Alkalische Modifikationen (A1-A3) wurden durch die Anwesenheit von monomeren Spezies (13,7 kDa) charakterisiert. Ein breiter Bereich von Dimeren (27,4 kDa) bis Tetrameren (54,8 kDa) wurde in den mittleren Fraktionen (A4 und A5) und überwiegend stark vernetzte RNase A in A6 und A7 nachgewiesen. Zweitens wurden alle aus der IEX gewonnenen Fraktionen mittels GPC (Abb. 19B) nach ihrem MW aufgetrennt (hier am Beispiel von Fraktion A5) und durch SDS-PAGE und IEF charakterisiert. Wie erwartet, zeichnen sich alle Spezies durch den gleichen pI-Bereich aus.

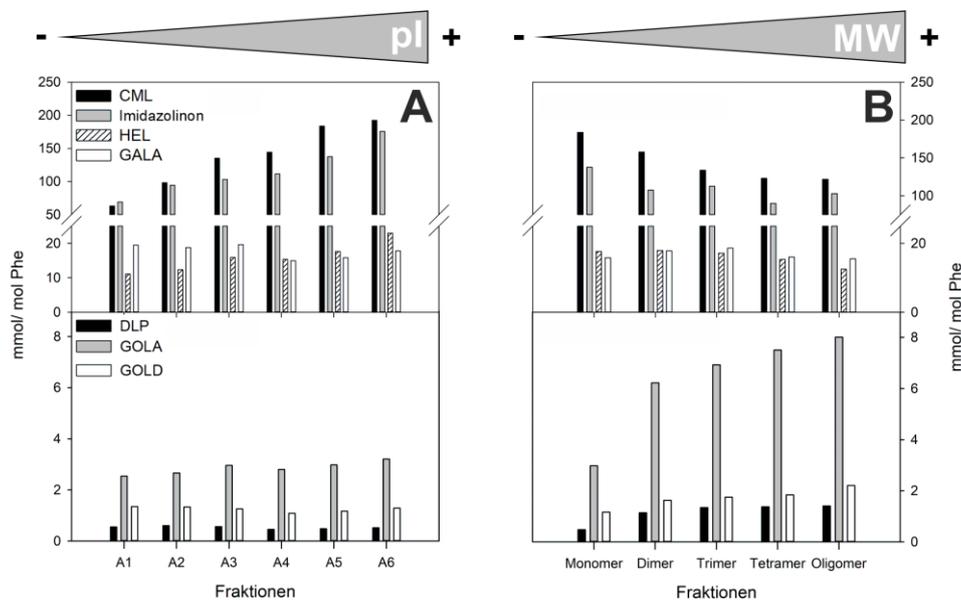


Abb. 20: Nachweis von AGEs aus definierten Proteinspezies von A) isolierten Monomeren mit unterschiedlichen isoelektrischem Punkt (pI) und B) Fraktion A5 (IEX) mit unterschiedlichem Molekulargewicht (MW)<sup>165</sup>

Im Anschluss an die Proteinaufreinigung war es möglich, die bestimmten Mengen an AGEs in den monomeren Proteinspezies der obigen IEX-Fraktionen mit variierenden pI miteinander zu vergleichen (Abb. 20A). Im Vergleich zu den anderen monovalenten AGEs korreliert vor allem die Menge an CML mit der Abnahme des pI. Dieser Umstand ist auf strukturelle Unterschiede der einzelnen Proteinmodifikationen zurückzuführen (Vergleich 2.1.3, Abb. 7). So kommt es z. B. bei CML durch die Einführung einer sauren Carboxylgruppe und infolge der Maskierung der basischen Aminofunktion von Lysin, zu einer Veränderung des pKa und des pI. Während bivalente AGEs keine Veränderung entlang des pI aufweisen, reflektierte die Bestimmung der

AGEs entlang ihres Polymerisationsgrads (Abb. 20B) bei konstantem pI das genaue Gegenteil. Anders als bei den isolierten Monomeren zeigten die quervernetzenden Strukturen 1-(5-Amino-5-carboxypentyl)-4-(5-amino-5-carboxypentyl-amino)-pyridiniumsalz (Dilysinopyridin, DLP), GOLD und Glyoxal-Lysin-Amid (GOLA) einen deutlichen Trend zu höheren Beträgen aufgrund der zunehmenden intermolekularen Quervernetzung.

Die Entdeckung von DLP (Abb. 21) als glycolaldehydspezifisches AGE gibt einen entscheidenden Hinweis über das unterschiedliche Quervernetzungspotential von Glycolaldehyd und Glyoxal. Obwohl nach Oxidation von Glycolaldehyd zu Glyoxal beide Aldehyde prinzipiell zum gleichen Spektrum an Proteinmodifikationen führen, werden in der Literatur zusätzliche Reaktionsmechanismen für Glycolaldehyd diskutiert. Neben der radikalisch unterstützten Bildung von AGEs („Namiki-Weg“) sind auch Aldolkondensationsreaktionen bekannt.<sup>38,47,157,168–171</sup> Ein möglicher Bildungsweg von DLP aus Glycolaldehyd sollte einen Aldolkondensations-ähnlichen Cyclisierungsschritt und den Verlust von Ameisensäure beinhalten. Zusätzlich modifiziert Glyoxal hauptsächlich Arginin, während Glycolaldehyd eine höhere Affinität zu Lysin aufweist.<sup>159,172</sup> Ein ähnliches Reaktionsverhalten konnte bei HSA festgestellt werden. Während vier Lysinreste die Zielstellen für die Glykierung von HSA in Gegenwart von Glucose sind, wurden bevorzugt fünf Argininreste von Methylglyoxal am gleichen Protein modifiziert.<sup>173,174</sup>

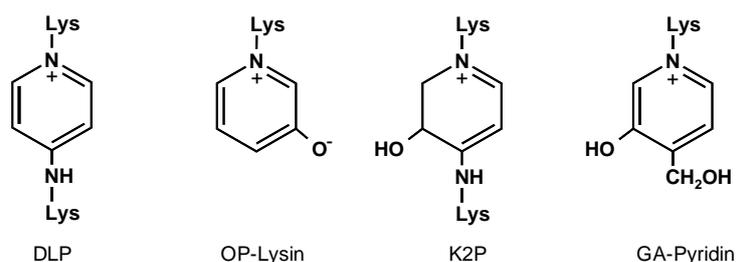


Abb. 21: Strukturformeln verschiedener Pyridinderivate<sup>169–171</sup>

Zusammenfassend konnte eine Struktur-Wirkungsbeziehung von AGEs auf die physikochemischen Eigenschaften von Proteinen hergestellt werden. Darüber hinaus wurde deutlich, dass für die selektive Modifikation von Proteinen die Aminosäuresequenz, die Anwesenheit von umgebenden funktionellen Gruppen wie Carbonsäuren (z.B. Asparaginsäure), und die Position einer Aminogruppe im Protein von entscheidender Bedeutung sind.<sup>175</sup> Die Modifikation von Proteinen wird durch die zugrunde liegenden Mechanismen und den daraus folgenden Produktspektrum bestimmt. Basierend auf vorliegender Arbeit scheint aber auch zusätzlich die wichtigste Determinante für die

unterschiedliche Modifikation von Proteinen die Art des Substrats sowie seine Affinität und Umsatzrate gegenüber der bevorzugten Aminosäure zu sein.

## 5 Zusammenfassung

Die posttranslationale Modifikation durch reaktive Carbonylverbindungen führt zu Veränderungen der biochemischen und physikalischen Eigenschaften von Proteinen in Bezug auf ihre Hydrophobizität, Ladung und biologische Funktion. Nicht-enzymatische Carbonyl-Amin-Reaktionen werden auch unter dem Begriff der Maillard-Reaktion zusammengefasst und die Endprodukte als Advanced Glycation Endproducts (AGEs) bezeichnet. Die ablaufenden Prozesse sind dabei nicht nur in Lebensmitteln sondern auch bei pathophysiologischen Veränderungen von besonderem Interesse. *In vivo* wird das mechanistische Verständnis durch die enzymatische Modulation von AGEs und ihrer Vorläuferstrukturen zusätzlich erschwert. Daher stehen die Rolle der enzymatischen Transketolase-Reaktion und ihr Einfluss auf die Bildung von AGEs im Fokus der vorliegenden Dissertation. Des Weiteren wurden die Proteinfunktionalisierung und ihr Effekt auf die physikochemischen Eigenschaften von Proteinen untersucht.

Transketolase A aus *Escherichia coli* und humane Transketolase wurden aus rekombinanten Zellen gewonnen und mittels Affinitätschromatographie aufgereinigt. Es wurden Modellinkubationen mit unterschiedlichen Substraten in Gegenwart und Abwesenheit von Glycolaldehyd durchgeführt. Parallel zur Abnahme der Glycolaldehydkonzentrationen konnte die enzymatische Umwandlung in Erythrose bestimmt werden. Die Schiff'sche Base, aus der Reaktion von Glycolaldehyd und Glyoxal mit Lysin, und die stabilen Folgeprodukte *N*<sup>6</sup>-Carboxymethyllysin einschließlich glyoxalspezifischer Argininmodifikationen wurden signifikant reduziert. Darüber hinaus deuten die erhaltenen Ergebnisse auf eine potentielle Rolle von Erythrose-4-phosphat bei der Bildung von *N*<sup>6</sup>-Carboxymethyllysin über oxidative Fragmentierungsmechanismen hin. Da die Bedeutung von Glycerinaldehyd-3-phosphat auf die Bildung von Proteinmodifikationen und dessen Modulierung über die Transketolase-Reaktion in der Literatur bekannt ist, sollte dieses Phänomen in zukünftigen Untersuchungen weiter verfolgt werden.

Für eine umfassende Bewertung der Transketolase-Reaktion *in vivo* wurden verschiedene Parameter einer Kontrollgruppe analysiert und mit nicht-diabetischen urämischen Patienten verglichen, die einer Hämodialyse unterzogen wurden. Basierend auf der Derivatisierung mit 1-Naphthylamin und Natriumcyanoborhydrid wurde eine neue LC-MS<sup>2</sup> Methode zur Quantifizierung von Glycolaldehyd sowie Zuckern und Zuckerphosphaten, die am Metabolismus von Transketolase beteiligt sind, etabliert und validiert. Die Quantifizierung

ergab Glycolaldehydkonzentrationen bis zu 2  $\mu\text{M}$  und untermauerte seine entscheidende Rolle bei der Bildung von AGEs *in vivo*.

Diesen Erkenntnissen folgend, wurden Modellinkubationen von Ribonuclease A mit Glycolaldehyd oder Glyoxal unter physiologischen Bedingungen durchgeführt. Es konnten zentrale Informationen über die unterschiedlichen Reaktionsmechanismen beider Aldehyde und ihren Einfluss auf die physikochemischen Eigenschaften von Proteinen gewonnen werden. Die aus den Inkubationen resultierenden Proteinspezies wurden erstmals durch Ionenaustauschchromatographie nach ihrem isoelektrischen Punkt und mithilfe der Gelpermeationschromatographie nach ihrem Polymerisationsgrad aufgetrennt und isoliert. Anschließend erfolgte die Quantifizierung der gebildeten AGEs nach saurer und enzymatischer Hydrolyse mithilfe von LC-MS<sup>2</sup>. Unter Verwendung von isoelektrischer Fokussierung und Natriumdodecylsulfat-Polyacrylamid-Gelelektrophorese (SDS-PAGE) konnte eine ausführliche Charakterisierung der einzelnen Proteinspezies durchgeführt werden. Die Korrelation der quantifizierten AGEs mit den variierenden isoelektrischen Punkten und Polymerisationsgraden der dazugehörigen Proteinspezies ermöglichte die Aufklärung von Struktur-Wirkungsbeziehungen relevanter AGEs. So führt vor allem die Bildung von N<sup>6</sup>-Carboxymethyllysin durch die Addition einer sauren Carboxylgruppe an die basische Aminofunktion von Lysin zu einer Verschiebung des isoelektrischen Punkts in den sauren Bereich. Weiterhin konnte das unterschiedliche Vernetzungspotential von Glycolaldehyd und Glyoxal entschlüsselt werden. Die Identifizierung von Dilysinopyridin als glycolaldehydspezifisches AGE führte zu (I) neuen Erkenntnissen über die Unterschiede des Reaktionsverhaltens von Glycolaldehyd und Glyoxal und impliziert (II) die Relevanz von Aldolkondensationsreaktionen in der Maillard-Reaktion.

Die vorliegende Dissertation erweitert das bisherige Wissen zur Rolle des Pentosephosphatwegs in der Unterdrückung von reaktiven Carbonylverbindungen und ihren Folgeprodukten. Die quantitative Bewertung dieser reaktiven Intermediate ist essentiell für das Verständnis von Transketolase-katalysierten Reaktionen auf molekularer Ebene. Darüber hinaus wird so die Entwicklung von möglichen therapeutischen Interventionen bei Krankheiten ermöglicht. Weiterhin konnten grundlegende Erkenntnisse über die seitenspezifische Modifikation von Proteinen gewonnen werden. Daher ist diese Arbeit essentiell für das Verständnis der physikochemischen Veränderungen von Proteinen und in der zukünftigen Forschung für die anschließende Bewertung ihrer Rolle in Nahrungsmitteln und *in vivo*.

## 6 Summary

Posttranslational modification by reactive carbonyl compounds leads to changes in the biochemical and physical properties of proteins in terms of their hydrophobicity, charge, and biological function. Non-enzymatic carbonyl-amine reactions are termed Maillard reactions and the final products are referred to as Advanced Glycation Endproducts (AGEs). They are of particular interest in foodstuffs and various pathologies. *In vivo*, the mechanistic formation of AGEs and their precursor compounds is influenced by a variety of enzymatic reactions. Therefore, the focus of the present dissertation was placed on the role of transketolase-catalyzed reactions and their influence on the formation of AGEs. Furthermore, protein functionalization and its effect on the physicochemical properties of proteins were investigated.

Transketolase A from *Escherichia coli* and human transketolase were gained from recombinant cells and purified via affinity chromatography. Model incubations with varying substrates in the presence and absence of glycolaldehyde were carried out and led to a decrease in glycolaldehyde concentrations paralleled by the enzymatic conversion to erythrulose. As a result, the Schiff base adducts of glycolaldehyde and glyoxal with lysine residues of proteins and their follow-up products *N*<sup>6</sup>-carboxymethyl lysine and glyoxal specific arginine modifications were significantly reduced. Furthermore, the obtained results indicate a potential role of erythrose-4-phosphate in the formation of *N*<sup>6</sup>-carboxymethyl lysine via oxidative fragmentation mechanisms. As the relevance of glyceraldehyde-3-phosphate on the modification of proteins is well-known in literature, this phenomenon should be clarified in future research.

For a comprehensive evaluation, parameters of the transketolase reaction were analyzed *in vivo* and compared to nondiabetic uremic patients undergoing hemodialysis. A novel LC-MS<sup>2</sup> method, based on derivatization with 1-naphthylamine and sodium cyanoborohydride, for quantitation of glycolaldehyde and other sugars and sugar phosphates involved in the transketolase metabolism was established and validated. Quantitation revealed amounts of glycolaldehyde up to 2  $\mu$ M and highlighted its crucial role in the formation of AGEs *in vivo*.

Driven by these insights, model incubations of ribonuclease A with glycolaldehyde or glyoxal under physiological conditions were carried out. Major information on the different reaction mechanisms and their influence on the physicochemical properties of proteins were obtained from both aldehydes. For the first time, various protein species derived from these aldehydes were successfully separated and isolated based on their isoelectric points by ion-exchange

chromatography and on their degree of polymerization by gel permeation chromatography. After acidic and enzymatic hydrolysis of the protein samples, AGEs were quantified by LC-MS<sup>2</sup>. Using isoelectric focusing and sodium dodecylsulfate-polyacrylamide gel electrophoresis (SDS-PAGE), a detailed characterization of each protein species was carried out. Comparison of the specific AGEs with varying isoelectric points and degrees of polymerization of the corresponding protein species enabled the elucidation of structure-activity relationships of relevant AGEs. Particularly, the formation of *N*<sup>6</sup>-carboxymethyl lysine leads to a shift of the isoelectric point towards the acidic region by addition of an extra carboxylic acid group to the amino function of lysine. Furthermore, the different cross-linking potential of glycolaldehyde and glyoxal was unraveled. The identification of Dilysinopyridine as a glycolaldehyde-specific AGE led to (I) new insights into the differences of the reaction behavior observed for glycolaldehyde and glyoxal and (II) implies the relevance of aldol condensation reactions in the Maillard reaction.

This dissertation extends the current knowledge on the role of the pentose phosphate pathway in the suppression of reactive carbonyl compounds and their follow-up products. The quantitative assessment of these reactive precursor compounds is essential in the understanding of the transketolase metabolism on a molecular level, and in future research on subsequent diseases and the development of possible therapeutic interventions. Furthermore, basic knowledge about the site-specific modification of proteins was obtained. Therefore, this work is essential for understanding the physicochemical changes of proteins and the subsequent assessment of their role in foodstuffs and *in vivo*.

## 7 Abbildungsverzeichnis

Abb. 1: Grundzüge der Maillard-Reaktion <sup>13</sup> .....	2
Abb. 2: Bildung des Amadori-Produktes am Beispiel der Glucose .....	3
Abb. 3: Bildung von $\alpha$ -Dicarbonylen ausgehend vom Amadori-Produkt der Glucose .....	4
Abb. 4: Reaktive Intermediate mit C2-C5 Kohlenstoff-Grundgerüst .....	4
Abb. 5: Mechanismus der oxidativen $\alpha$ -Dicarbonylsplaltung am Beispiel des 1-Desoxyglucosons nach Davidek et al. <sup>32</sup> .....	6
Abb. 6: Mechanismus der hydrolytischen $\beta$ -Dicarbonylsplaltung am Beispiel des Threosons nach Voigt et al. <sup>25</sup> .....	6
Abb. 7: Übersicht von mono- und bivalenten AGEs ausgehend von Glycolaldehyd und Glyoxal .....	8
Abb. 8: Übersicht über chemische, enzymatische und biologische Einflussfaktoren auf die Bildung von AGEs <i>in vivo</i> .....	9
Abb. 9: Glycolyse und Pentosephosphatweg .....	11
Abb. 10: Strukturformel von Thiamindiphosphat .....	12
Abb. 11: Reaktionsmechanismus der Katalyse am Beispiel von Xylulose-5-phosphat und Ribose-5-phosphat.....	14
Abb. 12: Rolle von Glycolaldehyd während der Transketolase-Reaktion.....	17
Abb. 13: Modellsystem A: Mechanismus der Transketolase-katalysierten Umsetzung von Glycolaldehyd in Gegenwart von BSA (übernommen von Klaus et al. 2017) <sup>119</sup> .....	18
Abb. 14: Modellsystem B: Umsetzung von Glycolaldehyd durch humane Transketolase, * und # markieren dabei <sup>13</sup> C-markierte Positionen (übernommen von Klaus et al. 2018) <sup>120</sup> .....	21
Abb. 15: Umsatzkurven von Modellsystem B in Gegenwart von Transketolase (geschlossene Symbole) und inaktivierter Transketolase (offene Symbole), sowie massenspektrometrischer Nachweis der Metabolisierung von Glycolaldehyd durch humane Transketolase nach reduktiver Aminierung A) Standard, B) 1- <sup>13</sup> C-Glycolaldehyd, C) 1- <sup>13</sup> C-Fructose-6-phosphat <sup>120</sup> .....	22
Abb. 16: Einfluss der Transketolase-Reaktion auf die Bildung glycolaldehyd- und glyoxalspezifischer Proteinmodifikationen <sup>120</sup> .....	23
Abb. 17: Unterscheidung von proteingebundenem Glycolaldehyd und Glyoxal durch Deuterierung <sup>47</sup> .....	25
Abb. 18: 2D-Gelelektrophorese nach Inkubation von RNase A mit Glycolaldehyd (A) und Glyoxal (B), die Position nativer RNase A wurde durch $\blacklozenge$ markiert <sup>165</sup> .....	27

Abb. 19: Isolation und Charakterisierung der gebildeten Proteinspezies nach Inkubation von RNase A mit Glycolaldehyd mithilfe von Ionenaustausch- (IEX) und Gelpermeationschromatographie (GPC) <sup>165</sup> .....	27
Abb. 20: Nachweis von AGEs aus definierten Proteinspezies von A) isolierten Monomeren mit unterschiedlichen isoelektrischem Punkt (pI) und B) Fraktion A5 (IEX) mit unterschiedlichem Molekulargewicht (MW) <sup>165</sup> .....	28
Abb. 21: Strukturformeln verschiedener Pyridinderivate <sup>169-171</sup> .....	29

## 8 Tabellenverzeichnis

Tab. 1: Substrate verschiedener Transketolasen .....	13
Tab. 2: Gehalte an Zucker [mol%, Ribose-5-phosphat] und Proteinmodifikationen [mmol/mol L-Leu] in Gegenwart von Transketolase A (TK) oder inaktivierter Transketolase A (ITK) nach 8 h mit und ohne Zusatz von 10 mol% Glycolaldehyd (GA). <sup>119</sup> .....	19
Tab. 3: Bestimmte Gehalte an Zucker und Transketolaseaktivität (TKA) in Vollblut, Erythrozyten (RBC) und Plasma von einer gesunden Kontrollgruppe und Urämie-Patienten. <sup>120,146</sup> .....	24

## 9 Literaturverzeichnis

- (1) Statistisches Bundesamt. *Pressemitteilung Nr. 370*, 2018.
- (2) Medvedev, Z. A. An Attempt at a Rational Classification of Theories of Ageing. *Biological Reviews* **1990**, *65*, 375–398.
- (3) Tessier, F. J. The Maillard reaction in the human body. The main discoveries and factors that affect glycation. *Pathologie-biologie* **2010**, *58*, 214–219.
- (4) Glomb, M. A.; Henning, C. Formation of Reactive Fragmentation Products during the Maillard Degradation of Reducing Sugars – A Review. In *Browned flavors: Analysis, formation, and physiology*; Granvogl, M., Peterson, D., Schieberle, P., Eds.; ACS Symposium Series 1237; American Chemical Society; Distributed in print by Oxford University Press: Washington, DC, Oxford, 2016; pp 117–131.
- (5) Khersonsky, O.; Tawfik, D. S. Enzyme promiscuity: A mechanistic and evolutionary perspective. *Annual review of biochemistry* **2010**, *79*, 471–505.
- (6) Gupta, R. D. Recent advances in enzyme promiscuity. *Sustainable Chemical Processes* **2016**, *4*, 471.
- (7) Hellwig, M.; Henle, T. Baking, ageing, diabetes: A short history of the Maillard reaction. *Angewandte Chemie International Edition in English* **2014**, *53*, 10316–10329.
- (8) Ledl, F.; Schleicher, E. New Aspects of the Maillard Reaction in Foods and in the Human Body. *Angewandte Chemie International Edition in English* **1990**, *29*, 565–594.
- (9) Huyghues-Despointes, A.; Yaylayan, V. A. Retro-Aldol and Redox Reactions of Amadori Compounds: Mechanistic Studies with Variouslly Labeled d-[<sup>13</sup>C]Glucose. *Journal of agricultural and food chemistry* **1996**, *44*, 672–681.
- (10) Martins, S. I.F.S.; van Boekel, M. A.J.S. Kinetics of the glucose/glycine Maillard reaction pathways: Influences of pH and reactant initial concentrations. *Food Chemistry* **2005**, *92*, 437–448.
- (11) Velíšek, J.; Davídek, J.; Pokorný, J.; Grundová, K.; Janíček, G. Reactions of glyoxal with glycine. *Zeitschrift für Lebensmittel-Untersuchung und -Forschung* **1972**, *149*, 323–329.
- (12) Hollnagel, A.; Kroh, L. W. Formation of  $\alpha$ -dicarbonyl fragments from mono- and disaccharides under caramelization and Maillard reaction conditions. *Zeitschrift für Lebensmitteluntersuchung und -Forschung A* **1998**, *207*, 50–54.
- (13) Brownlee, M. Biochemistry and molecular cell biology of diabetic complications. *Nature* **2001**, *414*, 813–820.

- (14) Hodge, J. E. Dehydrated Foods, Chemistry of Browning Reactions in Model Systems. *Journal of agricultural and food chemistry* **1953**, *1*, 928–943.
- (15) Bunn, H. F.; Higgins, P. J. Reaction of monosaccharides with proteins: Possible evolutionary significance. *Science (New York, N.Y.)* **1981**, *213*, 222–224.
- (16) Swamy, M. S.; Tsai, C.; Abraham, A.; Abraham, E. C. Glycation mediated lens crystallin aggregation and cross-linking by various sugars and sugar phosphates in vitro. *Experimental eye research* **1993**, *56*, 177–185.
- (17) Heyns, K.; Paulsen, H.; Eichstedt, R. Über die Gewinnung von 2-Amino-Aldosen Durch Umlagerung von Ketosylaminen: In: Chem. Ber. (90), S. 2039–2049. *Chemische Berichte* **1957**, 2039–2049.
- (18) Henning, C.; Glomb, M. A. Pathways of the Maillard reaction under physiological conditions. *Glycoconjugate journal* **2016**, *33*, 499–512.
- (19) Gobert, J.; Glomb, M. A. Degradation of glucose: Reinvestigation of reactive alpha-Dicarbonyl compounds. *Journal of agricultural and food chemistry* **2009**, *57*, 8591–8597.
- (20) Kawakishi, S.; Tsunehiro, J.; Uchida, K. Autoxidative degradation of Amadori compounds in the presence of copper ion. *Carbohydrate Research* **1991**, *211*, 167–171.
- (21) Smuda, M.; Glomb, M. A. Novel insights into the maillard catalyzed degradation of maltose. *Journal of agricultural and food chemistry* **2011**, *59*, 13254–13264.
- (22) Rakete, S.; Klaus, A.; Glomb, M. A. Investigations on the Maillard reaction of dextrans during aging of Pilsner type beer. *Journal of agricultural and food chemistry* **2014**, *62*, 9876–9884.
- (23) Voigt, M.; Glomb, M. A. Reactivity of 1-deoxy-D-erythro-hexo-2,3-diulose: A key intermediate in the maillard chemistry of hexoses. *Journal of agricultural and food chemistry* **2009**, *57*, 4765–4770.
- (24) Wang, Y.; Ho, C.-T. Flavour chemistry of methylglyoxal and glyoxal. *Chemical Society reviews* **2012**, *41*, 4140–4149.
- (25) Voigt, M.; Smuda, M.; Pfahler, C.; Glomb, M. A. Oxygen-dependent fragmentation reactions during the degradation of 1-deoxy-D-erythro-hexo-2,3-diulose. *Journal of agricultural and food chemistry* **2010**, *58*, 5685–5691.
- (26) Weenen, H. Reactive intermediates and carbohydrate fragmentation in Maillard chemistry. *Food Chemistry* **1998**, *62*, 393–401.
- (27) Tressl, R.; Rewicki, D. Heat Generated Flavors and Precursors. In *Flavor Chemistry: Thirty Years of Progress*; Teranishi, R., Wick, E. L., Hornstein, I., Eds.; Springer US: Boston, MA, s.l., 1999; pp 305–325.

- (28) Smuda, M.; Glomb, M. A. Fragmentation pathways during Maillard-induced carbohydrate degradation. *Journal of agricultural and food chemistry* **2013**, *61*, 10198–10208.
- (29) Pfeifer, Y. V.; Kroh, L. W. Investigation of reactive alpha-dicarbonyl compounds generated from the Maillard reactions of L-methionine with reducing sugars via their stable quinoxaline derivatives. *Journal of agricultural and food chemistry* **2010**, *58*, 8293–8299.
- (30) Singh, R.; Barden, A.; Mori, T.; Beilin, L. Advanced glycation end-products: A review. *Diabetologia* **2001**, *44*, 129–146.
- (31) Yaylayan, V. A.; Keyhani, A. The Origin and Fate of  $\alpha$ -Dicarbonyls Formed in Maillard Model Systems: Mechanistic Studies Using  $^{13}\text{C}$ - and  $^{15}\text{N}$ -Labelled Amino Acids. In *The Maillard reaction in foods and medicine*; O'Brien, J., Ed.; Woodhead Publishing series in food science, technology and nutrition 18; Woodhead Publishing Ltd: Cambridge, 1998; pp 51–56.
- (32) Davídek, T.; Robert, F.; Devaud, S.; Vera, F. A.; Blank, I. Sugar fragmentation in the maillard reaction cascade: Formation of short-chain carboxylic acids by a new oxidative alpha-dicarbonyl cleavage pathway. *Journal of agricultural and food chemistry* **2006**, *54*, 6677–6684.
- (33) Smuda, M.; Glomb, M. A. Maillard degradation pathways of vitamin C. *Angewandte Chemie International Edition in English* **2013**, *52*, 4887–4891.
- (34) Hayami, J.'i. Studies on the Chemical Decomposition of Simple Sugars. XII. Mechanism of the Acetol Formation. *Bulletin of the Chemical Society of Japan* **1961**, *34*, 927–932.
- (35) Henning, C.; Smuda, M.; Girndt, M.; Ulrich, C.; Glomb, M. A. Molecular basis of maillard amide-advanced glycation end product (AGE) formation in vivo. *The Journal of biological chemistry* **2011**, *286*, 44350–44356.
- (36) Wells-Knecht, K. J.; Zyzak, D. V.; Litchfield, J. E.; Thorpe, S. R.; Baynes, J. W. Identification of Glyoxal and Arabinose as Intermediates in the Autoxidative Modification of Proteins by Glucose. *Biochemistry* **2002**, *34*, 3702–3709.
- (37) Glomb, M. A.; Monnier, V. M. Mechanism of protein modification by glyoxal and glycolaldehyde, reactive intermediates of the Maillard reaction. *The Journal of biological chemistry* **1995**, *270*, 10017–10026.
- (38) Namiki, M.; Hayashi, T. A New Mechanism of the Maillard Reaction Involving Sugar Fragmentation and Free Radical Formation. In *Browned flavors: Analysis, formation, and physiology*; Granvogl, M., Peterson, D., Schieberle, P., Eds.; ACS Symposium Series 1237; American Chemical Society; Distributed in print by Oxford University Press: Washington, DC, Oxford, 2016; pp 21–46.

- (39) Heidland, A.; Sebekova, K.; Schinzel, R. Advanced glycation end products and the progressive course of renal disease. *American journal of kidney diseases : the official journal of the National Kidney Foundation* **2001**, *38*, S100-6.
- (40) Acharya, A. S.; Manning, J. M. Reaction of glycolaldehyde with proteins: Latent crosslinking potential of alpha-hydroxyaldehydes. *Proceedings of the National Academy of Sciences of the United States of America* **1983**, *80*, 3590–3594.
- (41) Mera, K.; Takeo, K.; Izumi, M.; Maruyama, T.; Nagai, R.; Otagiri, M. Effect of reactive-aldehydes on the modification and dysfunction of human serum albumin. *Journal of pharmaceutical sciences* **2010**, *99*, 1614–1625.
- (42) Brings, S.; Fleming, T.; Freichel, M.; Muckenthaler, M. U.; Herzig, S.; Nawroth, P. P. Dicarbonyls and Advanced Glycation End-Products in the Development of Diabetic Complications and Targets for Intervention. *International journal of molecular sciences* **2017**, *18*.
- (43) Smuda, M.; Voigt, M.; Glomb, M. A. Degradation of 1-deoxy-D-erythro-hexo-2,3-diulose in the presence of lysine leads to formation of carboxylic acid amides. *Journal of agricultural and food chemistry* **2010**, *58*, 6458–6464.
- (44) Vistoli, G.; Maddis, D. de; Cipak, A.; Zarkovic, N.; Carini, M.; Aldini, G. Advanced glycooxidation and lipoxidation end products (AGEs and ALEs): An overview of their mechanisms of formation. *Free radical research* **2013**, *47 Suppl 1*, 3–27.
- (45) Hull, G. L.J.; Woodside, J. V.; Ames, J. M.; Cuskelly, G. J. Nε-(carboxymethyl)lysine content of foods commonly consumed in a Western style diet. *Food Chemistry* **2012**, *131*, 170–174.
- (46) Thorpe, S. R.; Baynes, J. W. CML: A brief history. *International Congress Series* **2002**, *1245*, 91–99.
- (47) Henning, C.; Liehr, K.; Girndt, M.; Ulrich, C.; Glomb, M. A. Analysis and Chemistry of Novel Protein Oxidation Markers in Vivo. *Journal of agricultural and food chemistry* **2018**, *66*, 4692–4701.
- (48) Ahmed, M. U.; Thorpe, S. R.; Baynes, J. W. Identification of N epsilon-carboxymethyllysine as a degradation product of fructoselysine in glycated protein. *The Journal of biological chemistry* **1986**, *261*, 4889–4894.
- (49) Dunn, J. A.; Ahmed, M. U.; Murtiashaw, M. H.; Richardson, J. M.; Walla, M. D.; Thorpe, S. R.; Baynes, J. W. Reaction of ascorbate with lysine and protein under autoxidizing conditions: Formation of N.epsilon.-(carboxymethyl)lysine by reaction between lysine and products of autoxidation of ascorbate. *Biochemistry* **2002**, *29*, 10964–10970.

- (50) Fu, M. X.; Requena, J. R.; Jenkins, A. J.; Lyons, T. J.; Baynes, J. W.; Thorpe, S. R. The advanced glycation end product, Nepsilon-(carboxymethyl)lysine, is a product of both lipid peroxidation and glycooxidation reactions. *The Journal of biological chemistry* **1996**, *271*, 9982–9986.
- (51) Wolff, S. P.; Jiang, Z. Y.; Hunt, J. V. Protein glycation and oxidative stress in diabetes mellitus and ageing. *Free radical biology & medicine* **1991**, *10*, 339–352.
- (52) Ahmed, N.; Babaei-Jadidi, R.; Howell, S. K.; Beisswenger, P. J.; Thornalley, P. J. Degradation products of proteins damaged by glycation, oxidation and nitration in clinical type 1 diabetes. *Diabetologia* **2005**, *48*, 1590–1603.
- (53) Ahmed, N.; Ahmed, U.; Thornalley, P. J.; Hager, K.; Fleischer, G.; Münch, G. Protein glycation, oxidation and nitration adduct residues and free adducts of cerebrospinal fluid in Alzheimer's disease and link to cognitive impairment. *Journal of neurochemistry* **2005**, *92*, 255–263.
- (54) Baynes, J. W.; Thorpe, S. R. Role of oxidative stress in diabetic complications: A new perspective on an old paradigm. *Diabetes* **1999**, *48*, 1–9.
- (55) Baynes, J. W.; Thorpe, S. R. Glycooxidation and lipoxidation in atherogenesis. *Free radical biology & medicine* **2000**, *28*, 1708–1716.
- (56) Huebschmann, A. G.; Regensteiner, J. G.; Vlassara, H.; Reusch, J. E. B. Diabetes and advanced glycooxidation end products. *Diabetes care* **2006**, *29*, 1420–1432.
- (57) Olufemi, S.; Talwar, D.; Robb, D. A. The relative extent of glycation of haemoglobin and albumin. *Clinica chimica acta; international journal of clinical chemistry* **1987**, *163*, 125–136.
- (58) Delpierre, G.; Rider, M. H.; Collard, F.; Stroobant, V.; Vanstapel, F.; Santos, H.; van Schaftingen, E. Identification, cloning, and heterologous expression of a mammalian fructosamine-3-kinase. *Diabetes* **2000**, *49*, 1627–1634.
- (59) Szwegold, B. S.; Howell, S.; Beisswenger, P. J. Human Fructosamine-3-Kinase: Purification, Sequencing, Substrate Specificity, and Evidence of Activity In Vivo. *Diabetes* **2001**, *50*, 2139–2147.
- (60) Baynes, J. W. The role of AGEs in aging: Causation or correlation. *Experimental Gerontology* **2001**, *36*, 1527–1537.
- (61) Bailey, A. J. Molecular mechanisms of ageing in connective tissues. *Mechanisms of ageing and development* **2001**, *122*, 735–755.
- (62) Monnier, V. M.; Mustata, G. T.; Biemel, K. L.; Reihl, O.; Lederer, M. O.; Zhenyu, D.; Sell, D. R. Cross-linking of the extracellular matrix by the maillard reaction in aging and

diabetes: An update on "a puzzle nearing resolution". *Annals of the New York Academy of Sciences* **2005**, *1043*, 533–544.

(63) Smuda, M.; Henning, C.; Raghavan, C. T.; Johar, K.; Vasavada, A. R.; Nagaraj, R. H.; Glomb, M. A. Comprehensive analysis of maillard protein modifications in human lenses: Effect of age and cataract. *Biochemistry* **2015**, *54*, 2500–2507.

(64) Jost, T.; Zipprich, A.; Glomb, M. A. Analysis of Advanced Glycation Endproducts in Rat Tail Collagen and Correlation to Tendon Stiffening. *Journal of agricultural and food chemistry* **2018**, *66*, 3957–3965.

(65) Dinda, A. K.; Tripathy, D. R.; Dasgupta, S. Glycation of Ribonuclease A affects its enzymatic activity and DNA binding ability. *Biochimie* **2015**, *118*, 162–172.

(66) Bakala, H.; Hamelin, M.; Mary, J.; Borot-Laloi, C.; Friguet, B. Catalase, a target of glycation damage in rat liver mitochondria with aging. *Biochimica et biophysica acta* **2012**, *1822*, 1527–1534.

(67) Niyati-Shirkhodaee, F.; Shibamoto, T. Gas chromatographic analysis of glyoxal and methylglyoxal formed from lipids and related compounds upon ultraviolet irradiation. *Journal of agricultural and food chemistry* **1993**, *41*, 227–230.

(68) Kalapos, M. P. Methylglyoxal in living organisms: Chemistry, biochemistry, toxicology and biological implications. *Toxicology letters* **1999**, *110*, 145–175.

(69) Baynes, J. W. Chemical modification of proteins by lipids in diabetes. *Clinical chemistry and laboratory medicine* **2003**, *41*, 1159–1165.

(70) Lee, A. Y. W.; Chung, S. S. M. Contributions of polyol pathway to oxidative stress in diabetic cataract. *The FASEB Journal* **1999**, *13*, 23–30.

(71) Lorenzi, M. The polyol pathway as a mechanism for diabetic retinopathy: Attractive, elusive, and resilient. *Experimental diabetes research* **2007**, *2007*, 61038.

(72) Thornalley, P. J. Glutathione-dependent detoxification of alpha-oxoaldehydes by the glyoxalase system: Involvement in disease mechanisms and antiproliferative activity of glyoxalase I inhibitors. *Chemico-biological interactions* **1998**, *111-112*, 137–151.

(73) Thornalley, P. J. The potential role of thiamine (vitamin B1) in diabetic complications. *Current diabetes reviews* **2005**, *1*, 287–298.

(74) URATA, G.; GRANICK, S. Biosynthesis of alpha-aminoketones and the metabolism of aminoacetone. *The Journal of biological chemistry* **1963**, *238*, 811–820.

(75) Vander Jagt, D. L.; Hunsaker, L. A. Methylglyoxal metabolism and diabetic complications: Roles of aldose reductase, glyoxalase-I, betaine aldehyde dehydrogenase and 2-oxoaldehyde dehydrogenase. *Chemico-biological interactions* **2003**, *143-144*, 341–351.

- (76) Morgenstern, J.; Fleming, T.; Schumacher, D.; Eckstein, V.; Freichel, M.; Herzig, S.; Nawroth, P. Loss of Glyoxalase 1 Induces Compensatory Mechanism to Achieve Dicarbonyl Detoxification in Mammalian Schwann Cells. *The Journal of biological chemistry* **2017**, *292*, 3224–3238.
- (77) Hohmann, C.; Liehr, K.; Henning, C.; Fiedler, R.; Girndt, M.; Gebert, M.; Hulko, M.; Storr, M.; Glomb, M. A. Detection of Free Advanced Glycation End Products in Vivo during Hemodialysis. *Journal of agricultural and food chemistry* **2017**, *65*, 930–937.
- (78) Delgado-Andrade, C.; Fogliano, V. Dietary Advanced Glycosylation End-Products (dAGEs) and Melanoidins Formed through the Maillard Reaction: Physiological Consequences of their Intake. *Annual review of food science and technology* **2018**, *9*, 271–291.
- (79) Héroux, M.; Raghavendra Rao, V. L.; Lavoie, J.; Richardson, J. S.; Butterworth, R. F. Alterations of thiamine phosphorylation and of thiamine-dependent enzymes in Alzheimer's disease. *Metabolic Brain Disease* **1996**, *11*, 81–88.
- (80) Pácal, L.; Tomandl, J.; Svojanovsky, J.; Krusová, D.; Stepánková, S.; Rehorová, J.; Olsovsky, J.; Belobrádková, J.; Tanhäuserová, V.; Tomandlová, M. *et al.* Role of thiamine status and genetic variability in transketolase and other pentose phosphate cycle enzymes in the progression of diabetic nephropathy. *Nephrology, dialysis, transplantation : official publication of the European Dialysis and Transplant Association - European Renal Association* **2011**, *26*, 1229–1236.
- (81) Zahr, N. M.; Kaufman, K. L.; Harper, C. G. Clinical and pathological features of alcohol-related brain damage. *Nature reviews. Neurology* **2011**, *7*, 284–294.
- (82) Schenk, G.; Duggleby, R. G.; Nixon, P. F. Properties and functions of the thiamin diphosphate dependent enzyme transketolase. *The international journal of biochemistry & cell biology* **1998**, *30*, 1297–1318.
- (83) Berg, J. M.; Tymoczko, J. L.; Stryer, L.; Gatto, G. J. *Biochemie*, 7. Auflage; Springer Spektrum: Berlin, 2013.
- (84) Nelson, D. L.; Cox, M. M.; Lehninger, A. L.; Beginnen, K. *Lehninger Biochemie: Mit 40 Tabellen*, 3., vollst. überarb. und erw. Aufl.; Springer-Lehrbuch; Springer: Berlin, 2001.
- (85) Kruger, N. J.; Schaewen, A. von. The oxidative pentose phosphate pathway: Structure and organisation. *Current opinion in plant biology* **2003**, *6*, 236–246.
- (86) Tittmann, K. Sweet siblings with different faces: The mechanisms of FBP and F6P aldolase, transaldolase, transketolase and phosphoketolase revisited in light of recent structural data. *Bioorganic chemistry* **2014**, *57*, 263–280.

- (87) Kochetov, G. A.; Solovjeva, O. N. Structure and functioning mechanism of transketolase. *Biochimica et biophysica acta* **2014**, *1844*, 1608–1618.
- (88) Mitschke, L.; Parthier, C.; Schröder-Tittmann, K.; Coy, J.; Lüdtke, S.; Tittmann, K. The crystal structure of human transketolase and new insights into its mode of action. *The Journal of biological chemistry* **2010**, *285*, 31559–31570.
- (89) Kobori, Y.; Myles, D. C.; Whitesides, G. M. Substrate specificity and carbohydrate synthesis using transketolase. *The Journal of Organic Chemistry* **1992**, *57*, 5899–5907.
- (90) Nilsson, U.; Meshalkina, L.; Lindqvist, Y.; Schneider, G. Examination of substrate binding in thiamin diphosphate-dependent transketolase by protein crystallography and site-directed mutagenesis. *The Journal of biological chemistry* **1997**, *272*, 1864–1869.
- (91) Sprenger, G. A.; Schörken, U.; Sprenger, G.; Sahm, H. Transketolase A of *Escherichia coli* K12. Purification and properties of the enzyme from recombinant strains. *European journal of biochemistry* **1995**, *230*, 525–532.
- (92) Kato, N.; Higuchi, T.; Sakazawa, C.; Nishizawa, T.; Tani, Y.; Yamada, H. Purification and properties of a transketolase responsible for formaldehyde fixation in a methanol-utilizing yeast, *Candida boidinii* (Kloeckera sp.) No. 2201. *Biochimica et biophysica acta* **1982**, *715*, 143–150.
- (93) Janowicz, Z. A.; Eckart, M. R.; Drewke, C.; Roggenkamp, R. O.; Hollenberg, C. P.; Maat, J.; Ledebor, A. M.; Visser, C.; Verrips, C. T. Cloning and characterization of the DAS gene encoding the major methanol assimilatory enzyme from the methylotrophic yeast *Hansenula polymorpha*. *Nucleic acids research* **1985**, *13*, 3043–3062.
- (94) Ro, Y. T.; Eom, C. Y.; Song, T.; Cho, J. W.; Kim, Y. M. Dihydroxyacetone synthase from a methanol-utilizing carboxydobacterium, *Acinetobacter* sp. strain JC1 DSM 3803. *Journal of bacteriology* **1997**, *179*, 6041–6047.
- (95) Paoletti, F.; Mocali, A.; Marchi, M.; Truschi, F. Analysis of transketolase and identification of an enzyme variant in human leukocytes. *Biochemical and biophysical research communications* **1989**, *161*, 150–155.
- (96) Meshalkina, L. E.; Solovjeva, O. N.; Khodak, Y. A.; Drutsa, V. L.; Kochetov, G. A. Isolation and properties of human transketolase. *Biochemistry (Moscow)* **2010**, *75*, 873–880.
- (97) Kopple, J. D.; Dirige, O. V.; Jacob, M.; Wang, M.; Swendseid, M. E. Transketolase activity in red blood cells in chronic uremia. *Transactions - American Society for Artificial Internal Organs* **1972**, *18*, 250-6, 266.
- (98) Mocali, A.; Paoletti, F. Transketolase from human leukocytes. Isolation, properties and induction of polyclonal antibodies. *European journal of biochemistry* **1989**, *180*, 213–219.

- (99) Datta, A. G.; Racker, E. Mechanism of action of transketolase. I. Properties of the crystalline yeast enzyme. *Journal of Biological Chemistry* **1961**, 617–623.
- (100) Villafranca, J. J.; Axelrod, B. Heptulose synthesis from nonphosphorylated aldoses and ketoses by spinach transketolase. *The Journal of biological chemistry* **1971**, 246, 3126–3131.
- (101) Kochetov, G. A.; Meshalkina, L. E.; Usmanov, R. A. The number of active sites in a molecule of transketolase. *Biochemical and biophysical research communications* **1976**, 69, 839–843.
- (102) Meshalkina, L. E.; Kochetov, G. A. The functional identity of the active centres of transketolase. *Biochimica et Biophysica Acta (BBA) - Enzymology* **1979**, 571, 218–223.
- (103) Kochetov, G. A.; Philippov, P. P. Calcium: Cofactor of transketolase from baker's yeast. *Biochemical and biophysical research communications* **1970**, 38, 930–933.
- (104) Wikner, C.; Nilsson, U.; Meshalkina, L.; Udekwu, C.; Lindqvist, Y.; Schneider, G. Identification of catalytically important residues in yeast transketolase. *Biochemistry* **1997**, 36, 15643–15649.
- (105) Schneider, G.; Lindqvist, Y. Enzymatic Thiamine Catalysis: Mechanistic Implications from the Three-Dimensional Structure of Transketolase. *Bioorganic chemistry* **1993**, 21, 109–117.
- (106) Schneider, G.; Lindqvist, Y. Crystallography and mutagenesis of transketolase: Mechanistic implications for enzymatic thiamin catalysis. *Biochimica et Biophysica Acta (BBA) - Protein Structure and Molecular Enzymology* **1998**, 1385, 387–398.
- (107) Sevostyanova, I.; Solovjeva, O.; Selivanov, V.; Kochetov, G. Half-of-the-sites reactivity of transketolase from *Saccharomyces cerevisiae*. *Biochemical and biophysical research communications* **2009**, 379, 851–854.
- (108) Bykova, I. A.; Solovjeva, O. N.; Meshalkina, L. E.; Kovina, M. V.; Kochetov, G. A. One-substrate transketolase-catalyzed reaction. *Biochemical and biophysical research communications* **2001**, 280, 845–847.
- (109) Fiedler, E.; Golbik, R.; Schneider, G.; Tittmann, K.; Neef, H.; König, S.; Hübner, G. Examination of donor substrate conversion in yeast transketolase. *The Journal of biological chemistry* **2001**, 276, 16051–16058.
- (110) Solov'eva, O. N.; Bykova, I. A.; Meshalkina, L. E.; Kovina, M. V.; Kochetov, G. A. Cleaving of ketosubstrates by transketolase and the nature of the products formed. *Biochemistry Moscow* **2001**, 66, 932–936.

- (111) Agalou, S.; Ahmed, N.; Babaei-Jadidi, R.; Dawnay, A.; Thornalley, P. J. Profound mishandling of protein glycation degradation products in uremia and dialysis. *Journal of the American Society of Nephrology : JASN* **2005**, *16*, 1471–1485.
- (112) Ahmed, U.; Anwar, A.; Savage, R. S.; Thornalley, P. J.; Rabbani, N. Protein oxidation, nitration and glycation biomarkers for early-stage diagnosis of osteoarthritis of the knee and typing and progression of arthritic disease. *Arthritis research & therapy* **2016**, *18*, 250.
- (113) Odani, H.; Shinzato, T.; Matsumoto, Y.; Usami, J.; Maeda, K. Increase in three alpha,beta-dicarbonyl compound levels in human uremic plasma: Specific in vivo determination of intermediates in advanced Maillard reaction. *Biochemical and biophysical research communications* **1999**, *256*, 89–93.
- (114) Lapolla, A.; Reitano, R.; Seraglia, R.; Sartore, G.; Ragazzi, E.; Traldi, P. Evaluation of advanced glycation end products and carbonyl compounds in patients with different conditions of oxidative stress. *Molecular nutrition & food research* **2005**, *49*, 685–690.
- (115) Degenhardt, T. P.; Brinkmann-Frye, E.; Thorpe, S. R.; Baynes, J. W. Role of Carbonyl Stress in Aging and Age-Related Diseases. In *The Maillard reaction in foods and medicine*; O'Brien, J., Ed.; Woodhead Publishing series in food science, technology and nutrition 18; Woodhead Publishing Ltd: Cambridge, 1998; pp 3–10.
- (116) Ergin, V.; Hariry, R. E.; Karasu, C. Carbonyl stress in aging process: Role of vitamins and phytochemicals as redox regulators. *Aging and disease* **2013**, *4*, 276–294.
- (117) Thornalley, P. J. Glyoxalase I--structure, function and a critical role in the enzymatic defence against glycation. *Biochemical Society transactions* **2003**, *31*, 1343–1348.
- (118) Thornalley, P. J.; Jahan, I.; Ng, R. Suppression of the accumulation of triosephosphates and increased formation of methylglyoxal in human red blood cells during hyperglycaemia by thiamine in vitro. *Journal of biochemistry* **2001**, *129*, 543–549.
- (119) Klaus, A.; Pfirrmann, T.; Glomb, M. A. Transketolase A from E. coli Significantly Suppresses Protein Glycation by Glycolaldehyde and Glyoxal in Vitro. *Journal of agricultural and food chemistry* **2017**, *65*, 8196–8202.
- (120) Klaus, A.; Baldensperger, T.; Fiedler, R.; Girndt, M.; Glomb, M. A. Influence of Transketolase-Catalyzed Reactions on the Formation of Glycolaldehyde and Glyoxal Specific Posttranslational Modifications under Physiological Conditions. *Journal of agricultural and food chemistry* **2018**, *66*, 1498–1508.
- (121) Gyamerah, M.; Willetts, A. J. Kinetics of overexpressed transketolase from Escherichia coli JM 107/pQR 700. *Enzyme and Microbial Technology* **1997**, *20*, 127–134.

- (122) Mitra, R. K.; Woodley, J. M.; Lilly, M. D. Escherichia coli transketolase-catalyzed carbon-carbon bond formation: Biotransformation characterization for reactor evaluation and selection. *Enzyme and Microbial Technology* **1998**, *22*, 64–70.
- (123) Wei, Y.-C.; Braun-Galleani, S.; Henríquez, M. J.; Bandara, S.; Nesbeth, D. Biotransformation of  $\beta$ -hydroxypyruvate and glycolaldehyde to l-erythrulose by Pichia pastoris strain GS115 overexpressing native transketolase. *Biotechnology progress* **2018**, *34*, 99–106.
- (124) Sevostyanova, I. A.; Solovjeva, O. N.; Kochetov, G. A. A hitherto unknown transketolase-catalyzed reaction. *Biochemical and biophysical research communications* **2004**, *313*, 771–774.
- (125) Dickens, F.; Williamson, D. H. The preparation and properties of lithium hydroxypyruvate and hydroxypyruvic acid. *The Biochemical journal* **1958**, *68*, 74–81.
- (126) Lorillière, M.; Sousa, M. de; Bruna, F.; Heuson, E.; Gefflaut, T.; Berardinis, V. de; Saravanan, T.; Yi, D.; Fessner, W.-D.; Charmantray, F. *et al.* One-pot, two-step cascade synthesis of naturally rare l-erythro (3S,4S) ketoses by coupling a thermostable transaminase and transketolase. *Green Chemistry* **2017**, *19*, 425–435.
- (127) Hecquet, L.; Bolte, J.; Demuynck, C. New Assays for Transketolase. *Bioscience, Biotechnology, and Biochemistry* **2014**, *57*, 2174–2176.
- (128) Solovjeva, O. N.; Kovina, M. V.; Zavialova, M. G.; Zgoda, V. G.; Shcherbinin, D. S.; Kochetov, G. A. New in the mechanism of one-substrate transketolase reaction. *Bioscience reports* **2018**.
- (129) Asztalos, P.; Parthier, C.; Golbik, R.; Kleinschmidt, M.; Hübner, G.; Weiss, M. S.; Friedemann, R.; Wille, G.; Tittmann, K. Strain and near attack conformers in enzymic thiamin catalysis: X-ray crystallographic snapshots of bacterial transketolase in covalent complex with donor ketoses xylulose 5-phosphate and fructose 6-phosphate, and in noncovalent complex with acceptor aldose ribose 5-phosphate. *Biochemistry* **2007**, *46*, 12037–12052.
- (130) Huck, J. H. J.; Struys, E. A.; Verhoeven, N. M.; Jakobs, C.; van der Knaap, M. S. Profiling of pentose phosphate pathway intermediates in blood spots by tandem mass spectrometry: Application to transaldolase deficiency. *Clinical chemistry* **2003**, *49*, 1375–1380.
- (131) Rakete, S.; Glomb, M. A. A novel approach for the quantitation of carbohydrates in mash, wort, and beer with RP-HPLC using 1-naphthylamine for precolumn derivatization. *Journal of agricultural and food chemistry* **2013**, *61*, 3828–3833.
- (132) Glomb, M. A.; Pfahler, C. Amides are novel protein modifications formed by physiological sugars. *The Journal of biological chemistry* **2001**, *276*, 41638–41647.

- (133) Glomb, M. A.; Lang, G. Isolation and Characterization of Glyoxal–Arginine Modifications. *Journal of agricultural and food chemistry* **2001**, *49*, 1493–1501.
- (134) Chalmers, R. A.; Lawson, A. M.; Hauschildt, S.; Watts, R. W. E. The Urinary Excretion of Glycollic Acid and Threonic Acid by Xylitol-Infused Patients and their Relationship to the Possible Role of ‘Active Glycolaldehyde’ in the Transketolase Reaction in vivo. *Biochemical Society transactions* **1975**, *3*, 518–521.
- (135) Stinghen, A. E. M.; Massy, Z. A.; Vlassara, H.; Striker, G. E.; Boullier, A. Uremic Toxicity of Advanced Glycation End Products in CKD. *Journal of the American Society of Nephrology : JASN* **2016**, *27*, 354–370.
- (136) Modaresi, A.; Nafar, M.; Sahraei, Z. Oxidative stress in chronic kidney disease. *Iranian journal of kidney diseases* **2015**, *9*, 165–179.
- (137) Zhang, F.; Masania, J.; Anwar, A.; Xue, M.; Zehnder, D.; Kanji, H.; Rabbani, N.; Thornalley, P. J. The uremic toxin oxythiamine causes functional thiamine deficiency in end-stage renal disease by inhibiting transketolase activity. *Kidney international* **2016**, *90*, 396–403.
- (138) Pietrzak, I.; Baczyk, K. Erythrocyte transketolase activity and guanidino compounds in hemodialysis patients. *Kidney international. Supplement* **2001**, *78*, S97-101.
- (139) Filosa, S.; Fico, A.; Paglialunga, F.; Balestrieri, M.; Croke, A.; Verde, P.; Abrescia, P.; Bautista, J. M.; Martini, G. Failure to increase glucose consumption through the pentose-phosphate pathway results in the death of glucose-6-phosphate dehydrogenase gene-deleted mouse embryonic stem cells subjected to oxidative stress. *The Biochemical journal* **2003**, *370*, 935–943.
- (140) Fico, A.; Paglialunga, F.; Cigliano, L.; Abrescia, P.; Verde, P.; Martini, G.; Iaccarino, I.; Filosa, S. Glucose-6-phosphate dehydrogenase plays a crucial role in protection from redox-stress-induced apoptosis. *Cell death and differentiation* **2004**, *11*, 823–831.
- (141) Giacco, F.; Brownlee, M. Oxidative stress and diabetic complications. *Circulation research* **2010**, *107*, 1058–1070.
- (142) Kihm, L. P.; Müller-Krebs, S.; Klein, J.; Ehrlich, G.; Mertes, L.; Gross, M.-L.; Adaikalakoteswari, A.; Thornalley, P. J.; Hammes, H.-P.; Nawroth, P. P. *et al.* Benfotiamine protects against peritoneal and kidney damage in peritoneal dialysis. *Journal of the American Society of Nephrology : JASN* **2011**, *22*, 914–926.
- (143) Katare, R.; Oikawa, A.; Cesselli, D.; Beltrami, A. P.; Avolio, E.; Muthukrishnan, D.; Munasinghe, P. E.; Angelini, G.; Emanuelli, C.; Madeddu, P. Boosting the pentose phosphate pathway restores cardiac progenitor cell availability in diabetes. *Cardiovascular research* **2013**, *97*, 55–65.

- (144) Berrone, E.; Beltramo, E.; Solimine, C.; Ape, A. U.; Porta, M. Regulation of intracellular glucose and polyol pathway by thiamine and benfotiamine in vascular cells cultured in high glucose. *The Journal of biological chemistry* **2006**, *281*, 9307–9313.
- (145) Schupp, N.; Dette, E. M.; Schmid, U.; Bahner, U.; Winkler, M.; Heidland, A.; Stopper, H. Benfotiamine reduces genomic damage in peripheral lymphocytes of hemodialysis patients. *Naunyn-Schmiedeberg's archives of pharmacology* **2008**, *378*, 283–291.
- (146) Henning, C.; Liehr, K.; Girndt, M.; Ulrich, C.; Glomb, M. A. Extending the spectrum of  $\alpha$ -dicarbonyl compounds in vivo. *The Journal of biological chemistry* **2014**, *289*, 28676–28688.
- (147) Lonergan, E. T. Transketolase Activity in Uremia. *Archives of Internal Medicine* **1970**, *126*, 851.
- (148) Warnock, L. G.; Cullum, U. X.; Stouder, D. A.; Stone, W. J. Erythrocyte transketolase activity in dialysis patients with neuropathy. *Biochemical Medicine* **1974**, *10*, 351–359.
- (149) Masaru, K.; Atsumi, M.; Ryoko, Y.; Akihiro, I.; Yoshito, O. Erythrocyte transketolase activity in uremia. *Clinica Chimica Acta* **1980**, *108*, 169–177.
- (150) Loidl-Stahlhofen, A.; Spiteller, G.  $\alpha$ -Hydroxyaldehydes, products of lipid peroxidation. *Biochimica et biophysica acta* **1994**, *1211*, 156–160.
- (151) Anderson, M. M.; Requena, J. R.; Crowley, J. R.; Thorpe, S. R.; Heinecke, J. W. The myeloperoxidase system of human phagocytes generates N $\epsilon$ -s-(carboxymethyl)lysine on proteins: A mechanism for producing advanced glycation end products at sites of inflammation. *The Journal of clinical investigation* **1999**, *104*, 103–113.
- (152) Rakete, S.; Nagaraj, R. H. Identification of Kynoxazine, a Novel Fluorescent Product of the Reaction between 3-Hydroxykynurenine and Erythrulose in the Human Lens, and Its Role in Protein Modification. *The Journal of biological chemistry* **2016**, *291*, 9596–9609.
- (153) Ukeda, H.; Hasegawa, Y.; Ishi, T.; Sawamura, M. Inactivation of Cu,Zn-Superoxide Dismutase by Intermediates of Maillard Reaction and Glycolytic Pathway and Some Sugars. *Bioscience, Biotechnology, and Biochemistry* **2014**, *61*, 2039–2042.
- (154) Morgan, P. E.; Dean, R. T.; Davies, M. J. Inactivation of cellular enzymes by carbonyls and protein-bound glycation/glycoxidation products. *Archives of biochemistry and biophysics* **2002**, *403*, 259–269.
- (155) Brown, B. E.; Rashid, I.; van Reyk, D. M.; Davies, M. J. Glycation of low-density lipoprotein results in the time-dependent accumulation of cholesteryl esters and apolipoprotein B-100 protein in primary human monocyte-derived macrophages. *The FEBS journal* **2007**, *274*, 1530–1541.

- (156) Lorenzi, R.; Andrades, M. E.; Bortolin, R. C.; Nagai, R.; Dal-Pizzol, F.; Moreira, J. C. F. Circulating glycolaldehyde induces oxidative damage in the kidney of rats. *Diabetes research and clinical practice* **2010**, *89*, 262–267.
- (157) Hofmann, T.; Bors, W.; Stettmaier, K. Studies on Radical Intermediates in the Early Stage of the Nonenzymatic Browning Reaction of Carbohydrates and Amino Acids. *Journal of agricultural and food chemistry* **1999**, *47*, 379–390.
- (158) Harman, D. The free radical theory of aging. *Antioxidants & redox signaling* **2003**, *5*, 557–561.
- (159) Spanneberg, R.; Osswald, F.; Kolesov, I.; Anton, W.; Radusch, H.-J.; Glomb, M. A. Model studies on chemical and textural modifications in gelatin films by reaction with glyoxal and glycolaldehyde. *Journal of agricultural and food chemistry* **2010**, *58*, 3580–3585.
- (160) Spanneberg, R.; Schymanski, D.; Stechmann, H.; Figura, L.; Glomb, M. A. Glyoxal modification of gelatin leads to change in properties of solutions and resulting films. *Soft Matter* **2012**, *8*, 2222.
- (161) Steen, H.; Mann, M. The ABC's (and XYZ's) of peptide sequencing. *Nature reviews. Molecular cell biology* **2004**, *5*, 699–711.
- (162) Zhang, Q.; Ames, J. M.; Smith, R. D.; Baynes, J. W.; Metz, T. O. A perspective on the Maillard reaction and the analysis of protein glycation by mass spectrometry: Probing the pathogenesis of chronic disease. *Journal of proteome research* **2009**, *8*, 754–769.
- (163) Dai, Z.; Wang, B.; Sun, G.; Fan, X.; Anderson, V. E.; Monnier, V. M. Identification of glucose-derived cross-linking sites in ribonuclease A. *Journal of proteome research* **2008**, *7*, 2756–2768.
- (164) Brock, J. W. C.; Cotham, W. E.; Thorpe, S. R.; Baynes, J. W.; Ames, J. M. Detection and identification of arginine modifications on methylglyoxal-modified ribonuclease by mass spectrometric analysis. *Journal of mass spectrometry : JMS* **2007**, *42*, 89–100.
- (165) Klaus, A.; Rau, R.; Glomb, M. A. Modification and Cross-Linking of Proteins by Glycolaldehyde and Glyoxal: A Model System. *Journal of agricultural and food chemistry* **2018**, *66*, 10835–10843.
- (166) Barnard, E. A. Ribonucleases. *Annual review of biochemistry* **1969**, *38*, 677–732.
- (167) Tanford, C.; Hauenstein, J. D. Hydrogen Ion Equilibria of Ribonuclease 1. *Journal of the American Chemical Society* **1956**, *78*, 5287–5291.
- (168) Argirov, O. K.; Lin, B.; Olesen, P.; Ortwerth, B. J. Isolation and characterization of a new advanced glycation endproduct of dehydroascorbic acid and lysine. *Biochimica et Biophysica Acta (BBA) - General Subjects* **2003**, *1620*, 235–244.

- (169) Argirov, O. K.; Lin, B.; Ortwerth, B. J. 2-ammonio-6-(3-oxidopyridinium-1-yl)hexanoate (OP-lysine) is a newly identified advanced glycation end product in cataractous and aged human lenses. *The Journal of biological chemistry* **2004**, *279*, 6487–6495.
- (170) Cheng, R.; Feng, Q.; Argirov, O. K.; Ortwerth, B. J. Structure elucidation of a novel yellow chromophore from human lens protein. *The Journal of biological chemistry* **2004**, *279*, 45441–45449.
- (171) Nagai, R.; Hayashi, C. M.; Xia, L.; Takeya, M.; Horiuchi, S. Identification in human atherosclerotic lesions of GA-pyridine, a novel structure derived from glycolaldehyde-modified proteins. *The Journal of biological chemistry* **2002**, *277*, 48905–48912.
- (172) Cotham, W. E.; Metz, T. O.; Ferguson, P. L.; Brock, J. W. C.; Hinton, D. J. S.; Thorpe, S. R.; Baynes, J. W.; Ames, J. M. Proteomic analysis of arginine adducts on glyoxal-modified ribonuclease. *Molecular & cellular proteomics : MCP* **2004**, *3*, 1145–1153.
- (173) Iberg, N.; Flückiger, R. Nonenzymatic glycosylation of albumin in vivo. Identification of multiple glycosylated sites. *The Journal of biological chemistry* **1986**, *261*, 13542–13545.
- (174) Ahmed, N.; Thornalley, P. J. Peptide mapping of human serum albumin modified minimally by methylglyoxal in vitro and in vivo. *Annals of the New York Academy of Sciences* **2005**, *1043*, 260–266.
- (175) Reiser, K. M.; Amigable, M. A.; Last, J. A. Nonenzymatic glycation of type I collagen. The effects of aging on preferential glycation sites. *The Journal of biological chemistry* **1992**, *267*, 24207–24216.

## 10 Publikationen

## 10.1 Journal of Agricultural and Food Chemistry, 2017, 65, 8196-8202

JOURNAL OF  
**AGRICULTURAL AND  
 FOOD CHEMISTRY**

Article

pubs.acs.org/JAFC

## Transketolase A from *E. coli* Significantly Suppresses Protein Glycation by Glycolaldehyde and Glyoxal in Vitro

Alexander Klaus,<sup>±</sup> Thorsten Pfirrmann,<sup>‡</sup> and Marcus A. Glomb<sup>\*,±</sup>

<sup>±</sup>Institute of Chemistry, Food Chemistry, Martin-Luther-University Halle-Wittenberg, Kurt-Mothes-Str. 2, 06120 Halle/Saale, Germany

<sup>‡</sup>Institute of Physiological Chemistry, Martin-Luther-University Halle-Wittenberg, Hollystr. 1, 06114 Halle/Saale, Germany

**ABSTRACT:** Short-chained carbonyl species such as glycolaldehyde and its oxidized pendant glyoxal are highly reactive Maillard agents, leading to the formation of protein modifications. These advanced glycation endproducts have gained considerable interest as they have been linked to various pathologies in vivo. The ability of transketolase to use glycolaldehyde as a substrate suggested the possibility to modulate carbonyl-driven Maillard reactions. Model incubations with recombinant transketolase A from *Escherichia coli* in the presence of bovine serum albumin and glycolaldehyde indeed led to a decrease in glycolaldehyde concentrations paralleled by the enzymatic conversion to erythrulose. As a result, reversibly protein-bound glycolaldehyde and the major final endproduct N<sup>6</sup>-carboxymethyl lysine were significantly reduced by approximately 50%, respectively. Glycolaldehyde is easily oxidized to glyoxal in the presence of amines and oxygen. In the presence of transketolase, the lower amounts of glycolaldehyde therefore also strongly suppressed the formation of glyoxal specific arginine modifications, measured as 5-(2-imino-5-oxo-1-imidazolidinyl)norvaline after acid hydrolysis.

**KEYWORDS:** transketolase, glycolaldehyde, glyoxal, Maillard reaction, advanced glycation endproducts

### ■ INTRODUCTION

Transketolase (TK, EC 2.2.1.1) is an ubiquitous enzyme occurring in all organisms and of major importance in carbohydrate metabolism, as it interconnects the pentose phosphate pathway to glycolysis. The TK molecule is composed of two equal subunits, requiring thiamine diphosphate (ThDP) and bivalent cations for catalytic activity.<sup>1</sup>

The ThDP-mediated catalysis can be divided into two steps: the cleavage of a C–C-bond of a donor ketose and subsequent transfer of a covalently bound glycolaldehyde unit onto an acceptor aldose. Xylulose-5-phosphate, fructose-6-phosphate, and sedoheptulose-7-phosphate usually serve as donor substrates and ribose-5-phosphate, glyceraldehyde-3-phosphate, and erythrose-4-phosphate as acceptor substrates. TKs from nonmammalian cells are also able to utilize unphosphorylated sugars (e.g.,  $\beta$ -hydroxyppyruvate, dihydroxyacetone, and glycolaldehyde). In the case of  $\beta$ -hydroxyppyruvate, the reaction becomes irreversible due to the release of CO<sub>2</sub>. Apart from the two-substrate reaction, TK is able to perform one-substrate reactions, cleaving the donor substrate in the absence of an acceptor aldose. However, the rate is substantially lower than during two-substrate-catalyzed reactions.<sup>1–3</sup>

Short-chained aldehydes, like glycolaldehyde, play a major role in the reactions leading to post-translational protein modifications in vivo. Nonenzymatic carbonyl-amine reactions are termed Maillard reactions, and the final reaction products are also referred to as advanced glycation endproducts (AGEs) and accumulate over time.<sup>4–6</sup> Glomb et al. demonstrated that glycolaldehyde is initially reversibly bound to proteins via Schiff base adducts, but can be stabilized and analyzed by reduction as N<sup>6</sup>-(2-hydroxyethyl) lysine (HEL).<sup>5</sup> Furthermore, their data led to the conclusion that glycolaldehyde, next to glyoxal and the Amadori product of lysine and glucose, is one of the most

potent precursors of N<sup>6</sup>-carboxymethyl lysine, the quantitatively predominant AGE in vivo.<sup>5</sup> Surprisingly, literature on formation of glycolaldehyde in vivo is scarce. Several studies proposed the formation of glycolaldehyde during TK one-substrate-catalyzed reactions. However, the release of free glycolaldehyde from the enzyme was not detected. This might be explained by the immediate condensation with another glycolaldehyde residue, due to a decrease in the course of cleavage leading to erythrulose.<sup>3,7,8</sup> In addition to the nonenzymatic Maillard induced generation of glycolaldehyde, the myeloperoxidase system is the only known enzymatic source for glycolaldehyde in vivo.<sup>9</sup> Interestingly, Thornalley et al. described the suppression of methylglyoxal, due to a decrease in the triose phosphate pool via activation of the TK catalyzed metabolism.<sup>10</sup> As glycolaldehyde, methylglyoxal represents another potent glycating agent in vivo and is readily formed by the enzymatic and nonenzymatic degradation of triose phosphates.

The aim of the present study was to elucidate the role of free glycolaldehyde during two-substrate-catalyzed TK reactions and the impact on the formation of AGEs. Special emphasis was placed on the analysis of all mechanistic key intermediates leading to stable protein bound endproducts during model incubations with  $\beta$ -hydroxyppyruvate and ribose-5-phosphate. As a result, transketolase A (TKA) from *E. coli* lowered concentrations of Schiff base adducts and thereby suppressed synthesis of downstream modifications as N<sup>6</sup>-carboxymethyl lysine (CML) and 5-(2-imino-5-oxo-1-imidazolidinyl) norvaline (imidazolinone).

Received: July 11, 2017

Revised: August 25, 2017

Accepted: August 29, 2017

Published: September 7, 2017

## MATERIALS AND METHODS

**Chemicals.** All chemicals of the highest quality available were provided by Sigma-Aldrich (Munich/Steinheim, Germany), Fluka (Taufkirchen, Germany), Merck (Darmstadt, Germany), Roth (Karlsruhe, Germany), and Sigma (Taufkirchen, Germany), unless otherwise indicated.

HEL, CML, and imidazolinone were synthesized according to literature.<sup>5,11</sup>

**2-(Naphthalene-1-ylamino)-ethanol (GA-N).** GA-N was synthesized according to ref 18. In the first step, 1.65 mmol of glycolaldehyde was dissolved in 5 mL of water. An equimolar mixture of 1-naphthylamine in 5 mL of 15% acetic acid and dimethyl sulfoxide (50:50, v/v) and a solution of 3 mmol sodium cyanoborohydride in 5 mL of water were added and stirred at 40 °C overnight. The solution was extracted with hexane (50 mL), and the organic phase was concentrated under vacuum. Purification was carried out by column chromatography (silica gel 60, hexane-acetone 7:3). The combined fractions containing GA-N (TLC (silica gel):  $R_f$  0.35, hexane/acetone (7:3), UV detection) were concentrated under vacuum to obtain the compound as a brownish oil (0.86 mmol, 52%), which was identified by comparison of its <sup>1</sup>H and <sup>13</sup>C NMR spectra reported in literature.<sup>12</sup> HR-MS:  $m/z$  188.1070 (found);  $m/z$  188.1070 (calculated for C<sub>12</sub>H<sub>12</sub>NO [M + H]<sup>+</sup>).

**Sedoheptulose-7-phosphate.** Sedoheptulose-7-phosphate was synthesized with TKA *E. coli* according to literature. Synthesis was confirmed by comparison of its <sup>1</sup>H and <sup>13</sup>C NMR spectra to published data.<sup>13</sup> HR-MS:  $m/z$  289.0333 (found);  $m/z$  289.0330 (calculated for C<sub>7</sub>H<sub>14</sub>O<sub>10</sub>P [M - H]<sup>-</sup>). Purity was determined after derivatization by reductive amination as described below.

**Protein Expression and Purification.** The plasmid pGSJ427 carrying the gene for transketolase A from *E. coli* and His6-tag was kindly made available by Dr. Ralph Golbik (University of Halle, Germany). Expression and purification was carried out according to a modified method as described in the literature.<sup>14,15</sup> Transformation of the plasmid into *E. coli* Rosetta(DE3) (Novagen) strains was performed by electroporation. The transformed cells were incubated overnight on LB plates containing ampicillin 100 µg/mL and chloramphenicol 35 µg/mL at 37 °C. A single colony was inoculated into 300 mL of LB medium (100 µg/mL ampicillin, 35 µg/mL chloramphenicol) and grown overnight. The culture was then transferred to 4 L of fermentation medium (LB medium, 20 g glucose, 2.7 g MgSO<sub>4</sub>, 70 µM thiamine diphosphate (ThDP), 100 µg/mL ampicillin, 35 µg/mL chloramphenicol) at 37 °C. At an OD<sub>600</sub> of 5, cells were harvested by centrifugation (10 000g, 15 min, 4 °C).

For protein purification, 15 g of cells was suspended in lysis buffer (50 mM NaH<sub>2</sub>PO<sub>4</sub>, pH 8.0, 300 mM NaCl, 1 mM MgCl<sub>2</sub>, 10 mM imidazole), and lysozyme (1 mg/mL) was added on ice. After 30 min, cells were disrupted using a sonifier. Cell debris was pelleted by ultracentrifugation at 10 000g for 20 min. The supernatant was applied to a Ni<sup>2+</sup> NTA (Qiagen) column in a batch process and washed four times with lysis buffer and equilibration buffer (50 mM NaH<sub>2</sub>PO<sub>4</sub>, pH 8.0, 300 mM NaCl, 1 mM MgCl<sub>2</sub>, 20 mM imidazole), respectively. TKA was eluted stepwise with increasing concentrations of 125 mM imidazole and 250 mM imidazole. Fractions containing TKA were pooled, rebuffed to 20 mM glycyl-glycine with 1 mM dithiothreitol, and concentrated to 1.65 mg/mL by ultrafiltration using micro-concentrators (Vivaspin MWCO 30000, 4000 rpm, 4 °C) for storage.

Purity of isolated TKA was verified by SDS-Page, and protein concentration was determined spectrophotometrically at 280 nm.

**Transketolase Activity Assay.** TKA activity was measured spectrophotometrically according to a modified method of Hequet et al.<sup>16</sup> The reaction mixture (200 µL) contained 50 mM HEPES buffer (pH = 7.4), 10 mM ribose-5-phosphate, 10 mM L-erythrulose, 3 mM MgCl<sub>2</sub>, 2 mM thiamine diphosphate, 7.5 mM NAD<sup>+</sup>, and aldehyde dehydrogenase from *S. cerevisiae* (0.5 U) as auxiliary enzyme. The reaction was initiated by addition of TKA. The reduction of NAD<sup>+</sup> was monitored in a 96-well plate at 340 nm on a Tecan Infinite M200 plate reader at 25 °C. (Tecan, Groedich, AUT)

**Inactivation of Transketolase.** TKA was inactivated at 80 °C for 0.5, 1, and 2 h. No activity was observed by above assay after 0.5 h.

**Model Incubations.** Incubations were conducted in HEPES buffer at pH 7.4 and 25 °C. Ribose-5-phosphate and β-hydroxypruvate were incubated with TKA (0.06 mg/mL) and BSA (1 mg/mL) with and without addition of glycolaldehyde (1 mM). Blank values were obtained with inactivated TKA. The reaction mixture had the following composition: 25 mM HEPES, 10 mM ribose-5-phosphate, 10 mM β-hydroxypruvate, 3 mM MgCl<sub>2</sub>, and 2 mM thiamine diphosphate. Prior to incubations, TKA was rebuffed to 20 mM HEPES. The reaction was initiated by the addition of TKA. Solutions were degassed with helium and deaerated with argon before incubation.

**Analytical GC-FID.** Analysis of trimethylsilyl derivatives of ribose-5-phosphate, sedoheptulose-7-phosphate, and erythrulose was carried out adopting the method of Smuda et al.<sup>17</sup> To 100 µL aliquots of the samples, 100 µL of D-sorbit (1 mM) was added and centrifuged with MWCO 3000 at 5000 rpm, 4 °C. Samples were dried in vacuo, residues were dissolved in anhydrous pyridine (100 µL), and *N,O*-bis(trimethylsilyl)-acetamide with 5% trimethylchlorosilane (100 µL) was added. Samples were sonified for 30 min and kept at room temperature for 3 h prior to injection into the GC-FID system. Samples were analyzed on a HP 6890N chromatograph (Agilent Technologies, Palo Alto, CA) equipped with a flame ionization detector. The column was a HP-5 (30 m × 0.32 mm, film thickness 0.25 µm; Agilent Technologies, Palo Alto, CA); injector, 250 °C; split ratio, 1:10; detector, 270 °C. Helium 4.6 was used as carrier gas in constant flow mode (linear velocity 31 cm/s, flow 1.6 mL/min). The oven temperature program was as follows: 100 °C, 5 °C/min to 200 °C, 10 °C/min to 270 °C (held 10 min). Limit of detection and limit of quantitation (LOD/LOQ) and retention times were as follows: erythrulose (0.13/0.4 mol % ribose-5-phosphate)  $t_R$  = 9.72 min, sorbit  $t_R$  = 19.35 min, ribose-5-phosphate (0.2/0.6 mol %)  $t_R$  = 22.10 and 22.27 min and sedoheptulose-7-phosphate (0.5/1.7 mol %)  $t_R$  = 25.74, 22.85, and 22.94 min. Quantitation was carried out by comparison of peak areas obtained with those of standard solutions containing known amounts of the pure authentic reference compounds. Signals of target compounds were standardized using the signal of silylated sorbit.

**Analytical HPLC-FLD.** Determination of glycolaldehyde was carried out following a modified method of Rakete and Glomb.<sup>18,19</sup> To 50 µL of the samples, a solution of 25 µL of 0.4 M 1-naphthylamine (DMSO/15% acetic acid, 1:1, v/v) and 25 µL of 4 M sodium cyanoborohydride (DMSO/water, 1:1, v/v) were added and reincubated for 24 h. The derivatized samples were diluted with eluent B to concentrations appropriate for detection. Eluents were demineralized water (A) and a mixture of methanol and demineralized water (7:3, v/v; B). 0.6 mL/L Heptafluorobutyric acid (HFBA) was added to both eluents as ion pair reagent. Chromatographic separations were performed on a stainless steel column (KNAUER, Eurospher 100-5 C18, 250 × 4.6 mm, 5 µm, Berlin, Germany) using a flow rate of 1 mL min<sup>-1</sup> and a column temperature of 25 °C. Samples were injected (25 µL) at 40% B; the gradient was then changed to 100% B within 15 min and held for 10 min. Then gradient was changed to 40% B within 5 min, held 10 min. Glycolaldehyde naphthylamine derivative was detected at the retention time of  $t_R$  = 12.9 min with a LOD/LOQ of 0.006/0.02 mol % (ribose-5-phosphate). Quantitation was performed using the standard addition method with the pure authentic reference compound.

**Analytical HPLC-MS<sup>2</sup>.** A Jasco PU-2080 Plus quaternary gradient pump with degasser and a Jasco AS-2057 Plus autosampler (Jasco, Gross-Umstadt, Germany) were used. The mass analyses were performed using an Applied Biosystems API 4000 quadrupole instrument (Applied Biosystems, Foster City, CA, U.S.A.) equipped with an API source using an electrospray ionization (ESI) interface. The LC system was connected directly to the probe of the mass spectrometer. Nitrogen was used as sheath and auxiliary gas. To measure the analytes, the scheduled multiple-reaction monitoring (sMRM) mode of HPLC-MS<sup>2</sup> was used. Quantitation was based on the standard addition method using known amounts of the pure authentic reference compounds.

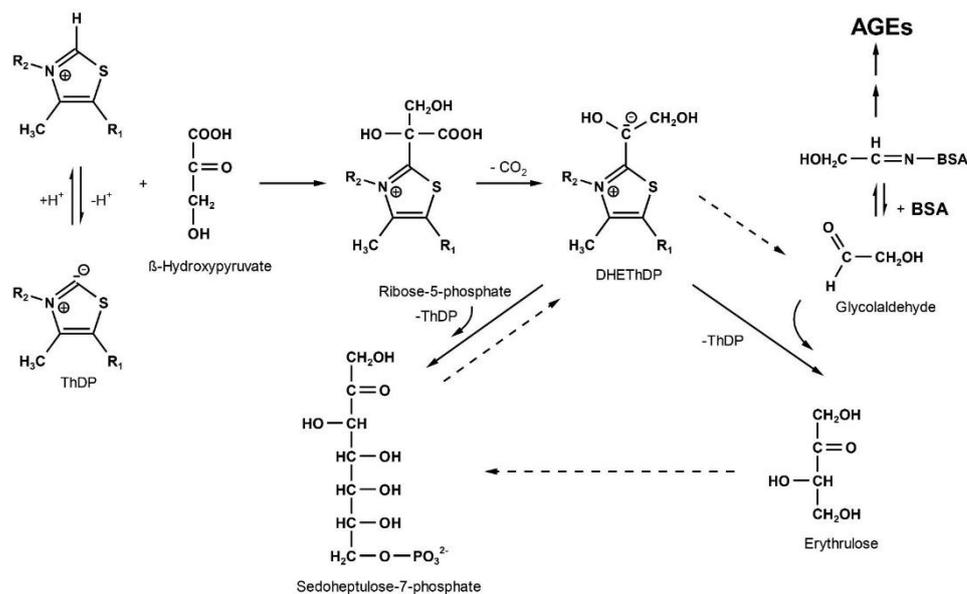


**Figure 1.** Transketolase-catalyzed metabolism of glycolaldehyde which reacts with BSA to form AGEs or alternatively serves as an acceptor aldose to give erythrose. Dashed arrows indicate alternative side-pathways.

**Glyoxal.** Sample aliquots were taken, and trichloroacetic acid was added to a final concentration of 12.5%. *o*-Phenylenediamine (3 mM) in 0.05 N HCl was added and reincubated for 5 h at 25 °C in the dark. The derivatized samples were diluted with water to concentrations appropriate for detection. The mobile phase used consisted of methanol/water (7:3 (v/v)), with 0.6 mL/L HFBA. Chromatographic parameters and optimized parameters for mass spectrometry were according to literature.<sup>20</sup>

**AGEs.** Acidic hydrolysis after reduction with NaBH<sub>4</sub> was carried out as described in literature.<sup>5</sup> Chromatographic separations were performed on a stainless steel column (VYDAC 218TP54, 250 × 4.6 mm, RP18, 5 μm, Hesperia, U.S.A.) using a flow rate of 1 mL min<sup>-1</sup> and a column temperature of 25 °C. Aliquots of the samples were diluted with water and injected (15 μL) at 2% B and run isocratic for 15 min; the gradient was changed to 100% B within 15 min (held for 10 min). Then the gradient was changed to 2% B within 5 min (held 15 min). Eluents were demineralized water (A) and a mixture of methanol and demineralized water (7:3, v/v; B), with 1.2 mL/L HFBA. For mass spectrometric detection, the sMRM mode was used, optimized MS parameters were as follows: HEL (*m/z* 191.2/84.0 (DP 42 V, CE 28.0 eV, CXP 6.0 V, quantifier), *m/z* 191.2/130.2 (DP 42 V, CE 18.0 eV, CXP 23.0 V, qualifier), *m/z* 191.2/56.2 (DP 42 V, CE 56.0 eV, CXP 4.0 V, qualifier), imidazolinone (*m/z* 215.1/100.1 (DP 48 V, CE 20.0 eV, CXP 8.0 V, quantifier), *m/z* 215.1/70.1 (DP 48 V, CE 38.0 eV, CXP 11.3 V, qualifier), *m/z* 215.1/116.2 (DP 48 V, CE 20.0 eV, CXP 9.0 V, qualifier) and CML.<sup>21</sup> Retention times were as follows: CML *t<sub>R</sub>* = 6.2 min, HEL *t<sub>R</sub>* = 10.0 min, and imidazolinone *t<sub>R</sub>* = 13.8 min.

**Ninhydrin Assay.** After complete workup, the content of amino acid modification was standardized to L-leucine according to a modified method of Smuda et al.<sup>21</sup> A calibration of L-leucine, concentrated between 0.5 and 10 nmol, was performed and referenced to the diluted samples. Each sample was prepared in duplicate.

**High-Resolution Mass Determination (HR-MS).** Positive- and negative-ion high-resolution ESI mass spectra were obtained from an Orbitrap Elite mass spectrometer (ThermoFisher Scientific, Bremen, DEU) equipped with an HESI electrospray ion source (spray voltage 4 kV; capillary temperature 275 °C, source heater temperature 40 °C; FTMS resolution > 30,000). Nitrogen was used as sheath and auxiliary

gas. The sample solutions were introduced continuously via a 500 μL Hamilton syringe pump with a flow rate of 5 μL min<sup>-1</sup>. The data were evaluated by the Xcalibur software 2.7 SP1.

**Nuclear Magnetic Resonance Spectroscopy (NMR).** NMR spectra were recorded on a Varian VXR 400 spectrometer operating at 400 MHz for <sup>1</sup>H and 100 MHz for <sup>13</sup>C or on a Varian Unity Inova 500 instrument operating at 500 MHz for <sup>1</sup>H and 125 MHz for <sup>13</sup>C, respectively. SiMe<sub>4</sub> was used as a reference for calibrating the chemical shift.

**Statistical Analysis.** Analyses were performed in triplicate for each model system and resulted in coefficients of variation less than 5% for sugar and sugar phosphate concentrations and less than 10% for AGE concentrations. All significance tests were performed by two-sample *t*-Test or WELCH-Test with a probability value of 95%. Limit of detection (LOD) and limit of quantitation (LOQ) were estimated according to DIN 32645.

## RESULTS AND DISCUSSION

**Characterization of Transketolase A (TKA) and Model Incubations.** Approximately 1.7 mg of TKA per g of wet cells was isolated with a specific activity of 0.2 U/mg. The comparatively low activity of TKA is most likely due to the use of a phosphate buffer during purification and an adopted assay, as described in Materials and Methods. Complete characterization and kinetic studies for TKA from *E. coli* were performed previously by Sprenger et al.<sup>22</sup>

To investigate the influence of TKA on the formation of AGEs, equimolar amounts of β-hydroxy pyruvate and ribose-5-phosphate with and without addition of 10 mol % glycolaldehyde were incubated in the presence of bovine serum albumin (BSA). As shown in Figure 1, the ThDP-mediated initial cleavage of β-hydroxy pyruvate results in the formation of CO<sub>2</sub> and dihydroxyethyl-thiamine diphosphate (DHETHDP), the carbanion-enamine intermediate. The ThDP bound glycolaldehyde unit is then transferred to ribose-5-phosphate forming sedoheptulose-7-phosphate as the major product. Addition of glycolaldehyde to the incubation mixture

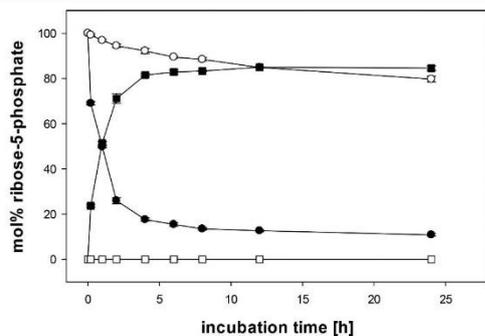
**Table 1.** Mean Concentration (mol %  $\pm$  Standard Deviation, Ribose-5-phosphate) of Sugar Phosphates, Sugars, and Glyoxal in the Presence of BSA and Transketolase A (TKA) or Inactivated Transketolase A (ITKA) at 8 h of Incubation Time, with and without Addition of 10 mol % Glycolaldehyde (GA)

	TKA without GA	ITKA without GA	TKA with GA	ITKA with GA
sedoheptulose-7-phosphate	87.3 $\pm$ 1.6	<LOD <sup>a</sup>	82.0 $\pm$ 1.9 <sup>c</sup>	<LOD
ribose-5-phosphate	11.5 $\pm$ 0.6	89.2 $\pm$ 0.7	13.5 $\pm$ 0.5 <sup>c</sup>	88.5 $\pm$ 0.8
glycolaldehyde	0.108 $\pm$ 0.006	0.536 $\pm$ 0.009	1.23 $\pm$ 0.03 <sup>d</sup>	3.7 $\pm$ 0.1 <sup>d</sup>
glyoxal	0.18 $\pm$ 0.02	0.31 $\pm$ 0.02	0.34 $\pm$ 0.02 <sup>c</sup>	1.17 $\pm$ 0.03 <sup>d</sup>
erythrose	0.58 $\pm$ 0.05	<LOQ <sup>b</sup>	5.3 $\pm$ 0.3 <sup>c</sup>	<LOQ

<sup>a</sup>LOD: limit of detection. <sup>b</sup>LOQ: limit of quantitation. <sup>c</sup>Significant difference compared to incubations without GA by *t*-Test ( $\alpha = 0.05$ ). <sup>d</sup>Significant difference compared to incubations without GA by WELCH-Test ( $\alpha = 0.05$ ).

can either result (I) in the spontaneous formation of Schiff base adducts with the amine moieties of BSA or (II) in the formation of erythrose by enzymatic condensation.  $\beta$ -Hydroxy-pyruvate is of advantage as a donor substrate in this model setup, as it renders the reaction irreversible. However, it is also prone to spontaneous decomposition reactions leading to glyoxylic acid, glycolaldehyde, and trace amounts of erythrose via nonenzymatic aldol condensation reactions.<sup>23–25</sup> In order to exclude the possibility of a significant impact on the formation of advanced glycation endproducts by Maillard-catalyzed degradation of the initial products or products formed during enzymatic conversion, incubations without addition of glycolaldehyde were carried out. Under our conditions, without addition of glycolaldehyde, only small amounts of free glycolaldehyde were detected (Table 1). Furthermore, incubations in the absence of BSA and TKA revealed formation of just 3 mol % glycolaldehyde after 24 h (data not shown).

**Conversion of Sugar Phosphates, Erythrose, Glycolaldehyde, and Glyoxal.** Figure 2 demonstrates the

**Figure 2.** Conversion of ribose-5-phosphate (●) to sedoheptulose-7-phosphate (■) by transketolase (closed symbols) or inactivated transketolase (open symbols) in the presence of BSA and glycolaldehyde.

irreversible enzymatic conversion of  $\beta$ -hydroxy-pyruvate and ribose-5-phosphate to sedoheptulose-7-phosphate. The level of sedoheptulose-7-phosphate quickly reached 82.0 mol % after 8 h and stayed nearly constant afterward. No formation of sedoheptulose-7-phosphate was observed in the presence of inactivated TKA. The concentrations of sugar phosphates, erythrose, glycolaldehyde, and glyoxal at 8 h of incubation are summarized in Table 1.

Interestingly, given the high-glycating activity of glycolaldehyde, TKs have been shown to be relatively resistant to high glycolaldehyde concentrations and therefore have been used in the production of L-erythrose.<sup>26,27</sup> Glycolaldehyde represents one of the best nonphosphorylated acceptor substrates for TKs from nonmammalian organisms ( $K_M = 14$  mM, glycolaldehyde for TKA).<sup>22</sup> Generally, however, phosphorylated substrates have higher affinities toward TK ( $K_M = 1.4$  mM, ribose-5-phosphate for TKA).<sup>22</sup> Obviously, the addition of glycolaldehyde as a competing acceptor substrate led to decreased formation of sedoheptulose-7-phosphate (82 vs 87 mol %). This was also envisioned by less depletion of ribose-5-phosphate in the presence of glycolaldehyde (13.5 vs 11.5 mol %). As the reaction proceeds, both  $\beta$ -hydroxy-pyruvate ( $K_M = 18$  mM)<sup>22</sup> and sedoheptulose-7-phosphate ( $K_M = 4$  mM)<sup>22</sup> can serve as donor substrates for glycolaldehyde, respectively.

As posted in the literature,<sup>3,7,8</sup> the theoretical cleavage of the carbanion DHETHDP intermediate by protonation might release glycolaldehyde and should entail an immediate conversion to erythrose during one-substrate-catalyzed reactions. However, the release of free glycolaldehyde was not substantiated so far. To further investigate this hypothesis in the present setup, BSA should serve as a trap for glycolaldehyde released from one-substrate reactions, which would result in elevated amounts of protein modifications. However, neither the formation of glycolaldehyde nor HEL significantly increased over time (Tables 1 and 2) in absence of externally added glycolaldehyde. Thus, the rate of formation of DHETHDP is considerably higher than its cleavage rate and due to the very small amounts of the intermediate actually present during the turnover in the presence of an acceptor aldose, cleavage of DHETHDP entailing a possible release of

**Table 2.** Formation of AGEs in mmol/mol L-Leucine (Mean Concentration  $\pm$  Standard Deviation) by Transketolase A (TKA) or Inactivated Transketolase A (ITKA) at 8 h of Incubation Time, with and without addition of 10 mol % Glycolaldehyde (GA)

	TKA without GA	ITKA without GA	TKA with GA	ITKA with GA
HEL	3.4 $\pm$ 0.2	4.1 $\pm$ 0.3 <sup>a</sup>	6.2 $\pm$ 0.2	18 $\pm$ 1 <sup>b</sup>
CML	0.62 $\pm$ 0.05	0.64 $\pm$ 0.03	0.85 $\pm$ 0.02	1.6 $\pm$ 0.1 <sup>b</sup>
imidazolinone	0.034 $\pm$ 0.002	0.033 $\pm$ 0.002	0.049 $\pm$ 0.002	0.09 $\pm$ 0.01 <sup>a</sup>

<sup>a</sup>Significant difference compared to TK by *t*-Test ( $\alpha = 0.05$ ). <sup>b</sup>Significant difference compared to TK by WELCH-Test ( $\alpha = 0.05$ ).

glycolaldehyde must be evaluated to have only a negligible impact, if any on the formation of AGEs *in vivo*.<sup>2,14</sup> Nevertheless, it has to be stated that despite the lack of evidence for the transketolase triggered release of glycolaldehyde, incubations without addition of glycolaldehyde indeed revealed detectable amounts of glycolaldehyde (0.1 mol %, TKA vs 0.5 mol %, inactivated TKA, 8 h). In the absence of transketolase activity, this has to be attributed to the spontaneous and Maillard-induced decomposition of  $\beta$ -hydroxypyruvate and other sugars. On the other hand, the significant decrease in the presence of transketolase was paralleled by an almost quantitative increase of erythrulose (0.6 mol %, 8 h), which again underpins the pronounced acceptor qualities of glycolaldehyde.

Consequently, transketolase led to a substantial formation of erythrulose in the presence of glycolaldehyde with up to 5 mol % after 8 h approaching a steady-state afterward (Figure 3A).

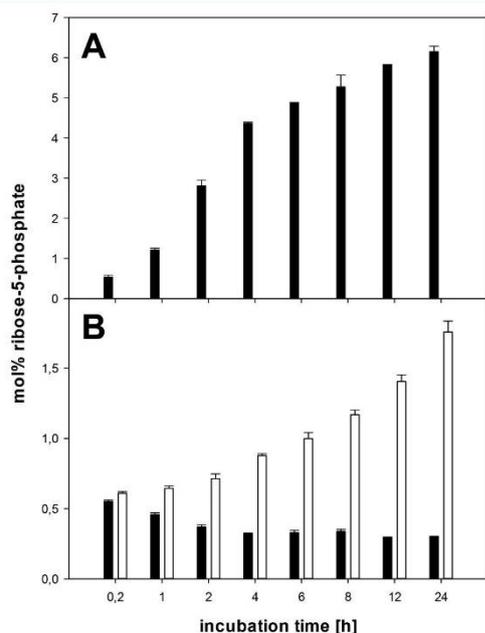


**Figure 3.** Formation of erythrulose (A) and glyoxal (B) in the presence of BSA and glycolaldehyde by transketolase (closed bars) or inactivated transketolase (open bars).

This exactly corresponded to the difference in the amounts of sedoheptulose-7-phosphate formed in presence vs absence of glycolaldehyde, and verifies the competitive character of glycolaldehyde and ribose-5-phosphate as acceptor aldoses leading to erythrulose and sedoheptulose-7-phosphate, respectively. More importantly, it also confirms the conversion of at least 50% glycolaldehyde after 8 h. Incubations with inactivated TKA in the presence of glycolaldehyde showed detectable but not quantifiable amounts of erythrulose, most likely formed via aldol condensation reactions. It has to be mentioned that the overall reaction proceeds much more complex as erythrulose itself represents a substrate of the TK reaction and may also lead to sedoheptulose-7-phosphate as depicted in Figure 1.

Nonenzymatic Maillard processes easily oxidize glycolaldehyde to glyoxal which is of major relevance *in vivo*.<sup>28</sup> Because it

basically leads to the very same AGEs, it was also monitored in the present study (Figure 3B). As expected, formation of glyoxal was up to 4 times higher after addition of glycolaldehyde (0.31 mol %, inactivated TKA vs 1.17 mol %, inactivated TKA). In the presence of active TKA, concentrations were significantly lowered (Table 1). Since glyoxal is not metabolized by TKs, these differences can only be explained by the enzymatic withdrawal of the precursor compound glycolaldehyde from the incubation system.

**Formation of Protein Modifications.** As TKA significantly renders concentrations of glycolaldehyde and other carbonyl compounds, all reactions were performed in the presence of BSA to explore the impact on the formation of Maillard protein modifications. The reaction of glycolaldehyde with the  $\epsilon$ -amino function of protein-bound lysine starts with the formation of the Schiff base adduct followed by rearrangement to the Amadori product.<sup>4,5</sup> Both forms were converted to  $N^{\epsilon}$ -(2-hydroxyethyl) lysine (HEL) by reduction with  $\text{NaBH}_4$  at the time of sampling, prior to acidic hydrolysis. Figure 4A demonstrates that during incubations with inactivated TKA, HEL was formed progressively until a plateau was reached at about 12–24 h with 21 mmol/mol L-leucine. On

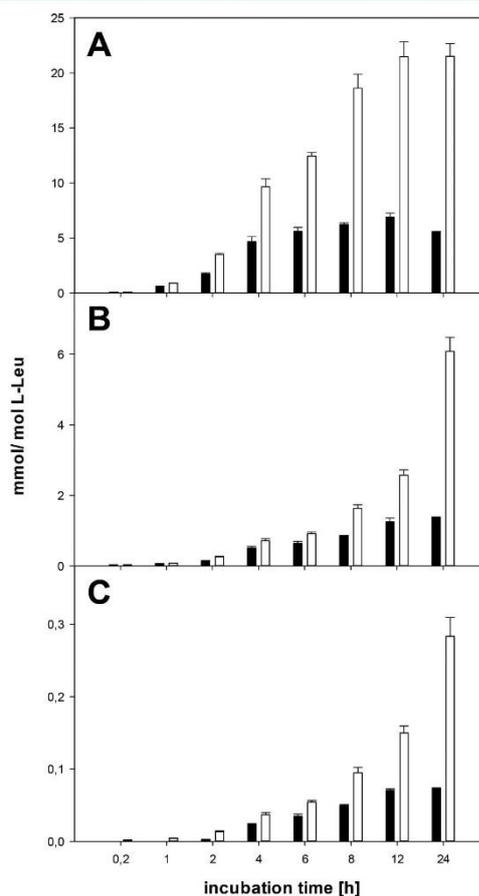


**Figure 4.** Formation of protein bound HEL (A), CML (B), and imidazolinone (C) in the presence of BSA and glycolaldehyde by transketolase (closed bars) or inactivated transketolase (open bars).

the other hand, the presence of TKA significantly hampered formation of HEL with maximum concentrations at 12 h with 7 mmol/mol L-leucine followed by degradation. Strikingly, the differences correlated with the enzymatic conversion of glycolaldehyde to the overall more-stable erythrulose. As already discussed above, the significant difference of HEL (3.4 mmol/mol L-leucine TKA vs 4.1 mmol/mol L-leucine, inactivated TKA) in incubations without addition of glycolaldehyde (Table 2) must be attributed to the nonenzymatic degradation of  $\beta$ -hydroxyppyruvate and other sugars to give glycolaldehyde followed by the enzyme-catalyzed formation of erythrulose. Nevertheless, the time course for HEL in Figure 4A highlights the glycolaldehyde-Schiff base adduct as an important transient intermediate of this Maillard reaction cascade with high reactivity.

After Amadori rearrangement to the aldoamine, oxidation, hydration, and isomerization results in the quantitatively most relevant formation of the stable advanced Maillard protein modification  $N^6$ -carboxymethyl lysine (CML) (Figure 4B). In incubations with inactivated TKA, levels of CML accumulated over time, which supports the mechanism and also nicely correlated to the accumulation of glyoxal (Figure 3B). In the presence of TKA, the formation was almost stalled leading to a 4:1 ratio ( $6.0 \pm 0.4$  mmol/mol L-leucine, inactivated TKA, vs  $1.37 \pm 0.02$  mmol/mol L-leucine, TKA) after 24 h. Contrary to the formation of HEL in incubations without addition of glycolaldehyde, levels of CML were almost identical whether with TKA or with inactivated TKA after 8 h (Table 2). These findings must be explained with the mechanistically more delayed formation of the stable endproduct.

As described by Glomb and Lang,<sup>11</sup> 5-(2-imino-5-oxo-1-imidazolidinyl) norvaline (imidazolinone) is a major arginine modification, arising from the acid-catalyzed conversion of  $N^7$ -carboxymethylarginine (CMA) and 5-(4,5-dihydroxy-2-imino-1-imidazolidinyl) norvaline (dihydroxyimidazolidine). It is important to understand that in contrast to HEL and CML, these three structures are formed exclusively from glyoxal. Figure 4C clearly depicts a comparable behavior of imidazolinone as for CML, with a nearly identical suppression of 50% after 8 h (Table 2). Arginine immediately traps glyoxal to give the dihydroxyimidazolidine, which is slowly converted to CMA. Thus, the considerably lower levels of imidazolinone compared to CML are expected given the lower concentrations of glyoxal (10–50 times less) formed by oxidation in the model setup.<sup>4,29,30</sup> As expected, no difference was observed during incubation without addition of glycolaldehyde.

In summary, on the basis of model systems we were able to identify significant changes in the formation of AGEs by the TK-catalyzed conversion of glycolaldehyde to erythrulose. The lowered formation of HEL and CML resulted unequivocally from the enzymatic conversion of glycolaldehyde. Less glycolaldehyde also led to decreased formation of glyoxal entailing suppressed formation of glyoxal specific AGEs as imidazolinone. Therefore, transketolase-catalyzed reactions contribute considerably to the degradation of Maillard reactive aldehydes, like glycolaldehyde, and thus can prevent the formation of advanced glycation endproducts. Further studies will now show if the results can be transferred to other TKs of mammalian organisms and to the situation in vivo.

## AUTHOR INFORMATION

### Corresponding Author

\*E-mail: marcus.glomb@chemie.uni-halle.de. Fax: ++049-345-5527341).

### ORCID

Alexander Klaus: 0000-0001-9289-5742

### Notes

The authors declare no competing financial interest.

## ACKNOWLEDGMENTS

We thank Prof. Dr. G. Sprenger (University of Stuttgart, Germany) and Dr. R. Golbik from the Institute for Biochemistry and Biotechnology/Microbial Biotechnology for providing the plasmid pGSJ427 encoding TKA. We would also like to thank Dr. D. Ströhl from the Institute of Organic Chemistry, Halle, Germany, for recording NMR spectra and Dr. A. Frolov from the Leibniz Institute of Plant Biochemistry, Halle, Germany, for performing accurate mass determination. Funding was supported by the Deutsche Forschungsgemeinschaft (DFG, Germany) Research Training Group 2155, ProMoAge.

## ABBREVIATIONS USED

AGEs, advanced glycation endproducts; BSA, bovine serum albumin; CMA,  $N^7$ -carboxymethylarginine; CML,  $N^6$ -carboxymethyl lysine; DHEThDP, dihydroxyethyl-thiamine diphosphate; dihydroxyimidazolidine, 5-(4,5-dihydroxy-2-imino-1-imidazolidinyl) norvaline; GA-N, 2-(naphthalene-1-ylamino)-ethanol; HEL,  $N^6$ -(2-hydroxyethyl) lysine; HFBA, heptafluorobutyric acid; imidazolinone, 5-(2-imino-5-oxo-1-imidazolidinyl) norvaline; ThDP, thiamine diphosphate; TK, transketolase; TKA, transketolase A

## REFERENCES

- (1) Schenk, G.; Duggleby, R. G.; Nixon, P. F. Properties and functions of the thiamin diphosphate dependent enzyme transketolase. *Int. J. Biochem. Cell Biol.* **1998**, *30*, 1297–1318.
- (2) Kochetov, G. A.; Solovjeva, O. N. Structure and functioning mechanism of transketolase. *Biochim. Biophys. Acta, Proteins Proteomics* **2014**, *1844*, 1608–1618.
- (3) Bykova, I. A.; Solovjeva, O. N.; Meshalkina, L. E.; Kovina, M. V.; Kochetov, G. A. One-Substrate Transketolase-Catalyzed Reaction. *Biochem. Biophys. Res. Commun.* **2001**, *280*, 845–847.
- (4) Acharya, A. S.; Manning, J. M. Reaction of glycolaldehyde with proteins: Latent crosslinking potential of  $\alpha$ -hydroxyaldehydes. *Proc. Natl. Acad. Sci. U. S. A.* **1983**, *80*, 3590–3594.
- (5) Glomb, M. A.; Monnier, V. M. Mechanism of Protein Modification by Glyoxal and Glycolaldehyde, Reactive Intermediates of the Maillard Reaction. *J. Biol. Chem.* **1995**, *270*, 10017–10026.
- (6) Henning, C.; Glomb, M. A. Pathways of the Maillard reaction under physiological conditions. *Glycoconjugate J.* **2016**, *33*, 499–512.
- (7) Fiedler, E.; Golbik, R.; Schneider, G.; Tittmann, K.; Neef, H.; König, S.; Hubner, G. Examination of Donor Substrate Conversion in Yeast Transketolase. *J. Biol. Chem.* **2001**, *276*, 16051–16058.
- (8) Solov'eva, O. N.; Bykova, I. A.; Meshalkina, L. E.; Kovina, M. V.; Kochetov, G. A. Cleaving of Ketosubstrates by Transketolase and the Nature of the Products Formed. *Biochemistry (Moscow)* **2001**, *66*, 932–936.
- (9) Anderson, M. M.; Requena, J. R.; Crowley, J. R.; Thorpe, S. R.; Heinecke, J. W. The myeloperoxidase system of human phagocytes generates N-(carboxymethyl)lysine on proteins. a mechanism for producing advanced glycation end products at sites of inflammation. *J. Clin. Invest.* **1999**, *104*, 103–113.

- (10) Thornalley, P. J.; Jahan, I.; Ng, R. Suppression of the Accumulation of Triosephosphates and Increased Formation of Methylglyoxal in Human Red Blood Cells during Hyperglycaemia by Thiamine In Vitro. *J. Biochem.* **2001**, *129*, 543–549.
- (11) Glomb, M. A.; Lang, G. Isolation and Characterization of Glyoxal–Arginine Modifications. *J. Agric. Food Chem.* **2001**, *49*, 1493–1501.
- (12) Guo, H.; Zhuang, Y.; Cao, J.; Zhang, G. Green and Efficient Protocol for the Synthesis of N-(2-Hydroxyethyl)anilines by the Alkylation Reaction in Ionic Liquid. *Synth. Commun.* **2014**, *44*, 3368–3374.
- (13) Charmantray, F.; Hélaine, V.; Legeret, B.; Hecquet, L. Preparative scale enzymatic synthesis of D-sedoheptulose-7-phosphate from  $\beta$ -hydroxypruvate and D-ribose-5-phosphate. *J. Mol. Catal. B: Enzym.* **2009**, *57*, 6–9.
- (14) Asztalos, P.; Parthier, C.; Golbik, R.; Kleinschmidt, M.; Hubner, G.; Weiss, M. S.; Friedemann, R.; Wille, G.; Tittmann, K. Strain and near attack conformers in enzymic thiamin catalysis: X-ray crystallographic snapshots of bacterial transketolase in covalent complex with donor ketoses xylulose 5-phosphate and fructose 6-phosphate, and in noncovalent complex with acceptor aldose ribose 5-phosphate. *Biochemistry* **2007**, *46*, 12037–12052.
- (15) Mitschke, L.; Parthier, C.; Schröder-Tittmann, K.; Coy, J.; Lüdtke, S.; Tittmann, K. The crystal structure of human transketolase and new insights into its mode of action. *J. Biol. Chem.* **2010**, *285*, 31559–31570.
- (16) Hecquet, L.; Bolte, J.; Demuyne, C. New Assays for Transketolase. *Biosci., Biotechnol., Biochem.* **1993**, *57*, 2174–2176.
- (17) Smuda, M.; Voigt, M.; Glomb, M. A. Degradation of 1-deoxy-D-erythro-hexo-2,3-diulose in the presence of lysine leads to formation of carboxylic acid amides. *J. Agric. Food Chem.* **2010**, *58*, 6458–6464.
- (18) Rakete, S.; Klaus, A.; Glomb, M. A. Investigations on the Maillard reaction of dextrans during aging of Pilsner type beer. *J. Agric. Food Chem.* **2014**, *62*, 9876–9884.
- (19) Rakete, S.; Glomb, M. A. A Novel Approach for the Quantitation of Carbohydrates in Mash, Wort, and Beer with RP-HPLC Using 1-Naphthylamine for Precolumn Derivatization. *J. Agric. Food Chem.* **2013**, *61*, 3828–3833.
- (20) Spanneberg, R.; Salzwedel, G.; Glomb, M. A. Formation of Early and Advanced Maillard Reaction Products Correlates to the Ripening of Cheese. *J. Agric. Food Chem.* **2012**, *60*, 600–607.
- (21) Smuda, M.; Henning, C.; Raghavan, C. T.; Johar, K.; Vasavada, A. R.; Nagaraj, R. H.; Glomb, M. A. Comprehensive Analysis of Maillard Protein Modifications in Human Lenses: Effect of Age and Cataract. *Biochemistry* **2015**, *54*, 2500–2507.
- (22) Sprenger, G. A.; Schorken, U.; Sprenger, G.; Sahn, H. Transketolase A of Escherichia coli K12 Purification and properties of the enzyme from recombinant strains. *Eur. J. Biochem.* **1995**, *230*, 525–535.
- (23) Lorillière, M.; De Sousa, M.; Bruna, F.; Heuson, E.; Gefflaut, T.; de Berardinis, V.; Saravanan, T.; Yi, D.; Fessner, W.-D.; Charmantray, F.; Hecquet, L. One-pot, two-step cascade synthesis of naturally rare L-erythro (3S,4S) ketoses by coupling a thermostable transaminase and transketolase. *Green Chem.* **2017**, *19*, 425–435.
- (24) Dickens, F.; Williamson, D. H. The Preparation and Properties of Lithium Hydroxypruvate and Hydroxypruvic Acid. *Biochem. J.* **1958**, *68*, 74–81.
- (25) Kobori, Y.; Myles, D. C.; Whitesides, G. M. Substrate Specificity and Carbohydrate Synthesis Using Transketolase. *J. Org. Chem.* **1992**, *57*, 5899–5907.
- (26) Mitra, R. K.; Woodley, J. M.; Lilly, M. D. Escherichia coli transketolase-catalyzed carbon-carbon bond formation: biotransformation characterization for reactor evaluation and selection. *Enzyme Microb. Technol.* **1998**, *22*, 64–70.
- (27) Gyamerah, M.; Willetts, A. J. Kinetics of overexpressed transketolase from Escherichia coli JM 107/pQR 700. *Enzyme Microb. Technol.* **1997**, *20*, 127–134.
- (28) Henning, C.; Liehr, K.; Girndt, M.; Ulrich, C.; Glomb, M. A. Extending the spectrum of alpha-dicarbonyl compounds in vivo. *J. Biol. Chem.* **2014**, *289*, 28676–28688.
- (29) Spanneberg, R.; Osswald, F.; Kolesov, I.; Anton, W.; Radusch, H.-J.; Glomb, M. A. Model studies on chemical and textural modifications in gelatin films by reaction with glyoxal and glycolaldehyde. *J. Agric. Food Chem.* **2010**, *58*, 3580–3585.
- (30) Schwarzenbolz, U.; Henle, T.; Haeßner, R.; Klostermeyer, H. On the reaction of glyoxal with proteins. *Z. Lebensm.-Unters.-Forsch. A* **1997**, *205*, 121–124.

Reprinted with permission from Klaus, A., Pffirmann, T., Glomb, M. A. Transketolase A From *E. Coli* Significantly Suppresses Protein Glycation By Glycolaldehyde And Glyoxal *in Vitro*. *Journal of Agricultural and Food Chemistry* **2017**, *65*, 8196-8202. Copyright 2017 American Chemical Society.

## 10.2 Journal of Agricultural and Food Chemistry, 2018, 66, 1498-1508

JOURNAL OF  
**AGRICULTURAL AND  
 FOOD CHEMISTRY**

Cite This: *J. Agric. Food Chem.* 2018, 66, 1498–1508

Article  
 pubs.acs.org/JAFC

## Influence of Transketolase-Catalyzed Reactions on the Formation of Glycolaldehyde and Glyoxal Specific Posttranslational Modifications under Physiological Conditions

Alexander Klaus,<sup>†</sup> Tim Baldensperger,<sup>†</sup> Roman Fiedler,<sup>‡</sup> Matthias Girndt,<sup>‡</sup> and Marcus A. Glomb<sup>\*,†</sup>

<sup>†</sup>Institute of Chemistry, Food Chemistry, Martin-Luther-University Halle-Wittenberg, Kurt-Mothes-Strasse 2, 06120 Halle/Saale, Germany

<sup>‡</sup>Department of Internal Medicine II, Martin-Luther-University Halle-Wittenberg, Ernst-Grube-Strasse 40, 06120 Halle/Saale, Germany

**S** Supporting Information

**ABSTRACT:** In the present study, we investigated the role of transketolase (TK) in the modulation of glycolaldehyde driven Maillard reactions. *In vitro* experiments with recombinant human TK reduced glycolaldehyde and glyoxal induced carbonyl stress and thereby suppressed the formation of advanced glycation endproducts up to 70% due to the enzyme-catalyzed conversion of glycolaldehyde to erythrose. This was further substantiated by the use of <sup>13</sup>C-labeled compounds. For the first time, glycolaldehyde and other sugars involved in the TK reaction were quantified *in vivo* and compared to nondiabetic uremic patients undergoing hemodialysis. Quantitation revealed amounts of glycolaldehyde up to 2 μM and highlighted its crucial role in the formation of AGEs *in vivo*. In this context, a LC–MS<sup>2</sup> method for the comprehensive detection of sedoheptulose-7-phosphate, fructose-6-phosphate, ribose-5-phosphate, erythrose-4-phosphate, erythrose, and glycolaldehyde in whole blood, plasma, and red blood cells was established and validated based on derivatization with 1-naphthylamine and sodium cyanoborohydride.

**KEYWORDS:** human transketolase, glycolaldehyde, glyoxal, sugar phosphates, Maillard reaction, advanced glycation endproducts

### ■ INTRODUCTION

Advanced glycation end products (AGEs) are a class of covalently modified amino acids that are formed oxidatively and nonoxidatively within the nonenzymatic pathways of Maillard reactions, also referred to as glycation. *In vivo*, the endogenous accumulation of AGEs is promoted by oxidative and carbonyl stress leading to altered structures and functions of proteins and therefore represents an important marker for tissue damage in aging and chronic diseases, including diabetes and uremia.<sup>1,2</sup>

Research on mechanistic pathways involving glycation has largely focused on the formation and reaction of short-chained aldehyde precursors like glycolaldehyde, glyoxal, and methylglyoxal.<sup>3–5</sup> In addition to their generation from Maillard induced fragmentation of longer-chained sugars, the peroxidation of lipids is considered as a major alternative source.<sup>6</sup> However, the formation of reactive carbonyls and their follow-up products is also influenced by a variety of enzymatic reactions, which regulate the metabolic flux and the redox state *in vivo*, e.g., the polyol pathway and the glyoxalase system. Particularly, a depletion of NADPH interferes with glutathione regeneration inducing oxidative stress.<sup>2,7,8</sup>

Recently, we described the suppression of the glycolaldehyde and glyoxal specific protein modifications *N*<sup>6</sup>-(2-hydroxyethyl) lysine, *N*<sup>6</sup>-carboxymethyl lysine, and 5-(2-imino-5-oxo-1-imidazolidinyl)norvaline by transketolase A from *Escherichia coli*.<sup>9</sup> Transketolase (TK), a thiamine (vitamin B<sub>1</sub>) dependent enzyme, catalyzes the conversion of sugar phosphates and links the pentose phosphate pathway (PPP) to glycolysis. The accumulation of glyceraldehyde-3-phosphate, a main intermediate of both pathways, and its degradation product

methylglyoxal under thiamine deficiency has been discussed as a major source of posttranslational protein modification.<sup>10</sup> On the other hand, studies have shown that an increased TK activity, induced by addition of thiamine or benfotiamine (a lipid-soluble precursor of vitamin B<sub>1</sub>), reduced concentrations of glucose and its metabolites, and was thereby proposed to also suppress accumulation of AGEs in hyperglycemia and uremia. Furthermore, a general activation of the PPP is desirable in the maintenance of antioxidative defense mechanisms by the production of NADPH. A decreased transketolase activity is often associated with multiple biochemical dysfunctions related to microvascular complications in hyperglycemia, e.g., mitochondrial and phagocyte dysfunction.<sup>11–13</sup> However, to our knowledge data on the specific impact of TK or PPP sugar intermediates on formation or profile of AGEs *in vivo* is lacking.

The aim of the present study therefore was to expand our work on TK A from *E. coli* to the situation *in vivo*. As glycolaldehyde was confirmed as a very good nonphosphorylated acceptor substrate, first, model incubations under physiological conditions with recombinant human TK, fructose-6-phosphate, and ribose-5-phosphate in the presence of glycolaldehyde and human serum albumin were carried out. Enzymatic conversion of sugars and protein modification were monitored in detail. As for TK A from *E. coli*, an essential

Received: November 24, 2017

Revised: January 20, 2018

Accepted: January 24, 2018

Published: February 5, 2018

reduction of glycolaldehyde and glyoxal by the human TK reaction was successfully attained, entailing a significant depletion of mechanistically related AGEs. Second, to access the importance of *in vivo* glycolaldehyde, TK activity as well as relevant sugar educts and products of the TK reaction were determined in whole blood, plasma, and red blood cells for the first time. With a novel optimized workup and LC-MS<sup>2</sup> method it was possible to compare healthy to uremic subjects, where renal failure generates an imbalance of the redox state and elevated amounts of reactive carbonyl species.<sup>1</sup>

## MATERIALS AND METHODS

**Chemicals.** Unless otherwise indicated, all chemicals of the highest quality available were provided by Sigma-Aldrich (Munich/Steinheim, Germany) (D-erythrose-4-phosphate, L-erythrulose, 1-<sup>13</sup>C-D-fructose, D-fructose-6-phosphate, glycolaldehyde, 1-naphthylamine, ortho-phenylenediamine, D-ribose-5-phosphate, sodium cyanoborohydride, thiamine diphosphate, and the auxiliary enzymes *sn*-glycero-3-phosphate dehydrogenase (GPH)/triose phosphate isomerase (TPI) from *rabbit muscle*); Sigma (Taufkirchen, Germany); Fluka (Taufkirchen, Germany) (hexokinase from *S. cerevisiae*); Merck (Darmstadt, Germany) (human serum albumin (HSA)); Omicron Biochemicals, Inc. (South Bend, USA) (1-<sup>13</sup>C-glycolaldehyde); Roth (Karlsruhe, Germany); ACROS Organics, (Geel, Belgium); and VWR Chemicals (Darmstadt, Germany).

N<sup>6</sup>-(2-Hydroxyethyl)lysine (HEL),<sup>4</sup> 5-(2-imino-5-oxo-1-imidazolidinyl)norvaline (imidazolinone),<sup>14</sup> N<sup>6</sup>-carboxymethyllysine (CML), 1,3-bis(5-amino-5-carboxypentyl)imidazolium salt (glyoxal-lysine dimer, GOLD),<sup>15</sup> D-sedoheptulose-7-phosphate, and 2-(naphthalene-1-ylamino)ethanol (GA-N)<sup>9</sup> were synthesized as reported previously.

**Synthesis of D-Glyceraldehyde-3-phosphate.** D-Glyceraldehyde-3-phosphate was synthesized with some modifications as described by Li et al.<sup>16</sup> Verification of correct synthesis was carried out by NMR spectroscopy and HR-MS: *m/z* 168.9908 (found); *m/z* 168.9907 (calculated for C<sub>3</sub>H<sub>6</sub>O<sub>6</sub>P [M - H]<sup>-</sup>).

**Synthesis of D-Xylulose-5-phosphate.** D-Xylulose-5-phosphate was synthesized with D-glyceraldehyde-3-phosphate, β-hydroxypropionate, and transketolase A from *E. coli* according to the literature.<sup>9,17</sup> Successful synthesis and purity was verified by <sup>1</sup>H and <sup>13</sup>C NMR spectroscopy,<sup>18</sup> HR-MS (*m/z* 229.0118 (found); *m/z* 229.0119 (calculated for C<sub>5</sub>H<sub>10</sub>O<sub>8</sub>P [M - H]<sup>-</sup>)), and the TK assay described below. The final product still contained 4% of unreacted D-glyceraldehyde-3-phosphate.

**Synthesis of 1-<sup>13</sup>C-D-Fructose-6-phosphate.** 1-<sup>13</sup>C-D-Fructose-6-phosphate was synthesized with 1-<sup>13</sup>C-D-fructose, adenosine 5'-triphosphate, and hexokinase following the method of Irvine et al.<sup>19</sup> Synthesis was verified by comparison of its <sup>1</sup>H and <sup>13</sup>C NMR spectra to the literature.<sup>20</sup> The 1-<sup>13</sup>C-labeled position led to an additional spin-spin coupling of 1Hz and 1Hz in the <sup>1</sup>H NMR spectra, with a coupling constant of <sup>1</sup>J<sub>C-H</sub> = 143.7 Hz. <sup>13</sup>C NMR peaks at position C1 were particularly intense at 62.8 (ppm, 1Cα) and 62.7 (ppm, 1Cβ), respectively. HR-MS: *m/z* 260.0254 (found); *m/z* 260.0247 (calculated for C<sub>5</sub><sup>13</sup>CH<sub>12</sub>O<sub>6</sub>P [M - H]<sup>-</sup>). The compound was referenced to commercially available D-fructose-6-phosphate via GC-FID (*t<sub>R</sub>* = 24.5, 24.6 min), as described previously.<sup>9</sup>

**Blood Samples.** Written informed consent was obtained from all patients. Samples were obtained from 9 healthy subjects and 10 nondiabetic uremic patients undergoing hemodialysis. Time of blood collection was predialysis. Hemodialysis was performed three times weekly for 4–5 h using polyamide dialyzers. All uremic patients were treated with bicarbonate hemodialysis (acid concentrate type 257, 8.4% sodium bicarbonate type 200, MTN Neubrandenburg GmbH, Neubrandenburg, Germany) with ultrapure water quality (by reverse osmosis and sterile filters). 5 mL aliquots of venous blood (EDTA monovette) were taken from each participant and immediately put on ice. Aliquots of whole blood were drawn and stored at -27 °C until further usage. The remaining blood was centrifuged (10 min, 3500

rpm, 4 °C), and plasma aliquots were taken and stored at -27 °C. Red blood cells (RBCs) were collected after removal of plasma and buffy coat via repeated washing with 0.9% saline, and frozen at -27 °C. Samples were hemolyzed by thawing and the addition of two volumes of ultrapure water (SIEMENS Ultra Clear, Munich, Germany) for 10 min in the dark. HbA1c, creatinine, and C-reactive protein were measured by routine methods at the laboratory Reising-Ackermann & Co. (Leipzig, Germany).

**Recombinant Human Transketolase (TK).** The vector pET28a(+) containing the human TK gene and His6-tag was kindly provided by Prof. Dr. Kai Tittmann.<sup>21</sup> Expression and purification was essentially carried out as described previously with minor modifications.<sup>9</sup> In short, transformation into *E. coli* Rosetta (DE3) (Novagen) was performed by electroporation. Cells containing the human TK gene were grown in LB medium (40 μg/mL kanamycin and 35 μg/mL chloramphenicol) at 37 °C. At an OD<sub>600</sub> of 0.8 expression was initiated by the addition of isopropyl-β-D-thiogalactopyranoside (100 μM), followed by incubation overnight at 20 °C. Cells were centrifuged, lysed with lysozyme, and disrupted by sonication. After pelleting of the cell debris, purification was carried out using a Ni<sup>2+</sup> NTA column (Qiagen). Fractions containing human TK were pooled, rebuffed to 50 mM triethanolamine and 1 mM dithiothreitol (pH = 7.4), and concentrated by ultrafiltration (Vivaspin MWCO 30000, 4000 rpm, 4 °C). Purity was checked using SDS-PAGE, and protein concentration was determined spectrophotometrically as described in the literature.<sup>22</sup>

**Transketolase Activity.** The oxidation of NADH was monitored in a 96 well plate at 340 nm with a Tecan Infinite M200 plate reader (Tecan, Groedig, AUT) at 37 °C for blood samples and 25 °C for recombinant human TK.

**Blood Samples.** Determination of TK activity with and without addition of thiamine diphosphate was carried out as described in the literature.<sup>23</sup> In brief, hemolyzed and diluted whole blood and RBC samples were added to a solution containing 14 mM ribose-5-phosphate, 0.2 mM NADH, and 0.1 M TRIS pH = 7.4 with and without addition of 385 μM thiamine diphosphate in a reaction tube (260 μL). The well mixed sample was preincubated at 37 °C for 30 min in the dark. Plasma samples were added directly to the reaction mixture. 197 μL aliquots were then transferred to a 96 well plate, and 3 μL GPH/TPI (≥2.25 U) was added.

**Recombinant Human Transketolase.** The reaction mixture (200 μL) contained 50 mM glycylglycine, 2 mM thiamine diphosphate, 3 mM MgCl<sub>2</sub>, 20 mM ribose-5-phosphate, 0.4 mM NADH, 1.21 mM xylulose-5-phosphate, and ≥2.25 U of GPH/TPI (pH = 8.0). The assay was initiated by addition of human TK. Due to minor impurities of D-glyceraldehyde-3-phosphate in synthesized xylulose-5-phosphate used for the assay, the reaction mixture was preincubated with GPH/TPI until no change in absorption was detectable.

**Inactivation of Human Transketolase.** Recombinant human TK was inactivated at 80 °C for 2 h. No activity was observed by the above assay.

**Model Systems.** All model setups were conducted in 50 mM triethanolamine buffer at pH = 7.4 and 37 °C. The reaction mixture had the following composition: 50 mM triethanolamine, 10 mM ribose-5-phosphate, 10 mM fructose-6-phosphate, 3 mM CaCl<sub>2</sub>, 2 mM thiamine diphosphate, 5 mg/mL HSA, 0.3 mM 1,4-dithiothreitol, and 0.4 mg/mL human TK. Blank values were obtained with the same composition and inactivated human transketolase (iTK). For mechanistic inquiries, 4 different model setups were carried out with and without addition of 5 mM glycolaldehyde in the presence of 1-<sup>13</sup>C-labeled fructose-6-phosphate, or with and without addition of 5 mM 1-<sup>13</sup>C-glycolaldehyde in the presence of unlabeled fructose-6-phosphate, respectively.

**Analytical HPLC-MS<sup>2</sup>.** A Jasco PU-2080 Plus quaternary gradient pump with degasser (LG-2080-02), a quaternary gradient mixer (LG-2080-04), and a Jasco AS-2057 Plus autosampler (Jasco, Gross-Umstadt, Germany) was used. The mass analyses were performed using an Applied Biosystems API 4000 quadrupole instrument (Applied Biosystems/MDS Sciex, Concord, ON, Canada) equipped with an API source using an electrospray ionization (ESI) interface. The LC system was connected directly to the probe of the mass

**Table 1. Mass Spectrometric Parameters for Sugar and Sugar Phosphate Naphthylamine Derivatives Monitored in Scheduled MRM Mode with Retention Times, Recovery Rates (RV), Limits of Detection (LOD), and Limits of Quantitation (LOQ)**

	retention time ( $t_R$ , min)	mass (amu)		DP (V)	CE (eV)	CXP (V)	limits ( $\mu\text{M}$ )		RV (%)	
		Q1	Q2 <sup>c</sup>				LOD	LOQ		
sedoheptulose-7-P	20.6, 24.6	418.2	Q1 <sup>a</sup>	85	23	12	0.1	0.3	107	
			Q2 <sup>b</sup>							400.1
			Q3 <sup>c</sup>							168.4
fructose-6-P	20.1, 24.3	388.1	Q1 <sup>a</sup>	75	26	11	0.3	0.7	37	
			Q2 <sup>b</sup>							290.1
			Q3 <sup>c</sup>							370.1
ribose-5-P	26.1	358.1	Q1 <sup>a</sup>	80	25	10	0.02	0.07	35	
			Q2 <sup>b</sup>							260.1
			Q3 <sup>c</sup>							156.2
erythrose-4-P	28.5	328.4	Q1 <sup>a</sup>	80	22	10	0.01	0.02	37	
			Q2 <sup>b</sup>							230.2
			Q3 <sup>c</sup>							194.2
erythrulose	48.0, 50.1	248.2	Q1 <sup>a</sup>	70	25	10	0.08	0.24	117	
			Q2 <sup>b</sup>							194.2
			Q3 <sup>c</sup>							143.2
glycolaldehyde	52.5	188.1	Q1 <sup>a</sup>	75	34	12	0.007	0.02	99	
			Q2 <sup>b</sup>							143.2
			Q3 <sup>c</sup>							170.2
			Q4 <sup>d</sup>							
			Q5 <sup>e</sup>							
			Q6 <sup>f</sup>							

<sup>a</sup>Q1: product ion 1 (quantifier, transition used for quantitation). <sup>b</sup>Q2: product ion 2 (qualifier 1, transition used for confirmation). <sup>c</sup>Q3: product ion 3 (qualifier 2, transition used for confirmation).

spectrometer. Nitrogen was used as sheath and auxiliary gas. To measure the analytes the scheduled multiple-reaction monitoring (sMRM) mode of HPLC-MS<sup>2</sup> was used. Labeled carbons of target compounds were identified by addition of 1 amu to Q1 and their corresponding Q3 transitions containing the labeled fragment. Since GOLD results from the reaction of two molecules of glyoxal with two lysine residues under the possible loss of one labeled position, 1 and 2 amu were added to Q1 and Q3 transitions, respectively. To resolve potential matrix interferences, increasing amounts of authentic reference standards were added to mixed aliquots of the sample and a regression of response vs concentration was generated for quantitation. All synthesized compounds were referenced to commercially available authentic reference standards (e.g., 1-<sup>13</sup>C-glycolaldehyde, purity 97%; 1-<sup>13</sup>C-fructose-6-phosphate, purity 88%).

**Glyoxal.** Determination of glyoxal was carried out as described previously.<sup>9</sup>

**Sugar and Sugar Phosphates.** Plasma, hemolyzed whole blood, and hemolyzed RBC samples were first filtered through a centrifugal filter with a pore size of 0.45  $\mu\text{m}$  (cellulose acetate membrane, Corning Costar Spin-X, Sigma). The filtrate was then placed in a 3000 Da MWCO cutoff filter (PES, VWR North America) and centrifuged. Centrifugation was carried out at 16100g and 4 °C. The clear eluate (300  $\mu\text{L}$ ) was then freeze-dried and derivatized with 25  $\mu\text{L}$  of 1-naphthylamine (0.1 M) and 25  $\mu\text{L}$  of sodium cyanoborohydride (1 M), as described in the literature.<sup>24</sup> Glycolaldehyde concentrations were determined without lyophilization. Derivatization of model incubations was carried out as described previously.<sup>9</sup> Chromatographic separations were performed on a stainless steel column (KNAUER, Eurospher 100-5 C18, 250  $\times$  4.6 mm, 5  $\mu\text{m}$ , Berlin, Germany) using a flow rate of 1 mL min<sup>-1</sup>. An injection volume of 25  $\mu\text{L}$  and column temperature of 25 °C were used. Eluents were ultrapure water (A) and a mixture of methanol and ultrapure water (7:3, v/v; B). 0.6 mL/L heptafluorobutyric acid was added to both eluents as ion pair reagent. Samples were injected at 20% B, and gradient was then changed to 40% B within 35 min and 100% B within 25 min and held for 10 min. Then gradient was changed to 20% B within 5 min and held for 15 min. ESI in positive mode was used: sprayer capillary voltage, 2.5 kV;

nebulizing gas flow, 60 mL/min; heating gas, 80 mL/min at 600 °C; collision gas, high and curtain gas, 40 mL/min.

Determination of the compound-specific orifice potentials and fragment-specific collision energies was carried out with authentic reference material. Sugar and sugar phosphates were derivatized as described above and isolated by preparative high performance liquid chromatography. The identity of all naphthylamine compounds was secured by HR-MS. HR-MS for the respective naphthylamine derivatives was as follows: fructose-6-phosphate  $m/z$  388.1156 (found),  $m/z$  388.1156 (calculated for C<sub>16</sub>H<sub>23</sub>O<sub>8</sub>NP [M + H]<sup>+</sup>); sedoheptulose-7-phosphate  $m/z$  416.1116 (found),  $m/z$  416.1116 (calculated for C<sub>17</sub>H<sub>23</sub>O<sub>8</sub>NP [M - H]<sup>-</sup>); ribose-5-phosphate  $m/z$  358.1049 (found),  $m/z$  358.1050 (calculated for C<sub>15</sub>H<sub>21</sub>O<sub>7</sub>NP [M + H]<sup>+</sup>); erythrose-4-phosphate  $m/z$  326.0788 (found),  $m/z$  326.0788 (calculated for C<sub>14</sub>H<sub>17</sub>O<sub>6</sub>NP [M + H]<sup>+</sup>); and erythrulose  $m/z$  248.1282 (found),  $m/z$  248.1281 (calculated for C<sub>14</sub>H<sub>18</sub>O<sub>3</sub>N [M + H]<sup>+</sup>). The optimized parameters for compound-specific mass spectrometry, recovery rate (RV), retention times ( $t_R$ ), and limits of detection (LOD) and quantitation (LOQ) are shown in Table 1. Recovery rates were determined by addition of the respective sugar and sugar phosphates at three different concentrations to plasma, freshly hemolyzed whole blood, and RBCs of one subject. The native and the spiked samples were subjected to the workup procedure and analyzed as described above. The RV was estimated as the quotient of (spiked amount - amount in native sample)/amount of added sample  $\times$  100%.

Glucose concentrations were determined via HPLC-FLD (excitation 318 nm and emission 440 nm) at a retention time of  $t_R$  = 45.0 min and with a LOD/LOQ of 0.07/0.21  $\mu\text{M}$ . Chromatographic parameters were as described above.

**Protein Modifications.** Workup, chromatographic parameters, and the optimized parameters for mass spectrometry for HEL, CML, and imidazolinone were according to previous work.<sup>9</sup> Optimized mass spectrometric parameters for GOLD ( $t_R$  = 26.4 min) were as follows:  $m/z$  327.2/84.1 (declustering potential (DP) 60 V, collision energy (CE) 51.0 eV, cell exit potential (CXP) 13.0 V, quantifier),  $m/z$  327.2/282.3 (DP 60 V, CE 31.0 eV, CXP 14.0 V, qualifier 1),  $m/z$  327.2/198.1 (DP 60 V, CE 28.0 eV, CXP 14.0 V, qualifier 2).

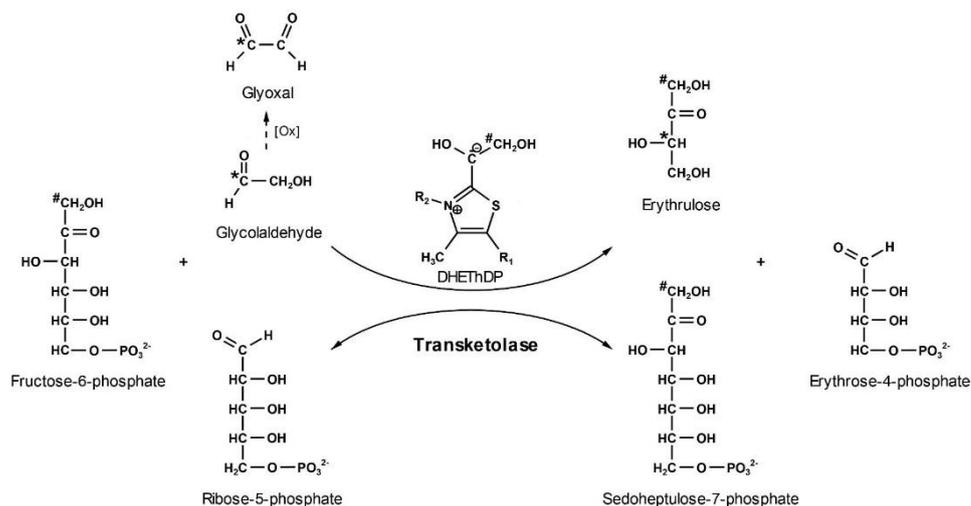


**Figure 1.** Reaction mechanism of the transketolase-catalyzed transformation of glycolaldehyde into erythrulose in the presence of the donor ketose fructose-6-phosphate and the acceptor aldose ribose-5-phosphate (\* and # represent  $^{13}\text{C}$  labeled positions).

**Product Ion MS<sup>2</sup> by Collision-Induced Dissociation (CID).** Samples were derivatized as described above and injected into the HPLC–MS<sup>2</sup> system using a CID experiment after chromatographic separation. The fragmentation spectra of the authentic references and samples were obtained with the same parameters for DP as in Table 1. Parameters for CE and CXP of naphthylamine derivatives were as follows: erythrulose, 24 eV (CE), 10 V (CXP); glycolaldehyde, 22 eV (CE), 10 V (CXP).

**High Resolution Mass Determination (HR-MS).** Positive and negative ion high resolution ESI mass spectra were obtained from an Orbitrap Elite mass spectrometer (ThermoFisher Scientific, Bremen, DEU) equipped with an HESI electrospray ion source (spray voltage 4 kV; capillary temperature 275 °C, source heater temperature 40 °C; FTMS resolution >30,000). Nitrogen was used as sheath and auxiliary gas. The sample solutions were introduced continuously via a 500  $\mu\text{L}$  Hamilton syringe pump with a flow rate of 5  $\mu\text{L min}^{-1}$ . The data were evaluated by the Xcalibur software 2.7 SP1.

**Nuclear Magnetic Resonance Spectroscopy (NMR).** NMR spectra were recorded on a Varian VXR 400 spectrometer operating at 400 MHz for  $^1\text{H}$  and 100 MHz for  $^{13}\text{C}$ .  $\text{SiMe}_4$  was used as a reference for calibrating the chemical shift.

**Statistical Analysis.** Analyses were performed in triplicate for each model system and resulted in coefficients of variation less than 5% for sugars, glyoxal, and sugar phosphates and less than 10% for protein modifications detected. All significance tests were performed by two-sample *t*-test with a probability value of 95% (\*) for each model system and 95% (\*) and 99% (\*\*) for blood samples. LOD and LOQ were estimated for sugar and sugar phosphate naphthylamine derivatives, at a signal-to-noise ratio of 3 for LOD and 9 for LOQ.

## RESULTS AND DISCUSSION

**In Vitro Model Incubations with Recombinant Human Transketolase.** Approximately 0.5 mg of recombinant human transketolase (TK) per g of wet cells was isolated from *E. coli* with a specific activity of 0.6 U/mg. Properties and enzymatic characteristics were studied previously.<sup>21,22,25</sup> To investigate the influence of human TK on the formation of glycolaldehyde and glyoxal specific advanced glycation endproducts (AGEs), model incubations with fructose-6-phosphate (F6P) and ribose-5-phosphate (R5P) in the presence of human serum albumin (HSA) with and without addition of glycolaldehyde were carried out under physiological conditions (pH 7.4, 37 °C) and

compared to incubations with inactivated transketolase (iTK). The ratio of the initial reaction educts F6P, R5P, and glycolaldehyde was adapted to the concentrations *in vivo*, based on our findings (Table 4) and the data presented in the literature.<sup>26</sup> Sugar and sugar phosphates were trapped by postincubation with 1-naphthylamine and sodium cyanoborohydride following established methods.<sup>9,24</sup> Reductive amination yields the respective naphthylamine derivatives with one peak for aldoses and two peaks for ketoses, due to the formed diastereoisomers. As expected, the ratio of peak areas of derivatized ketose isomers was stable. For detailed mechanistic insights into the TK-catalyzed reactions and the formation of protein modifications, either 1- $^{13}\text{C}$ -labeled F6P or 1- $^{13}\text{C}$ -glycolaldehyde was used in the reaction setup. Quantitation of the isotopologues was corrected by the naturally occurring isotope distribution. Time course experiments showed that the use of labeled chemicals had virtually no influence on the quantitative data.

**Characterization of the Transketolase Reaction.** As depicted in Figure 1, the initial reaction of F6P with thiamine diphosphate leads to the formation of erythrulose-4-phosphate (E4P), as the first product, and the dihydroxyethyl-thiamine diphosphate (DHETHDP) intermediate. Subsequent transfer of the covalently bound glycolaldehyde unit to R5P yields sedoheptulose-7-phosphate (S7P), as the second product. Addition of glycolaldehyde as a competing acceptor substrate entails the formation of erythrulose. The TK-catalyzed conversion of sugar phosphates in the presence of 1- $^{13}\text{C}$ -glycolaldehyde is shown in Figure 2. Reduction of the educts F6P (52.3 mol %, TK, vs 86 mol %, iTK, 24 h) and R5P (22.7 mol %, TK, vs 38.0 mol %, iTK) was accompanied by an almost equimolar formation of S7P (19.5 mol %). Surprisingly, E4P was formed progressively at the early stages of the reaction (8.0 mol %, 2 h), followed by degradation (4.2 mol %, 24 h). Theoretically, amounts of E4P formed during incubations should be in the range of S7P. Compared to S7P, however, only about 20% of the expected levels were detected after 24 h. It should be noted that in contrast to our previously published model setup with TK from *E. coli* this is an equilibrium reaction

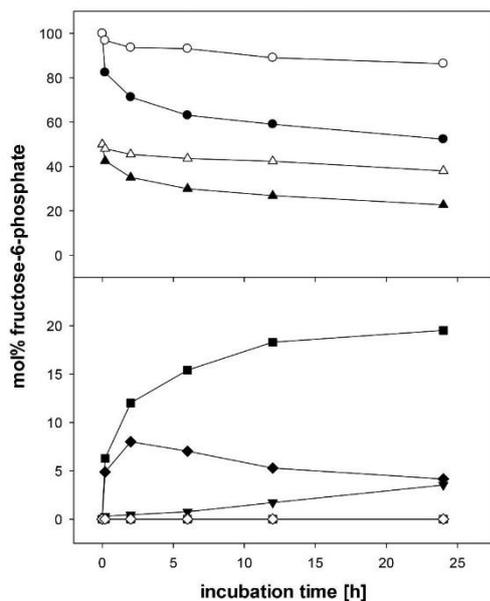


**Figure 2.** Conversion of fructose-6-phosphate (●), ribose-5-phosphate (▲), and 1-<sup>13</sup>C-glycolaldehyde to sedoheptulose-7-phosphate (■), erythrose-4-phosphate (◆), and 3-<sup>13</sup>C-erythrulose (▼) by human transketolase (closed symbols) or inactivated human transketolase (open symbols) in the presence of HSA.

with an educts to products ratio of approximately 80:20, which increasingly proceeds by the nonenzymatic depletion of E4P. This development is recognizable on the basis of erythrulose formation, which was generated continuously up to 24 h, by the reaction of both added and from E4P degradation formed glycolaldehyde with the donor ketoses F6P and S7P, respectively. In general, the reactivity of sugars and sugar phosphates follows their mutarotation rate and chain length. The stability increases with increasing chain length, since carbohydrates with more than 5 carbon atoms (aldose phosphates) or more than 6 carbon atoms (ketose phosphates) are essentially hemiacetalic ring structures in aqueous solution. As a result, open-chained C4 sugars as erythrulose and especially E4P are prone to Maillard-catalyzed nonenzymatic degradation and significantly add to HSA glycation. However, this notion is also the reason why we deliberately chose the present model since the alternative setup with xylulose-5-phosphate leading to glyceraldehyde-3-phosphate represents a mechanistically even more reactive and difficult to interpret system. As expected, in the present setup, neither the formation of S7P nor E4P or erythrulose was observed during incubations with iTK. Conversion of sugar phosphates during incubation with 1-<sup>13</sup>C-F6P in the absence of glycolaldehyde led to isotopic labeling of S7P and traces of erythrulose at position C1, respectively. This again underpinned the high reactivity of E4P by the disposal of nonlabeled glycolaldehyde. The results are summarized in Table 2.

3-<sup>13</sup>C-Erythrulose was generated continuously up to 24 h in the presence of 1-<sup>13</sup>C-glycolaldehyde and revealed 50-fold higher concentrations compared to incubations in the absence of glycolaldehyde (3.5 vs 0.07 mol %). In the presence of 1-<sup>13</sup>C-glycolaldehyde, comparable amounts of 1-<sup>13</sup>C-glycolaldehyde

**Table 2.** Mean Concentration of Sugar Phosphates, Sugars, and Glyoxal (mol % ± SD, Fructose-6-phosphate) and AGEs (mmol/mol L-leucine ± SD) in the Presence of HSA and Human Transketolase (TK) or Inactivated Human Transketolase (iTK) at 24 h of Incubation Time, with and without Addition of 50 mol % 1-<sup>13</sup>C-Glycolaldehyde (GA) or 1-<sup>13</sup>C-Fructose-6-phosphate (F6P)

	TK 1- <sup>13</sup> C F6P without GA		iTK 1- <sup>13</sup> C F6P without GA		TK F6P with 1- <sup>13</sup> C GA		iTK F6P with 1- <sup>13</sup> C GA	
	12C	13C	12C	13C	12C	13C	12C	13C
fructose-6-P	<LOD <sup>a</sup>	56 ± 2	<LOD	86 ± 3	52.3 ± 0.6	<LOD	86 ± 1	<LOD
ribose-5-P	20.9 ± 0.3	<LOD	39 ± 2	<LOD	22.7 ± 0.6	<LOD	38.0 ± 0.8	<LOD
sedoheptulose-7-P	<LOD	20.6 ± 0.2	<LOD	<LOD	19.5 ± 0.5	<LOD	<LOD	<LOD
erythrose-4-P	4.0 ± 0.1	<LOD	<LOD	<LOD	4.2 ± 0.1	<LOD	<LOD	<LOD
glycolaldehyde	0.19 ± 0.01	<LOD	0.12 ± 0.01	<LOD	0.14 ± 0.01	16.8 ± 0.2	0.13 ± 0.01	17.5 ± 0.7
glyoxal	0.43 ± 0.01	<LOQ <sup>b</sup>	0.23 ± 0.01	<LOQ	0.21 ± 0.01	1.34 ± 0.06	0.16 ± 0.01	1.76 ± 0.05
erythrulose	<LOD	0.07 ± 0.01	<LOD	<LOD	<LOQ	3.5 ± 0.2	<LOD	<LOD
HEL	0.16 ± 0.01	<LOD	0.092 ± 0.004 <sup>c</sup>	<LOD	0.108 ± 0.005	6.6 ± 0.8	0.095 ± 0.002 <sup>*</sup>	9.4 ± 0.2 <sup>*</sup>
CML	0.48 ± 0.03	0.0034 ± 0.0003	0.28 ± 0.02 <sup>*</sup>	0.0034 ± 0.0002	0.51 ± 0.03	1.30 ± 0.09	0.15 ± 0.01 <sup>*</sup>	1.28 ± 0.08
imidazolinone	0.057 ± 0.004	<LOD	0.027 ± 0.001 <sup>*</sup>	<LOD	0.041 ± 0.002	0.168 ± 0.008	0.029 ± 0.002 <sup>*</sup>	0.38 ± 0.02 <sup>*</sup>
GOLD	0.0049 ± 0.0002	<LOD	0.0054 ± 0.0003	<LOD	0.0035 ± 0.0005	0.051 ± 0.002	0.0038 ± 0.0002	0.18 ± 0.01 <sup>*</sup>

<sup>a</sup>LOD: limit of detection. <sup>b</sup>LOQ: limit of quantitation. <sup>c</sup>\*Significant difference compared to incubations with TK by *t*-test ( $\alpha = 0.05$ ).

(16.8 mol %, TK, vs 17.5 mol %, iTK) and up to 140-fold lower concentrations of  $^{12}\text{C}$ -glycolaldehyde were detected after 24 h. Incubations conducted in the absence of glycolaldehyde showed slightly elevated amounts of  $^{12}\text{C}$ -glycolaldehyde (0.19 mol %, TK, vs 0.12 mol %, iTK) and were found to be approximately equal to the results observed for  $^{12}\text{C}$ -glycolaldehyde in the presence of  $1\text{-}^{13}\text{C}$ -glycolaldehyde.

**Verification of the Transketolase-Catalyzed Conversion of Glycolaldehyde to Erythrulose.** To our knowledge, the use of glycolaldehyde as an acceptor substrate for human TK has only been described by Meshalkina et al. but without tangible substrate characteristics.<sup>22</sup> Though no apparent difference of glycolaldehyde was observed in the presence and absence of TK, the nature of erythrulose formation by the reaction of DHETHDP with glycolaldehyde was unequivocally proven by comparison of the fragmentation spectra of erythrulose formed during model incubations to the reference standard. The proposed fragmentation was supported by the elemental composition based on high resolution mass determination (Supporting Information). As shown in Figure 3, the

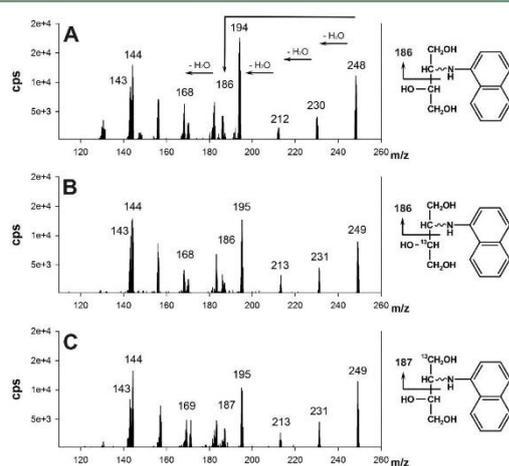


**Figure 3.** Mass spectra of the human transketolase-catalyzed formation of erythrulose from glycolaldehyde by collision-induced dissociation (CID), detected as their naphthylamine derivatives (A) nonlabeled standard, (B)  $1\text{-}^{13}\text{C}$ -glycolaldehyde, and (C)  $1\text{-}^{13}\text{C}$ -fructose-6-phosphate.

protonated molecular ion  $[\text{M} + \text{H}]^+$  of the erythrulose naphthylamine derivative (Figure 3A) at  $m/z$  248 is expected to undergo multiple dehydration reactions to  $m/z$  230, 212, and 194. Elimination of the 1,2-dihydroxyethyl group and dehydration give ions at  $m/z$  186 and 168, respectively. The ions at  $m/z$  143 and 144 represent the naphthylamine backbone after cleavage of erythrulose. Model incubations of F6P in the presence of  $1\text{-}^{13}\text{C}$ -glycolaldehyde (Figure 3B) and of  $1\text{-}^{13}\text{C}$ -F6P in the presence of glycolaldehyde (Figure 3C) led to incorporation of a  $^{13}\text{C}$ -label into the erythrulose backbone and thus increased the  $m/z$  of the molecular ion and its subsequent dehydration products by 1 amu. As the reaction of F6P with  $1\text{-}^{13}\text{C}$ -glycolaldehyde results in  $3\text{-}^{13}\text{C}$ -erythrulose, elimination of the 1,2-dihydroxyethyl group and dehydration led to the loss of the  $^{13}\text{C}$ -label at  $m/z$  186 and 168 during fragmentation, whereas with  $1\text{-}^{13}\text{C}$ -F6P and glycolaldehyde the label was retained in  $1\text{-}^{13}\text{C}$ -erythrulose.

**Formation of Glyoxal.** In the presence of oxygen and amines glycolaldehyde is easily oxidized to glyoxal.<sup>4</sup> The results are depicted in Figure 4 and Table 2. Amounts of  $^{13}\text{C}$ -glyoxal

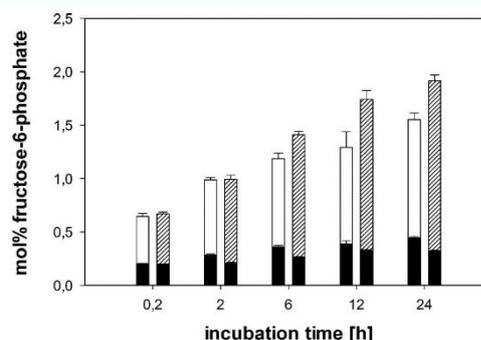


**Figure 4.** Formation of glyoxal in the presence of HSA and  $1\text{-}^{13}\text{C}$ -glycolaldehyde by human transketolase (open bars) or human inactivated transketolase (hatched bars). Black bars represent the  $^{13}\text{C}$  portion of glyoxal formed during incubation.

formed during incubations with  $1\text{-}^{13}\text{C}$ -glycolaldehyde were reduced up to 24% in the presence of TK (1.34 vs 1.76 mol %).  $^{12}\text{C}$ -Glyoxal levels were 6- to 10-fold lower and showed an opposing time-course development resulting in elevated amounts of  $^{12}\text{C}$ -glyoxal formed in the presence of TK (0.21 vs 0.16 mol %). The same was observed during incubations without the addition of glycolaldehyde (0.43 vs 0.23 mol %). The reversal of the unlabeled glyoxal ratio (TK vs iTK) compared to the labeled glyoxal ratio must be attributed foremost to Maillard-triggered fragmentation reactions of unlabeled E4P formed in the presence of TK, while  $^{13}\text{C}$ -glyoxal can only be formed by oxidation of  $^{13}\text{C}$ -glycolaldehyde and is thus decreased by TK. This was further confirmed by incubations carried out without addition of glycolaldehyde since comparable levels of unlabeled glycolaldehyde and glyoxal were detected.

**Formation of Posttranslational Protein Modifications.** As human TK renders concentrations of glycolaldehyde, glyoxal, and other carbonyl compounds, all reactions were performed in the presence of HSA to explore the impact on the formation of Maillard protein modifications. In essence the reaction of glycolaldehyde and glyoxal leads to the very same AGEs, however, an additional radicalic pathway for the reaction of glycolaldehyde with amines leading to quaternary pyrazine species and glyoxal imines has been described.<sup>27</sup> According to the scheme outlined in Figure 5, initially, the carbonyl function of glycolaldehyde or glyoxal reacts with the  $\epsilon$ -amino group of protein-bound lysine to yield the corresponding imines. Prior to acidic hydrolysis, both Schiff base adducts were converted to  $N^6$ -(2-hydroxyethyl)lysine (HEL) by reduction with  $\text{NaBH}_4$ , representing the reversible protein-bound portions of glycolaldehyde and glyoxal during model incubations.<sup>4,28</sup> The time-dependent formation of the AGEs  $N^6$ -carboxymethyl lysine (CML), 5-(2-imino-5-oxo-1-imidazolidinyl)norvaline (imidazolinone), and glyoxal-lysine dimer (GOLD) in the presence of  $1\text{-}^{13}\text{C}$ -glycolaldehyde is depicted in Figure 6. Values obtained for HEL, CML, imidazolinone, and GOLD during incubations with and without addition of glycolaldehyde after 24 h are summarized in Table 2.

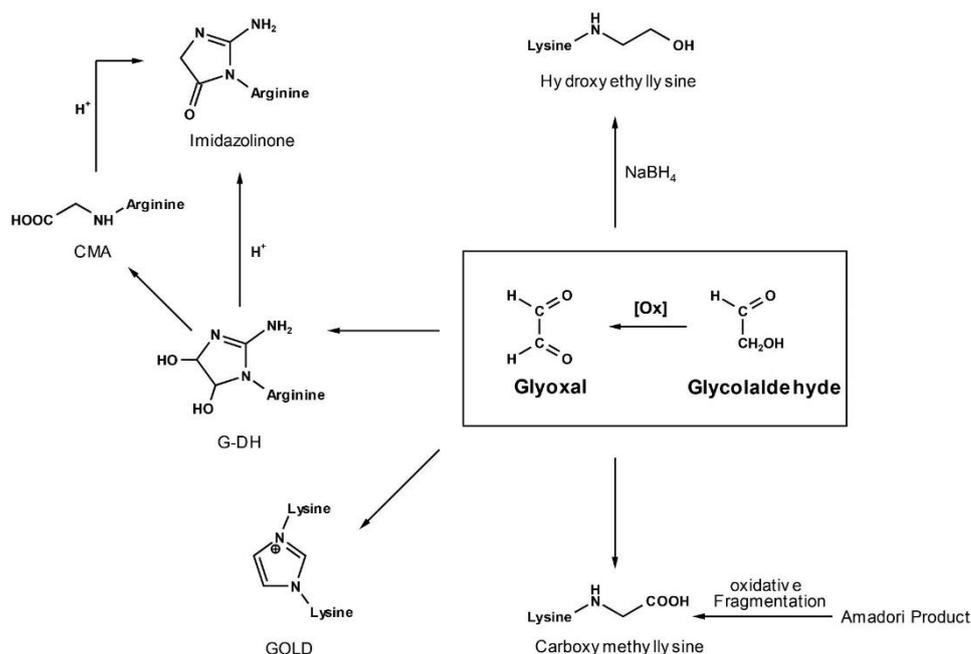


**Figure 5.** Formation of glycolaldehyde- and glyoxal-specific protein modifications in the presence of HSA.

Amounts of <sup>13</sup>C-HEL formed during incubations in the presence of L-<sup>13</sup>C-glycolaldehyde were significantly reduced by 30% (6.6 mmol/mol L-leucine, TK, vs 9.4 mmol/mol L-leucine, iTK). Up to one hundred times less <sup>12</sup>C-HEL was determined. <sup>12</sup>C-HEL contents were significantly higher in the presence of TK during incubations with and without addition of glycolaldehyde. As HEL represents the reversible lysine bound glycolaldehyde and glyoxal, this data was in good agreement to the parallel analyzed unbound concentration reported in Table 2. Unexpectedly, total amounts of CML were significantly elevated in the presence of TK (1.8 vs 1.4 mmol/mol L-leucine). Furthermore, <sup>12</sup>C-CML had a share of 30% of total amounts of CML formed (0.51 mmol/mol L-leucine, <sup>12</sup>C-CML, vs 1.81 mmol/mol L-leucine, total-CML) in the presence of TK and a more than 3-fold higher concentration compared to iTK (0.51 vs 0.15 mmol/mol L-leucine). This cannot be explained by the above-discussed moderate (still significant) increase of free and reversible bound C2 carbonyls. While, HEL, GH-3, and GOLD are exclusively formed by the reaction of glycolaldehyde and glyoxal with lysine and arginine, respectively, the oxidative fragmentation of the Amadori product has been described as a major alternative pathway for CML.<sup>4</sup> Obviously, highly reactive E4P, formed and degraded by more than 80% during the TK reaction, enters to a major portion this reaction route. This reasoning was further substantiated (I) as comparable amounts of unlabeled CML were formed in the absence of glycolaldehyde and (II) as <sup>13</sup>C-CML generated in absence of glycolaldehyde was negligible, excluding an impact of F6P and S7P on oxidative fragmentation.

In contrast to HEL and CML, formation of imidazolinone and the bivalent AGE GOLD solely depends upon explicitly glyoxal.<sup>14,15</sup> The initial reaction leads to the formation of 5-(4,5-dihydroxy-2-imino-1-imidazolidinyl)norvaline (GDH),

which is slowly degraded to N<sup>7</sup>-carboxymethyl arginine (CMA). Both forms are converted to imidazolinone under acidic protein hydrolysis, which therefore represents a sum parameter for the total extent of glyoxal-arginine modifications.<sup>14</sup> Imidazolinone was suppressed by approximately 50% in the presence of TK (0.21 vs 0.41 mmol/mol L-leucine) after 24 h. Total reduction however was primarily based on the decrease in <sup>13</sup>C-imidazolinone. The <sup>12</sup>C-imidazolinone portion was small, but still significantly elevated in the presence of TK (0.041 vs 0.029 mmol/mol L-leucine). GOLD was most strongly suppressed up to 70% (0.05 vs 0.18 mmol/mol L-leucine, total-GOLD) after 24 h. This was expected because the cross-link structure results from reaction of two equivalents of glyoxal with two lysine residues under release of formic acid, while for imidazolinone only one molecule of glyoxal is needed.<sup>15</sup> It also explains why the slightly higher levels of unlabeled glyoxal in the presence of TK had virtually no impact on <sup>12</sup>C-GOLD formation (0.0035 mmol/mol L-leucine, TK, vs 0.0038 mmol/mol L-leucine, iTK).

**Transketolase Activity and Sugar and Sugar Phosphate Concentrations of Healthy Subjects and Uremic Patients.** To gain insights into TK metabolism, enzyme activity and related sugars were measured in blood from 9 healthy subjects and 10 nondiabetic uremic patients undergoing hemodialysis. As shown in Table 3, renal function was assessed from serum creatinine and the inflammatory status from C-reactive protein. Normal renal function was defined as serum creatinine levels below 101 μM. Nondiabetic conditions were verified by the determination of HbA1c. Time of blood sampling for uremic patients was predialysis. Handling and processing were carried out in the cold (4 °C) to exclude possible alterations of the blood samples. The correct separation of blood compartments was verified by the

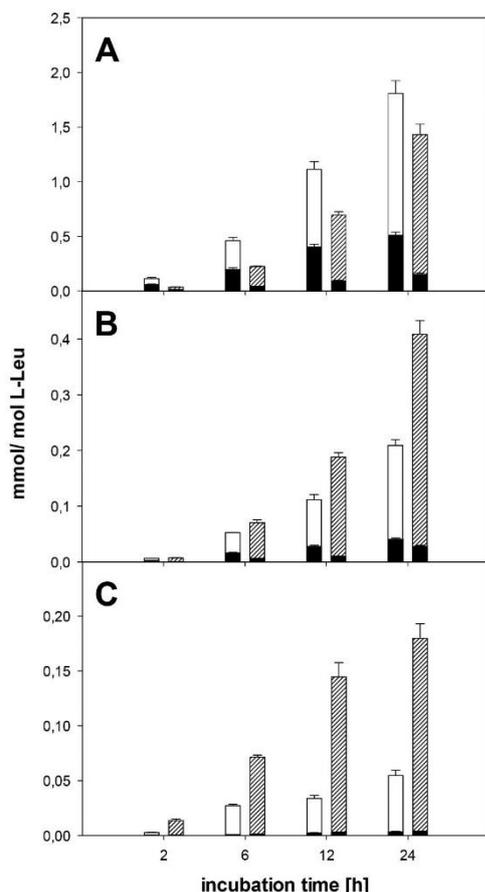


**Figure 6.** Influence of the transketolase reaction on the formation of CML (A) imidazolone (B) and GOLD (C) in the presence of  $1\text{-}^{13}\text{C}$ -glycolaldehyde: open bars, human transketolase; hatched bars, inactivated human transketolase; and black bars,  $^{12}\text{C}$  portion of AGEs formed during incubation.

**Table 3.** Profile of Healthy Subjects vs Nondiabetic Uremic Patients

	healthy subjects	uremic patients
no. of participants	9	10
sex, female/male	3/6	3/7
age (years)	56 (48–72)	55 (31–67)
HbA1c (mmol/mol)	$33 \pm 4$	$31 \pm 5$
serum creatinine ( $\mu\text{M}$ )	$85 \pm 11$	$999 \pm 256$
C-reactive protein (mg/L)	$2.0 \pm 1.6$	$4.9 \pm 7.0$

determination of glucose levels. The results are summarized in Table 4.

Loss of renal clearance leads to the accumulation of waste products and has been linked to an impaired metabolic function of the PPP.<sup>29</sup> The percentage increase in activity of TK in red blood cells (RBCs) and leukocytes upon addition of thiamine diphosphate is often used to detect thiamine deficiency. However, contradictory data on TK activity have been published. Different authors have observed normal and even enhanced TK activity in uremic patients while others reported a

significantly suppressed TK activity.<sup>30</sup> Reversible inhibition of TK remains a complex and yet not fully understood phenomenon, and its suppression by uremic toxins has been subject to recent investigations.<sup>29</sup> In our study, we could not determine a significant difference in TK activity with or without addition of thiamine diphosphate between uremic patients and the control group in RBCs (0.68 U/g Hb, 116%, healthy subjects, vs 0.73 U/g Hb, 113%, uremic patients) or whole blood (0.87 U/g Hb, 111%, healthy subjects, vs 0.99 U/g Hb, 104%, uremic patients). As anticipated, no TK activity was detected in plasma.

Determination of sugars and sugar phosphates in blood is a difficult task and has never been compared to patients with chronic renal failure. We herein present a novel approach for the quantitation of these important intermediates *in vivo*. A simple workup procedure followed by analysis via LC–MS<sup>2</sup> for the detection of sugar and sugar phosphates was developed and validated. In contrast to the model incubations, for F6P only the first peak was evaluated for quantitation, as the second was disturbed by matrix interferences. A LC–MS<sup>2</sup> chromatogram of a standard mix and a RBC sample is given in the Supporting Information. All workup samples of healthy subjects and uremic patients were analyzed in single batches to exclude interassay variations. However, the intraassay variation (CV) was  $\leq 10\%$ . Levels of S7P and R5P detected in whole blood of the control group were in good agreement with the data presented in the literature.<sup>26</sup> R5P levels were nearly doubled in uremic patients (3.1 vs 5.6  $\mu\text{M}$ , RBCs), while concentrations of F6P were almost identical (4.7  $\mu\text{M}$ , healthy subjects, vs 5.5  $\mu\text{M}$ , uremic patients in RBCs). The significantly elevated levels of S7P (1.4  $\mu\text{M}$ , healthy subjects, vs 2.6  $\mu\text{M}$ , uremic patients in RBCs) are expected to be caused by the increased amounts of R5P. To our knowledge, E4P was detected and quantified for the first time and exhibited significantly lower concentrations in patients with loss of renal function (0.070  $\mu\text{M}$  vs 0.039  $\mu\text{M}$ , RBCs). This may be explained by the increased oxidative stress in uremia to promote the nonenzymatic oxidative degradation of E4P, as shown in our above *in vitro* studies.

Physiological concentrations of glycolaldehyde have not been determined so far but were believed to range from 0.1 to 1 mM.<sup>31</sup> For the first time, we measured glycolaldehyde concentrations in RBCs (up to 2.06  $\mu\text{M}$ ), whole blood (up to 1.48  $\mu\text{M}$ ), and plasma (up to 0.95  $\mu\text{M}$ ) with a clear shift to elevated levels in RBCs indicating endogenous formation pathways. As shown in Figure 7, the identity of glycolaldehyde in plasma was confirmed by comparison of retention time and fragmentation pattern with the synthesized authentic reference standard (GA-N). Dehydration of the quasi molecular ion  $[\text{M} + \text{H}]^+$  at  $m/z$  188 gives fragment  $m/z$  170. Peaks at  $m/z$  143/144 represent the naphthylamine ion after elimination of the hydroxyethyl group. Until now, the degradation of L-serine by myeloperoxidase at chronic sites of inflammation and the Maillard reaction have been the only known source of glycolaldehyde *in vivo*.<sup>5</sup> However, more recent studies showed no connection between myeloperoxidase levels and the etiology of complications in advancing renal disease.<sup>32</sup> Furthermore, our data strongly emphasized the high kinetic stability of the DHETHDP intermediate excluding a possible release of glycolaldehyde, as levels of  $^{13}\text{C}$ -glycolaldehyde and  $^{13}\text{C}$ -glyoxal and their corresponding lysine-derived imines ( $^{13}\text{C}$ -HEL) during incubations of  $1\text{-}^{13}\text{C}$ -F6P were below LOD and LOQ, respectively. Thus, the source of glycolaldehyde *in vivo* remains uncertain but is likely to be generated enzymatically. The

**Table 4.** Values (Mean Concentration [ $\mu\text{M}$ ]  $\pm$  SD) of Sugars, Sugar Phosphates, and Transketolase Activity with and without Addition of Thiamine Diphosphate Determined in Whole Blood, Red Blood Cells (RBC), and Plasma of Healthy Subjects vs Uremic Patients

	healthy subjects			uremic patients		
	whole blood	RBC	plasma	whole blood	RBC	plasma
fructose-6-phosphate	2.03 $\pm$ 0.82	4.7 $\pm$ 1.3	<LOD <sup>a</sup>	2.2 $\pm$ 1.0	5.5 $\pm$ 2.8	<LOD
ribose-5-phosphate	0.69 $\pm$ 0.20	3.1 $\pm$ 1.4 <sup>*c</sup>	<LOQ <sup>b</sup>	0.99 $\pm$ 0.29	5.6 $\pm$ 1.4	<LOQ
sedoheptulose-7-phosphate	1.06 $\pm$ 0.32	1.36 $\pm$ 0.36 <sup>*</sup>	<LOD	1.29 $\pm$ 0.60	2.6 $\pm$ 1.3	<LOD
erythrose-4-phosphate	<LOQ	0.070 $\pm$ 0.009 <sup>**</sup>	<LOD	<LOQ	0.039 $\pm$ 0.007	<LOD
glucose	4719 $\pm$ 597	1.15 $\pm$ 0.46	6258 $\pm$ 627	5036 $\pm$ 910	1.20 $\pm$ 0.46	7873 $\pm$ 2122
erythrose	0.98 $\pm$ 0.37 <sup>**</sup>	<LOQ	4.0 $\pm$ 1.2 <sup>*</sup>	0.43 $\pm$ 0.26	<LOQ	2.4 $\pm$ 1.1
glycolaldehyde	1.39 $\pm$ 0.62	2.06 $\pm$ 0.65	0.58 $\pm$ 0.16 <sup>*</sup>	1.48 $\pm$ 0.47	1.75 $\pm$ 0.91	0.95 $\pm$ 0.22
TK activity						
−ThDP [U/g Hb]	0.87 $\pm$ 0.10	0.68 $\pm$ 0.07	<LOD	0.99 $\pm$ 0.16	0.73 $\pm$ 0.12	<LOD
+ThDP [%]	111 $\pm$ 12	116 $\pm$ 20	<LOD	104 $\pm$ 13	113 $\pm$ 10	<LOD

<sup>a</sup>LOD: limit of detection. <sup>b</sup>LOQ: limit of quantitation. <sup>c</sup>\*Significant difference compared to uremic patients by *t*-test ( $\alpha = 0.05$ ). <sup>\*\*</sup>Significant difference compared to uremic patients by *t*-test ( $\alpha = 0.01$ ).

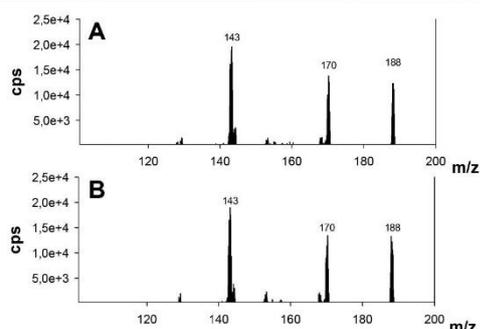


**Figure 7.** Product ion MS<sup>2</sup> of glycolaldehyde naphthylamine derivative in plasma by collision-induced dissociation (CID) of  $m/z$  188 [ $\text{M} + \text{H}$ ]<sup>+</sup>: (A) plasma workup and (B) authentic standard.

relevance of glycolaldehyde and glyoxal to modify and to cross-link proteins in the course of the Maillard reaction has been studied extensively.<sup>1,4,27,28</sup> Glyoxal is formed by oxidative degradation of sugars, lipids, DNA, and glycated proteins but also detoxified by the glyoxalase system.<sup>4,6,7</sup> The content of glyoxal in plasma was estimated at  $0.49 \pm 0.05 \mu\text{M}$  and is approximately equal to our results detected for glycolaldehyde ( $0.58 \pm 0.16$ ) in healthy subjects.<sup>1</sup> Hofmann et al. described the reduction of glyoxal to glycolaldehyde by a redox reaction in the presence of a reductone.<sup>27</sup> However, Henning et al. reported 3-fold higher concentrations of glyoxal in plasma of uremic patients,<sup>1</sup> whereas we detected a 1.6-fold increase of glycolaldehyde ( $0.58$  vs  $0.95 \mu\text{M}$ ). Consequently, oxidation of glycolaldehyde to glyoxal can be directly correlated to oxidative stress and thus must be regarded as a major pathway leading to protein modification *in vivo*.

Erythrose has been described as a major degradation product of ascorbate,<sup>33</sup> however, literature on the detection *in vivo* is scarce. As the TK-catalyzed conversion of glycolaldehyde results in the formation of erythrose, elevated amounts of erythrose were expected to occur in RBCs. Indeed, we were able to detect erythrose in RBCs, but the concentrations remained below LOQ, and, in contrast to the distribution of glycolaldehyde, a clear shift of erythrose toward plasma was determined. In comparison to the control group, significantly lower amounts of erythrose were detected in uremic patients

( $0.98 \mu\text{M}$  vs  $0.43 \mu\text{M}$ , whole blood, and  $4.0 \mu\text{M}$  vs  $2.4 \mu\text{M}$ , plasma). We conclude three possible mechanisms for the difference in erythrose concentrations observed: (I) increased amounts of RSP act as a competing acceptor substrate with glycolaldehyde, (II) nonenzymatic degradation of erythrose may be enhanced in uremia, and (III) oxidation of glycolaldehyde to glyoxal results in the withdrawal of glycolaldehyde as a substrate for TK.

In conclusion, we were able to identify significant changes in the sugar and sugar phosphate profile of uremic patients and to emphasize the role of the PPP as a shunt for reactive intermediates. In this context, glycolaldehyde, erythrose, and E4P were quantified for the first time *in vivo*. *In vitro*, studies with recombinant human TK significantly suppressed the formation of glycolaldehyde and glyoxal specific AGEs by the conversion of glycolaldehyde to erythrose. Furthermore, knowledge of these mechanisms will help in the evaluation of chemical processes and changes occurring in diseases with an altered TK activity. In this context, glycolaldehyde was unequivocally established as a crucial intermediate. However, its origin *in vivo* remains unclear.

## ■ ASSOCIATED CONTENT

### ● Supporting Information

The Supporting Information is available free of charge on the ACS Publications website at DOI: 10.1021/acs.jafc.7b05472.

LC–MS<sup>2</sup> chromatograms and verification of the fragmentation pattern of the erythrose naphthylamine reference standard by HR-MS (PDF)

## ■ AUTHOR INFORMATION

### Corresponding Author

\*E-mail: marcus.glomb@chemie.uni-halle.de. Fax: ++049-345-5527341.

### ORCID

Alexander Klaus: 0000-0001-9289-5742  
Tim Baldensperger: 0000-0002-9653-3156  
Marcus A. Glomb: 0000-0001-8826-0808

### Funding

Funding was supported by the Deutsche Forschungsgemeinschaft (DFG, Germany) Research Training Group 2155, ProMoAge.

## Notes

The authors declare no competing financial interest.

## ACKNOWLEDGMENTS

We thank Prof. Dr. K. Tittmann (University of Göttingen, Germany) for providing the vector pET28a(+) encoding human TK, Dr. T. Pfirrmann from the Institute of Physiological Chemistry, Halle, for his support with the expression and purification of human TK, Dr. D. Ströhl from the Institute of Organic Chemistry, Halle, Germany, for recording NMR spectra, and Dr. A. Frolov and A. Laub from the Leibniz Institute of Plant Biochemistry, Halle, Germany, for performing accurate mass determination. We would also like to thank the employees at the KfH Nierenzentrum Halle (Saale), Germany, for their help.

## ABBREVIATIONS USED

AGEs, advanced glycation endproducts; CMA, N<sup>7</sup>-carboxymethyl arginine; CML, N<sup>ε</sup>-carboxymethyl lysine; DHETHDP, dihydroxyethyl-thiamine diphosphate; E4P, erythrulose-4-phosphate; F6P, fructose-6-phosphate; GDH, 5-(4,5-dihydroxy-2-imino-1-imidazolidinyl)norvaline; GOLD, glyoxal-lysine dimer, 1,3-bis(5-amino-5-carboxypentyl)imidazolium salt; GPH, sn-glycero-3-phosphate dehydrogenase; HEL, N<sup>ε</sup>-(2-hydroxyethyl)lysine; HSA, human serum albumin; imidazolone, 5-(2-imino-5-oxo-1-imidazolidinyl)norvaline; iTK, inactivated transketolase; PPP, pentose phosphate pathway; RBCs, red blood cells; R5P, ribose-5-phosphate; S7P, sedoheptulose-7-phosphate; TK, transketolase; TPI, triose phosphate isomerase; ESI, electron spray ionization; sMRM, scheduled multiple-reaction monitoring; CID, collision-induced dissociation; DP, declustering potential; CE, collision energy; CXP, collision cell exit potential; LOD, limit of detection; LOQ, limit of quantitation; RV, recovery rate

## REFERENCES

- (1) Henning, C.; Liehr, K.; Girndt, M.; Ulrich, C.; Glomb, M. A. Extending the spectrum of  $\alpha$ -dicarbonyl compounds in vivo. *J. Biol. Chem.* **2014**, *289*, 28676–28688.
- (2) Brownlee, M. Biochemistry and molecular cell biology of diabetic complications. *Nature* **2001**, *414*, 813–820.
- (3) Henning, C.; Glomb, M. A. Pathways of the Maillard reaction under physiological conditions. *Glycoconjugate J.* **2016**, *33*, 499–512.
- (4) Glomb, M. A.; Monnier, V. M. Mechanism of Protein Modification by Glyoxal and Glycolaldehyde, Reactive Intermediates of the Maillard Reaction. *J. Biol. Chem.* **1995**, *270*, 10017–10026.
- (5) Anderson, M. M.; Requena, J. R.; Crowley, J. R.; Thorpe, S. R.; Heinecke, J. W. The myeloperoxidase system of human phagocytes generates N<sup>ε</sup>-(carboxymethyl)lysine on proteins: a mechanism for producing advanced glycation end products at sites of inflammation. *J. Clin. Invest.* **1999**, *104*, 103–113.
- (6) Fu, M.-X.; Requena, J. R.; Jenkins, A. J.; Lyons, T. J.; Baynes, J. W.; Thorpe, S. R. The Advanced Glycation End Product, N<sup>ε</sup>-(Carboxymethyl)lysine, Is a Product of both Lipid Peroxidation and Glycoxidation Reactions. *J. Biol. Chem.* **1996**, *271*, 9982–9986.
- (7) Thornalley, P. J. Glutathione-dependent detoxification of  $\alpha$ -oxoaldehydes by the glyoxalase system: involvement in disease mechanisms and antiproliferative activity of glyoxalase I inhibitors. *Chem.-Biol. Interact.* **1998**, *111-112*, 137–151.
- (8) Giacco, F.; Brownlee, M. Oxidative Stress and Diabetic Complications. *Circ. Res.* **2010**, *107*, 1058–1070.
- (9) Klaus, A.; Pfirrmann, T.; Glomb, M. A. Transketolase A From *E. Coli* Significantly Suppresses Protein Glycation By Glycolaldehyde And Glyoxal in Vitro. *J. Agric. Food Chem.* **2017**, *65*, 8196–8202.
- (10) Thornalley, P. J.; Jahan, I.; Ng, R. Suppression of the Accumulation of Triosephosphates and Increased Formation of Methylglyoxal in Human Red Blood Cells during Hyperglycaemia by Thiamine In Vitro. *J. Biochem.* **2001**, *129*, 543–549.
- (11) Katare, R.; Oikawa, A.; Cesselli, D.; Beltrami, A. P.; Avolio, E.; Muthukrishnan, D.; Munasinghe, P. E.; Angelini, G.; Emanuelli, C.; Madeddu, P. Boosting the pentose phosphate pathway restores cardiac progenitor cell availability in diabetes. *Cardiovasc. Res.* **2013**, *97*, 55–65.
- (12) Kihm, L. P.; Müller-Krebs, S.; Klein, J.; Ehrlich, G.; Mertes, L.; Gross, M.-L.; Adaikalakoteswari, A.; Thornalley, P. J.; Hammes, H.-P.; Nawroth, P. P.; Zeier, M.; Schwenger, V. Benfotiamine protects against peritoneal and kidney damage in peritoneal dialysis. *J. Am. Soc. Nephrol.* **2011**, *22*, 914–926.
- (13) Berrone, E.; Beltramo, E.; Solimine, C.; Ape, A. U.; Porta, M. Regulation of intracellular glucose and polyol pathway by thiamine and benfotiamine in vascular cells cultured in high glucose. *J. Biol. Chem.* **2006**, *281*, 9307–9313.
- (14) Glomb, M. A.; Lang, G. Isolation and Characterization of Glyoxal-Arginine Modifications. *J. Agric. Food Chem.* **2001**, *49*, 1493–1501.
- (15) Glomb, M. A.; Pfahler, C. Amides are novel protein modifications formed by physiological sugars. *J. Biol. Chem.* **2001**, *276*, 41638–41647.
- (16) Li, H.; Tian, J.; Wang, H.; Yang, S.-Q.; Gao, W.-Y. An Improved Preparation of D-Glyceraldehyde 3-Phosphate and Its Use in the Synthesis of 1-Deoxy-D-xylulose 5-Phosphate. *Helv. Chim. Acta* **2010**, *93*, 1745–1750.
- (17) Solovjeva, O. N.; Kochetov, G. A. Enzymatic synthesis of d-xylulose 5-phosphate from hydroxypyruvate and d-glyceraldehyde-3-phosphate. *J. Mol. Catal. B: Enzym.* **2008**, *54*, 90–92.
- (18) Guérard-Hélaine, C.; Debacker, M.; Clapés, P.; Szekrenyi, A.; Hélaine, V.; Lemaire, M. Efficient biocatalytic processes for highly valuable terminally phosphorylated C5 to C9 D-ketoses. *Green Chem.* **2014**, *16*, 1109–1113.
- (19) Irvine, R. W.; Flanagan, I. L.; MacLeod, J. K.; Collins, J. G.; Williams, J. F. Mass spectrometric studies of the path of carbon in photosynthesis: Positional isotopic analysis of <sup>13</sup>C-labelled 2-oxoaldehydes. *Org. Mass Spectrom.* **1992**, *27*, 1052–1060.
- (20) Sánchez-Moreno, I.; Hélaine, V.; Poupard, N.; Charmantray, F.; Légeret, B.; Hecquet, L.; García-Junceda, E.; Wohlgemuth, R.; Guérard-Hélaine, C.; Lemaire, M. One-Pot Cascade Reactions using Fructose-6-phosphate Aldolase. Efficient Synthesis of D-Arabinose 5-Phosphate, D-Fructose 6-Phosphate and Analogues. *Adv. Synth. Catal.* **2012**, *354*, 1725–1730.
- (21) Mitschke, L.; Parthier, C.; Schröder-Tittmann, K.; Coy, J.; Lüdtke, S.; Tittmann, K. The crystal structure of human transketolase and new insights into its mode of action. *J. Biol. Chem.* **2010**, *285*, 31559–31570.
- (22) Meshalkina, L. E.; Solovjeva, O. N.; Khodak, Y. A.; Drutsa, V. L.; Kochetov, G. A. Isolation and properties of human transketolase. *Biochemistry* **2010**, *75*, 873–880.
- (23) Bayoumi, R. A.; Rosalki, S. B. Evaluation of methods of coenzyme activation of erythrocyte enzymes for detection of deficiency of vitamins B1, B2, and B6. *Clin. Chem.* **1976**, *22*, 327–335.
- (24) Rakete, S.; Glomb, M. A. A novel approach for the quantitation of carbohydrates in mash, wort, and beer with RP-HPLC using 1-naphthylamine for precolumn derivatization. *J. Agric. Food Chem.* **2013**, *61*, 3828–3833.
- (25) Schenk, G.; Duggleby, R. G.; Nixon, P. F. Heterologous expression of human transketolase. *Int. J. Biochem. Cell Biol.* **1998**, *30*, 369–378.
- (26) Huck, J. H.; Struys, E. A.; Verhoeven, N. M.; Jakobs, C. Profiling of Pentose Phosphate Pathway Intermediates in Blood Spots by Tandem Mass Spectrometry. Application to Transaldolase Deficiency. *Clin. Chem.* **2003**, *49*, 1375–1380.
- (27) Hofmann, T.; Bors, W.; Stettmaier, K. Studies on Radical Intermediates in the Early Stage of the Nonenzymatic Browning

Reaction of Carbohydrates and Amino Acids. *J. Agric. Food Chem.* **1999**, *47*, 379–390.

(28) Acharya, A. S.; Manning, J. M. Reaction of glycolaldehyde with proteins: Latent crosslinking potential of  $\alpha$ -hydroxyaldehydes. *Proc. Natl. Acad. Sci. U. S. A.* **1983**, *80*, 3590–3594.

(29) Zhang, F.; Masania, J.; Anwar, A.; Xue, M.; Zehnder, D.; Kanji, H.; Rabbani, N.; Thornalley, P. J. The uremic toxin oxythiamine causes functional thiamine deficiency in end-stage renal disease by inhibiting transketolase activity. *Kidney International. Kidney Int.* **2016**, *90*, 396–403.

(30) Masaru, K.; Atsumi, M.; Ryoko, Y.; Akihiro, I.; Yoshito, O. Erythrocyte Transketolase Activity in Uremia. *Clin. Chim. Acta* **1980**, *108*, 169–177.

(31) Lorenzi, R.; Andrades, M. E.; Bortolin, R. C.; Nagai, R.; Dal-Pizzol, F.; Moreira, J. C. F. Circulating glycolaldehyde induces oxidative damage in the kidney of rats. *Diabetes Res. Clin. Pract.* **2010**, *89*, 262–267.

(32) Madhusudhana Rao, A.; Anand, U.; Anand, C. V. Myeloperoxidase in Chronic Kidney Disease. *Indian J. Clin. Biochem.* **2011**, *26*, 28–31.

(33) Rakete, S.; Nagaraj, R. H. Identification of Kynoxazine, a Novel Fluorescent Product of the Reaction between 3-Hydroxykynurenine and Erythrulose in the Human Lens, and Its Role in Protein Modification\*. *J. Biol. Chem.* **2016**, *291*, 9596–9609.

Reprinted with permission from Klaus, A., Baldensperger, T., Fiedler, R., Girndt, M., Glomb, M. A. Influence of Transketolase-Catalyzed Reactions on the Formation of Glycolaldehyde and Glyoxal Specific Posttranslational Modifications under Physiological Conditions. *Journal of Agricultural and Food Chemistry* **2018**, *66*, 1498-1508. Copyright 2018 American Chemical Society.

## 10.3 Journal of Agricultural and Food Chemistry, 2018, 66, 10835–10843

## Modification and Cross-Linking of Proteins by Glycolaldehyde and Glyoxal: A Model System

Alexander Klaus,<sup>✉</sup> Robert Rau, and Marcus A. Glomb\*<sup>✉</sup>

Institute of Chemistry, Food Chemistry, Martin-Luther-University Halle-Wittenberg, Kurt-Mothes-Straße 2, 06120 Halle/Saale, Germany

**S** Supporting Information

**ABSTRACT:** Highly reactive intermediates of the Maillard reaction, such as glycolaldehyde and glyoxal, are precursors in the modification and cross-linking of proteins. Therefore, we investigated ribonuclease A modified by glycolaldehyde and glyoxal, separately. For the first time, various protein species derived by these aldehydes were successfully separated by ion-exchange chromatography and gel permeation chromatography. Highly cross-linked ribonuclease A was obtained in glycolaldehyde incubations. In contrast, glyoxal predominantly led to modified monomeric protein species. These results were verified by sodium dodecyl sulfate polyacrylamide gel electrophoresis and isoelectric focusing. Quantitation of mono- and bivalent protein modifications of the isolated protein species led to a positive correlation between the degree of protein modification and the change of the isoelectric point and molecular weight, respectively. Glycolaldehyde is easily oxidized to glyoxal. However, significantly lower levels of bivalent glyoxal modifications were detected in glycolaldehyde versus glyoxal incubations (glyoxal–lysine dimer,  $1.58 \pm 0.02$  versus  $2.86 \pm 0.04$  mmol/mol of phenylalanine; glyoxal–lysine amide,  $2.7 \pm 0.1$  versus  $5.6 \pm 0.1$  mmol/mol of phenylalanine). In addition, a novel glycolaldehyde-specific lysine–lysine cross-link was identified and putatively assigned as 1-(5-amino-5-carboxypentyl)-4-(5-amino-5-carboxypentyl-amino)pyridinium salt.

**KEYWORDS:** Maillard reaction, glycolaldehyde, glyoxal, cross-linking, advanced glycation endproducts, ribonuclease A

### ■ INTRODUCTION

At the beginning of the 20th century, Louis-Camille Maillard described the reaction of reducing carbohydrates with amino compounds. The so-called Maillard reaction or non-enzymatic browning leads to a variety of structurally diverse compounds in foodstuffs and *in vivo*. Especially highly reactive carbonyls, such as glycolaldehyde, glyoxal, and methylglyoxal, represent an important class of intermediates. These short-chained aldehydes readily react with amino groups of amino acids, peptides, and proteins to form unstable Schiff base adducts, followed by rearrangement reactions that ultimately lead to advanced glycation end products (AGEs).<sup>1</sup> The association between AGEs and chronic and age-related diseases, such as diabetes, atherosclerosis, and Alzheimer's disease, and their formation pathways *in vivo* has been described in many studies.<sup>2,3</sup> This might also be due to conformational changes; e.g., prolonged glycation of enzymes affects the enzymatic activity.<sup>4</sup> However, specific information about the effects of AGEs on the physicochemical properties of proteins is lacking.

Recently, we quantified glycolaldehyde in the blood of healthy subjects and uremic patients. Furthermore, our working group detected approximately equal levels of free ( $0.58 \pm 0.16 \mu\text{M}$  glycolaldehyde versus  $0.49 \pm 0.05 \mu\text{M}$  glyoxal) and protein-bound glycolaldehyde and glyoxal in blood plasma of healthy subjects.<sup>5–7</sup> The formation of glycolaldehyde *in vivo* can occur non-enzymatically by the degradation of carbohydrates but also enzymatically by the myeloperoxidase system at sites of inflammation.<sup>8,9</sup> On the other side, glyoxal represents the oxidative pendant to glycolaldehyde. It evolves during the Maillard reaction or autoxidation of unsaturated fatty acids via mechanisms including hydroperoxide formation and  $\beta$ -fragmentation or is

formed directly from autoxidation of glucose.<sup>10,11</sup> Both aldehydes react with the  $\epsilon$ -amino group of lysine to the monovalent protein modifications *N*<sup>6</sup>-carboxymethyl lysine (CML) or *N*<sup>6</sup>-glycolyl lysine (GALA) and bivalent cross-links, such as glyoxal–lysine dimer (GOLD). Although they are similar in structure, specific AGEs and reaction patterns were identified. Glyoxal prefers to react with the guanidino function of arginine to form *N*<sup>7</sup>-carboxymethyl arginine (CMA) and dihydroxyimidazolidine.<sup>12</sup> On the other hand, for glycolaldehyde to form these structures, oxidation to glyoxal is a prerequisite.<sup>13</sup>

The aim of the present work was the investigation of protein species and AGEs formed by the reaction of glycolaldehyde and glyoxal, separately. Therefore, we incubated these carbonyl compounds with ribonuclease A (RNase A) under physiological conditions. We were able to separate a variety of protein species with different isoelectric points and degrees of polymerization by ion-exchange chromatography (IEX) and gel permeation chromatography (GPC). Liquid chromatography–tandem mass spectrometry (LC–MS<sup>2</sup>) analysis revealed a direct correlation between the properties of protein species and detected AGEs and also led to the identification of a novel glycolaldehyde-specific lysine–lysine cross-link structure.

### ■ MATERIALS AND METHODS

**Chemicals.** All chemicals of the highest quality available were provided by Sigma-Aldrich (Munich/Steinheim, Germany), Fluka

Received: July 27, 2018

Revised: September 21, 2018

Accepted: September 22, 2018

(Taufkirchen, Germany), Merck (Darmstadt, Germany), Roth (Karlsruhe, Germany), Serva (Heidelberg, Germany), ACROS Organics (Geel, Belgium), Grüssing (Filsium, Germany), Omicron Biochemicals, Inc. (South Bend, IN, U.S.A.), AppliChem (Darmstadt, Germany), and VWR Chemicals (Darmstadt, Germany), unless otherwise indicated.

$N^6$ -Glycoloyl lysine (glycolic acid lysine amide, GALA),  $N^6$ -(2-[(5-amino-5-carboxypentyl)amino]-2-oxoethyl)lysine (glyoxal-lysine amide, GOLA), 2-ammonio-6-({2-[(4-ammonio-5-oxido-5-oxopentyl)amino]-4,5-dihydro-1H-imidazol-5-ylidene}amino)hexanoate (glyoxal imidazolimine, GODIC), CMA,  $N^6$ -(2-hydroxyethyl)lysine (HEL), 5-(2-imino-5-oxo-1-imidazolidinyl)norvaline (imidazolinone),  $N^6$ -carboxymethyl lysine (CML), and 1,3-bis(5-amino-5-carboxypentyl)imidazolium salt (glyoxal-lysine dimer, GOLD) were synthesized or isolated from glyoxal lysine/arginine reaction mixtures as described in the literature.<sup>1,12,14–16</sup>

**Isolation and Characterization of 1-(5-Amino-5-carboxypentyl)-4-(5-amino-5-carboxypentyl-aminopyridinium) Salt (DLP).** Glycolaldehyde (21 mM), glyceraldehyde (21 mM), and  $N^2$ -(*tert*-butoxycarbonyl)-L-lysine (42 mM) were dissolved in triethanolamine-buffered solution (0.1 M, pH 8.5) and incubated at 37 °C for 7 days under deaerated conditions. These conditions were achieved by the addition of 1 mM diethylenetriaminepentaacetic acid (DTPA). Buffer was degassed with helium before incubation. Chromatographic separations were performed with Lobar 310-25 LiChroprep RP-18 (40–63  $\mu$ m) at a flow rate of 5 mL/min. Fractions containing DLP were verified by analytical high-performance liquid chromatography (HPLC), combined, concentrated under vacuum, and diluted with 6 M HCl to a final HCl concentration of 3 M. For quantitative removal of the *tert*-butoxycarbonyl (BOC) protection group, the samples were kept at room temperature for 30 min. Further purification was carried out by preparative HPLC (not shown). As a result of the instability of the obtained product, we were not able to isolate appropriate amounts for nuclear magnetic resonance (NMR). The identity of the bivalent modification was secured by high-resolution mass spectrometry (HR-MS):  $m/z$  353.2182 (found); 353.2183 (calculated for  $C_{17}H_{29}O_4N_4 [M]^+$ ). For semi-quantitative determination of DLP, it was referenced to GOLA by analytical HPLC–fluorescence detection (FLD) after post-column derivatization with *o*-phthalaldehyde, as described below.

**Fluorescence Measurements.** The fluorescent characteristics of DLP were determined in a 96-well plate on a Tecan Infinite M200 plate reader (Tecan, Groedec, Austria) at 25 °C after dilution to appropriate concentrations.

**Model Incubations with RNase A.** In general, incubations were conducted in 0.1 M phosphate buffer at pH 7.4 and 37 °C for 7 days. Glycolaldehyde or glyoxal (4 mM) were incubated with RNase A from bovine pancreas (0.5 mM). Incubations were performed under deaerated conditions. Deaeration was achieved by degassing of the buffer with helium and the addition of 1 mM DTPA using a minimum headspace volume saturated with argon during incubation.

**Model Incubations with  $N^2$ -(*tert*-Butoxycarbonyl)-L-lysine.** The model incubation was conducted in 0.1 M triethanolamine buffer at pH 8.5 and 37 °C under deaerated conditions for 7 days. For mechanistic inquiries,  $N^2$ -(*tert*-butoxycarbonyl)-L-lysine (42 mM) was incubated in the presence of glycolaldehyde (42 mM) or a mixture of glycolaldehyde (21 mM) and glyceraldehyde (21 mM). The addition of 6 M hydrochloric acid to a final concentration of 3 M hydrochloric acid was followed by incubation at room temperature for 30 min. After removal of the acidic solvent in a vacuum concentrator, the residue was resuspended and analyzed by HPLC–MS<sup>2</sup>.

**Glycolaldehyde or Glyceraldehyde Artifact Control Experiment.** Glycolaldehyde or glyceraldehyde was derivatized by reductive amination as described previously.<sup>17</sup> The retention time of the glycolaldehyde naphthylamine derivative was at  $t_R = 11.7$  min.

**IEX.** A XK 26/20 column (GE Healthcare, Uppsala, Sweden) packed with Capto Q (bed height, 100 mm; diameter, 26 mm; GE Healthcare, Uppsala, Sweden), and a peristaltic pump (Ismatec, Wertheim, Germany) was used. The protein concentration was adjusted to 100 mg/mL with equilibration buffer (20 mM 1,3-diaminopropane and 50 mM NaCl at pH 10.5), and 1 mL was applied to the column. Chromatographic separations were performed at a flow rate of 10 mL/min. Protein

samples were fractionated stepwise using the following eluents: 300 mL (20 mM 1,3-diaminopropane and 50 mM NaCl at pH 10.5), 700 mL (20 mM 1,3-diaminopropane and 100 mM NaCl at pH 10.5), 700 mL (20 mM 1,3-diaminopropane and 150 mM NaCl at pH 10.5), 600 mL (20 mM 1,3-diaminopropane and 150 mM NaCl at pH 10.0), 300 mL (20 mM 1,3-diaminopropane and 150 mM NaCl at pH 9.5), 200 mL (20 mM 1,3-diaminopropane and 150 mM NaCl at pH 9.0), 200 mL (20 mM 1,3-diaminopropane and 150 mM NaCl at pH 8.5), and 200 mL (20 mM 1,3-diaminopropane and 1000 mM NaCl at pH 8.5). The 10 mL fractions were collected, and the protein content was determined spectrophotometrically at 595 nm by the Lowry protein assay. As depicted in Figure 1b, the corresponding fractions were combined, dialyzed, and lyophilized until further usage.

**GPC.** A XK 26/100 column (GE Healthcare, Uppsala, Sweden) packed with Superdex 75 prep grade (bed height, 950 mm; diameter, 26 mm; GE Healthcare, Uppsala, Sweden) and a peristaltic pump (Ismatec, Wertheim, Germany) were used. The protein concentration was adjusted to 10 mg/mL with running buffer (10 mM phosphate and 150 mM NaCl at pH 7.4), and 1 mL was applied to the column. Chromatographic separations were performed with running buffer at a flow rate of 0.5 mL/min. Detection was carried out spectrophotometrically at 280 nm. As depicted in Figure 1a, the corresponding fractions were combined, dialyzed, and lyophilized until further usage.

**Sodium Dodecyl Sulfate–Polyacrylamide Gel Electrophoresis (SDS–PAGE).** A Mini-PROTEAN 3 (Bio-Rad, Munich, Germany) and a PowerPac basic power supply (Bio-Rad, Munich, Germany) were used. The protein concentration was adjusted to 0.3  $\mu$ g/ $\mu$ L with Laemmli buffer [pH 6.8, 125 mM Tris–HCl, 0.1 M 1,4-dithiothreitol, 1 mM ethylenediaminetetraacetic acid (EDTA), 4.8% (w/v) sodium dodecyl sulfate (SDS), 20% (w/v) glycerol, and 0.5% (w/v) bromophenol blue]. A total of 10  $\mu$ L (3  $\mu$ g) of sample solutions and 5  $\mu$ L of molecular weight marker were applied to the wells of 5% acrylamide stacking gels with a cross-linking of 1.1% and analyzed on 15% acrylamide separation gels with a cross-linking of 3.3% using a running buffer [0.1 M Tris, 1 M glycine, and 0.5% (w/v) SDS]. The running condition was 10 min at 100 V and 70 min at 200 V. After separation, gels were stained with Coomassie Brilliant Blue G250 following the method of Kang et al.<sup>18</sup> After decoloration, gels were scanned and analyzed with a gel documentation system (ChemiDoc XRS, Bio-Rad, Munich, Germany) and ImageLab software.

**Isoelectric Focusing (IEF).** A Multiphor II (Amersham Biosciences), a Multitemp II thermostatic circulator (LKB Bromma), and an electrophoresis power supply 3501 (Amersham Biosciences) were used. The protein concentration was adjusted to 3  $\mu$ g/ $\mu$ L, and 7.5  $\mu$ L of sample solutions and 1  $\mu$ L of IEF marker were applied on the gels (5% acrylamide with a cross-linking of 1.1% 1.5 M glycerol, 7.3 M urea, 5% SERVALYT 3-10, and 5% SERVALYT 6-8). The running condition was 60 min (550 V, 5 mA, and 3 W), 45 min (600 V, 3 mA, and 3 W), 105 min (1000 V, 3 mA, and 5W), and 15 min (1400 V, 3 mA, and 5W). After separation, gels were soaked in 20% (w/v) trichloroacetic acid for 30 min, washed [5:13:2 (v/v/v) methanol/distilled water/acetic acid] for 30 min, and stained [0.1% (w/v) Serva Violet in distilled water] for 10 min. After decoloration, gels were scanned and analyzed with a gel documentation system (ChemiDoc XRS, Bio-Rad, Munich, Germany) and ImageLab software.

**Acidic and Enzymatic Hydrolysis of Protein Samples.** In brief, acidic and enzymatic hydrolyses of the isolated and purified protein samples were carried out with some modifications as described by Smuda et al.<sup>19</sup> Prior to acidic hydrolysis, protein samples were reduced by the addition of sodium borohydride (80 mM, 1 h, and 4 °C). The efficiencies of both hydrolysis methods were compared and referenced to the content of CML in acidic hydrolysis as 100%.

**Analytical HPLC–MS<sup>2</sup>.** For the determination of post-translational protein modifications, a Jasco PU-2080 Plus quaternary gradient pump with a degasser (LG-2080-02), a quaternary gradient mixer (LG-2080-04), and a Jasco AS-2057 Plus autosampler (Jasco, Gross-Umstadt, Germany) was used. The mass analyses were performed using an Applied Biosystems API 4000 quadrupole instrument (Applied Biosystems/MDS Sciex, Concord, Ontario, Canada) equipped with an API source using an electrospray ionization (ESI) interface. The LC

system was connected directly to the probe of the mass spectrometer. Nitrogen was used as sheath and auxiliary gas. To measure the analytes, the scheduled multiple-reaction monitoring (sMRM) mode of HPLC-MS<sup>2</sup> was used. Chromatographic separations were performed on stainless-steel columns (Waters XSelect HSS T3, 250 × 3 mm, 5 μm, Dublin, IRL) using a flow rate of 0.7 mL/min and a column oven set at 25 °C. The mobile phase used consisted of ultrapure water (solvent A) and MeOH/water [7:3 (v/v), solvent B]. To both solvents (A and B), 1.2 mL/L of heptafluorobutyric acid (HFBA) was added. Samples were injected (5 μL) at 2% B and run isocratic for 2 min, and the gradient then changed to 14% B in 10 min, 87% B in 22 min, and 100% B in 0.5 min, was held at 100% for 7 min, then changed again to 2% B in 2.5 min, and was held for 8 min. Optimized parameters for MS for GALA, GOLA, GOLD, CMA, HEL, CML, and imidazolinone were according to previous works.<sup>5,19,17</sup> Limit of detection and limit of quantitation (LOD/LOQ) and retention times (*t<sub>R</sub>*) were as follows: GALA (0.05/0.15 mmol/mol of phenylalanine (Phe)), *t<sub>R</sub>* = 11.4 min; GOLA (0.15/0.46 mmol/mol of Phe), *t<sub>R</sub>* = 27.6 min; GOLD (0.05/0.15 mmol/mol of Phe), *t<sub>R</sub>* = 27.3 min; CMA (0.06/0.18 mmol/mol of Phe), *t<sub>R</sub>* = 18.6 min; HEL (0.03/0.10 mmol/mol of Phe), *t<sub>R</sub>* = 15.7 min; CML (0.09/0.28 mmol/mol of Phe), *t<sub>R</sub>* = 10.6 min; and imidazolinone, *t<sub>R</sub>* = 18.5 min. Optimized mass spectrometric parameters for GODIC and DLP were as follows: GODIC (0.05/0.15 mmol/mol of Phe; *t<sub>R</sub>* = 29.0 min), *m/z* 343.3/298.4 [declustering potential (DP), 20 V; collision energy (CE), 32.0 eV; cell exit potential (CXP), 7.0 V; quantifier], *m/z* 343.3/183.2 (DP, 20 V; CE, 44.0 eV; CXP, 13.0 V; qualifier 1), *m/z* 343.3/70.2 (DP, 20 V; CE, 74.0 eV; CXP, 11.0 V; qualifier 2); DLP (0.03/0.09 mmol/mol of Phe; *t<sub>R</sub>* = 29.8 min), *m/z* 353.2/84.1 (DP, 85 V; CE, 51.0 eV; CXP, 6.0 V; quantifier), *m/z* 353.2/179.1 (DP, 85 V; CE, 45.0 eV; CXP, 9.5 V; qualifier 1), *m/z* 353.2/224.2 (DP, 85 V; CE, 31.0 eV; CXP, 11.5 V; qualifier 2). To resolve potential matrix interferences, increasing amounts of authentic reference standards were added to mixed aliquots of the sample and a regression of response versus concentration was generated for quantitation.

**Analytical HPLC-FLD.** For determination of the amino acids lysine, arginine, and phenylalanine, a Jasco ternary gradient unit (980-PU-ND) with a degasser (DG-980-50), an autosampler (851-AS), a column oven set at 25 °C, and a fluorescence detector (FP-920, Jasco, Gross-Umstadt, Germany) was used. Chromatographic separations were performed on stainless-steel columns (VYDAC 218TP54, 250 × 4.6 mm, RP18, 5 μm, Hesperia, CA, U.S.A.) using a flow rate of 1.0 mL/min. The mobile phase used was ultrapure water (solvent A) and MeOH/water [7:3 (v/v), solvent B]. To both solvents (A and B), 1.2 mL/L of HFBA was added. The diluted samples were injected (10 μL) at 2% B and run isocratic for 15 min, and the gradient then changed to 90% B in 45 min and 100% B in 1 min, was held at 100% for 10 min, then changed again to 2% B in 4 min, and was held for 15 min. The fluorescence detector was attuned to 340 nm for excitation and 455 nm for emission. Retention times (*t<sub>R</sub>*) were as follows: lysine, *t<sub>R</sub>* = 9.7 min; arginine, *t<sub>R</sub>* = 16.7 min; and phenylalanine, *t<sub>R</sub>* = 35.8 min. Prior, a post-column derivatization reagent was added at 0.5 mL/min. This reagent consisted of 0.8 g of *o*-phthalaldehyde, 24.73 g of boric acid, 2 mL of 2-mercaptoethanol, and 1 g of Brij35 in 1 L of water adjusted to pH 9.75 with KOH.

**Product Ion MS<sup>2</sup> by Collision-Induced Dissociation (CID).** Samples were injected into the HPLC-MS<sup>2</sup> system using a CID experiment after chromatographic separation. The fragmentation spectra of the authentic reference and sample were obtained with the same parameters for DP as described above. Parameters for CE and CXP of DLP were as follows: 30 eV (CE) and 10 V (CXP).

**HR-MS.** Positive-ion high-resolution ESI mass spectra were obtained from an Orbitrap Elite mass spectrometer (Thermo Fisher Scientific, Bremen, Germany) equipped with a HESI electrospray ion source [spray voltage, 4 kV; capillary temperature, 275 °C; source heater temperature, 40 °C; and Fourier transform mass spectrometry (FTMS) resolution, >30 000]. The calculated mass errors were less than 3 ppm. Nitrogen was used as sheath and auxiliary gas. The sample solutions were introduced continuously via a 500 μL Hamilton syringe pump with a flow rate of 5 μL min<sup>-1</sup>. The data were evaluated by the Xcalibur software 2.7 SP1.

**Statistical Analysis.** Analyses were performed at least in duplicate and resulted in coefficients of variation less than 10% for protein modifications detected. All significance tests were performed by a two-sample *t* test with a probability value of 95 or 99%. LOD and LOQ were estimated at a signal/noise ratio of 3 for LOD and 9 for LOQ.

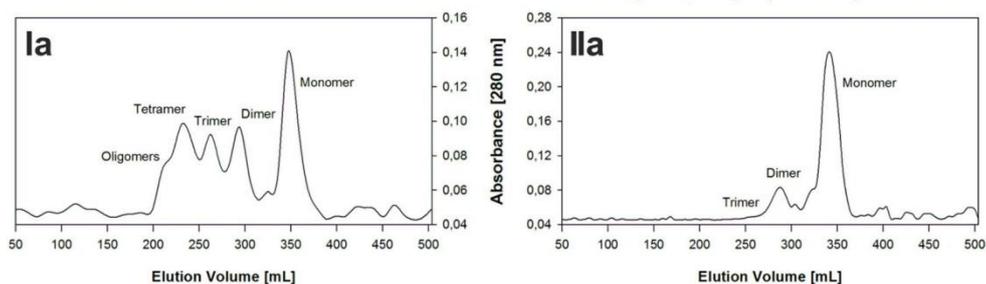
## RESULTS

**In Vitro Model Incubations and Isolation of Protein Species.** To investigate the formation of modified protein species and AGEs by glycolaldehyde or glyoxal, model incubations with RNase A under physiological conditions (pH 7.4, 37 °C, deaerated) were carried out. With the aim to isolate the different protein species, a workup procedure was developed (Figure 1). The quantitation of the AGEs formed during incubations of glycolaldehyde in the presence of RNase A was implemented and compared to the protein modifications derived from glyoxal.

A general survey regarding the isolation and fractionation of the various protein species formed during incubations with RNase A is shown in Figure 1. Different degrees of polymerization were induced by glycolaldehyde compared to glyoxal incubations, as detected by GPC (panels Ia and IIa of Figure 1; for SDS-PAGE, IEF, and 2D-PAGE of total incubations, see Figures SI 1 and SI 2 of the Supporting Information). Modification of RNase A by glyoxal (IIa) predominantly led to monomeric protein species. Only small amounts of the dimer and trimer were verified. In contrast, glycolaldehyde incubations (Ia) led, besides, monomer, dimer, and trimer, also to highly cross-linked polymers. First, fractionation of protein species was achieved by IEX (panels Ib and IIb of Figure 1) using decreasing pH values and increasing NaCl concentrations. Seven fractions (A1–A7) were collected from glycolaldehyde incubations, and nine fractions (X1–X9) were collected from glyoxal incubations. Modifications with high pI (A1–A3 and X1–X3) were characterized by the presence of monomeric species (13.7 kDa). A wide range of dimers (27.4 kDa) to tetramers (54.8 kDa) was detected in the middle fractions (A4 and A5) and predominantly highly cross-linked RNase A in A6 and A7. In contrast, with glyoxal, the fractions X5–X9 showed low amounts of monomeric, dimeric, and trimeric protein species. The isoelectric point (pI) of native RNase is 9.6.<sup>20</sup> According to IEF, the pI of the protein species shifted from alkaline (9.6) to acidic (6.0). Second, after IEX, the fractions were purified by means of GPC and verified by SDS-PAGE and IEF. Figure 2A shows the GPC isolation of mono- to tetrameric and oligomeric species from glycolaldehyde IEX fraction A5. As expected, all of these species were characterized by the same pI range (Figure 2B).

**Quantitation of AGEs in Model Incubations.** As glycolaldehyde and glyoxal incubations led to different protein species, the formation of Maillard-derived protein modifications was investigated. Glyoxal is directly formed by amine-catalyzed oxidation of glycolaldehyde; thus, in addition to specific AGEs, both carbonyl compounds react with lysine or arginine to a broad range of identical AGEs. Values obtained for the total incubation regarding mono- and bivalent protein modifications during reaction with glycolaldehyde or glyoxal are summarized in Table 1. To ensure standardization of AGE to protein content, all values were referenced to the Maillard-inert and acid-stable amino acid Phe. In general, higher amounts of monovalent modifications were detected in glyoxal incubations, except for HEL (9.66 ± 0.2 mmol/mol of Phe versus 19.2 ± 0.6 mmol/mol of Phe), which is formed by the reduction of Schiff base adducts of both carbonyls with lysine by sodium borohydride.<sup>1</sup>

## Gel Permeation Chromatography (GPC)



## Ion Exchange Chromatography (IEX)

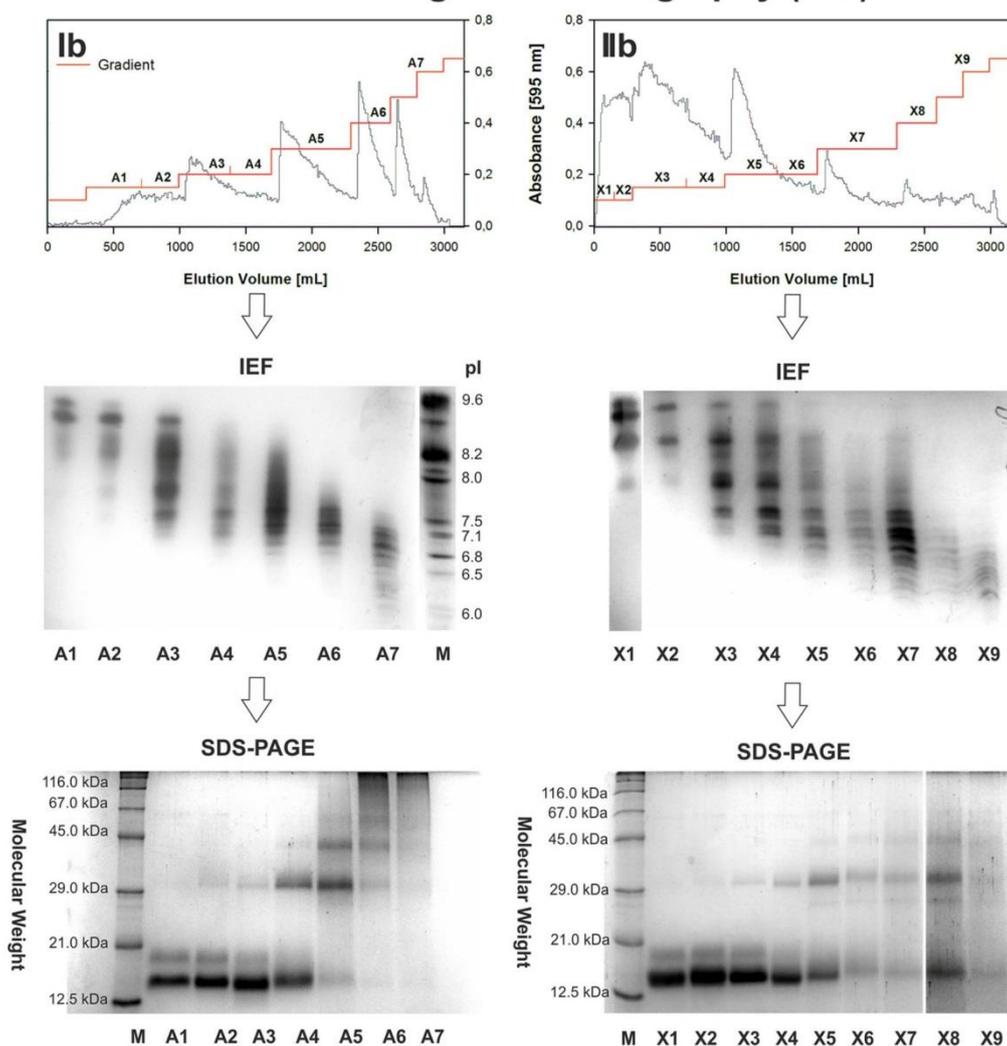


**Figure 1.** Workup scheme for the isolation of protein species resulting from incubations of RNase A with glycolaldehyde (I) and glyoxal (II) by (a) GPC of total incubation and (b) IEX of total incubation. Single IEX fractions were characterized by IEF and SDS-PAGE.

In comparison to glycolaldehyde, concentrations of GALA were 3-fold higher in glyoxal incubations ( $16.9 \pm 0.5$  mmol/mol of Phe versus  $52.2 \pm 0.9$  mmol/mol of Phe). Similar ratios were detected for imidazolinone ( $109 \pm 2$  mmol/mol of Phe versus  $207 \pm 11$  mmol/mol of Phe). It should be noted that

imidazolinone represents a pure artifact generated by the acidic workup procedure and is not directly formed during incubation. However, calculated from the acidic protein hydrolysis, it can serve as a sum parameter for CMA and dihydroxyimidazolinone (G-DH).<sup>12</sup> The examined bivalent modifications

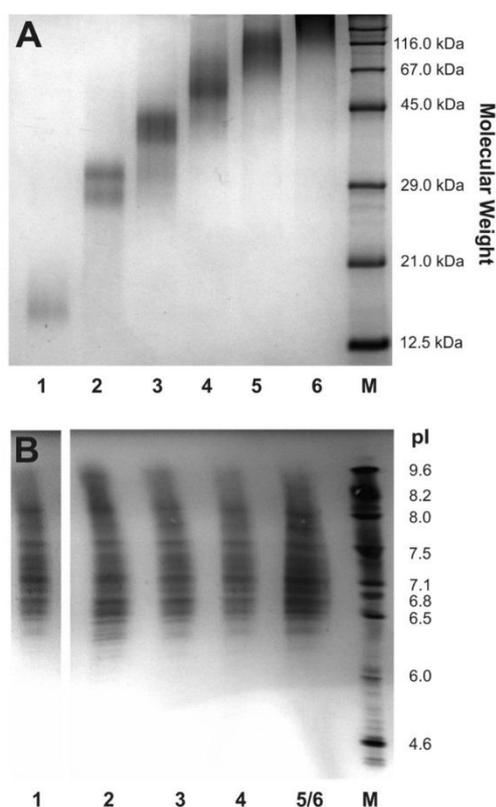


**Figure 2.** (A) SDS-PAGE and (B) IEF of isolated monomer, dimer, trimer, tetramer, and oligomers of fraction A5 after IEX and GPC. Lanes: 1, monomer; 2, dimer; 3, trimer; 4, tetramer; 5, oligomeric fraction 1; 6, oligomeric fraction 2; and M, molecular weight and IEF standard marker.

**Table 1. Comparison of Arginine, Lysine, and AGEs (mmol/mol of Phenylalanine  $\pm$  Standard Deviation) Formed during Incubations of Glycolaldehyde or Glyoxal in the Presence of RNase A (pH 7.4, 7 Days)**

	glycolaldehyde	glyoxal	native RNase A
GALA	16.9 $\pm$ 0.5	52.2 $\pm$ 0.9 <sup>a</sup>	<LOD
CML	94 $\pm$ 2	108 $\pm$ 4 <sup>b</sup>	<LOD
HEL	19.2 $\pm$ 0.6	9.66 $\pm$ 0.2 <sup>b</sup>	<LOQ <sup>c</sup>
CMA	62.7 $\pm$ 0.8	105 $\pm$ 3 <sup>a</sup>	<LOD
imidazolinone	109 $\pm$ 2	207 $\pm$ 11 <sup>a</sup>	<LOD
GOLD	1.58 $\pm$ 0.02	2.86 $\pm$ 0.04 <sup>a</sup>	<LOD
GOLA	2.7 $\pm$ 0.1	5.6 $\pm$ 0.1 <sup>a</sup>	<LOD
GODIC	5.6 $\pm$ 0.2	10.3 $\pm$ 0.3 <sup>a</sup>	<LOD
DLP	0.76 $\pm$ 0.03	<LOD <sup>d</sup>	<LOD
total lysine modification	140	188	<LOQ
total arginine modification	114	217	<LOQ
arginine <sup>e</sup>	1020 $\pm$ 10	670 $\pm$ 10 <sup>a</sup>	1440 $\pm$ 60
lysine <sup>e</sup>	3030 $\pm$ 60	3250 $\pm$ 20 <sup>b</sup>	3420 $\pm$ 60

<sup>a</sup>Significant difference compared to glycolaldehyde incubations by the *t* test ( $\alpha = 0.01$ ). <sup>b</sup>Significant difference compared to glycolaldehyde incubations by the *t* test ( $\alpha = 0.05$ ). <sup>c</sup>LOQ = limit of quantitation. <sup>d</sup>LOD = limit of detection. <sup>e</sup>Unmodified concentration remaining in the incubation setup.

glyoxal–lysine-derived dimer (GOLD), glyoxal–lysine amide (GOLA), and lysine arginine cross-link (GODIC) showed

2-fold higher concentrations in glyoxal incubations. In the presence of glyoxal, arginine side chains were more degraded than lysine (arginine, 670  $\pm$  10 mmol/mol of Phe versus lysine, 3250  $\pm$  20 mmol/mol of Phe). Incubations with glycolaldehyde reflected precisely the opposite (arginine, 1020  $\pm$  10 mmol/mol of Phe versus lysine, 3030  $\pm$  60 mmol/mol of Phe).

Furthermore, AGEs were quantified after chromatographic separation with IEX. Results for mono- and bivalent protein modifications from fraction A1 versus fraction A7 (glycolaldehyde) and from fraction X1 versus fraction X9 (glyoxal) are summarized in Table 2 (all fractions are shown in Figures SI 3 and SI 4 of the Supporting Information). For all measured protein modifications, a significant increase from alkaline to acidic fractions was detected. In general, fractions X1–X9 showed higher amounts of AGEs compared to fractions A1–A7. CML reached the highest concentrations in fractions A7 and X9. It increased from 52.8  $\pm$  0.9 mmol/mol of Phe in fraction A1 to 183  $\pm$  4 mmol/mol of Phe in fraction A7 and from 51  $\pm$  1 mmol/mol of Phe in fraction X1 to 514  $\pm$  50 mmol/mol of Phe in fraction X9. As a result of the acid–base equilibrium of CMA and the high pH value used during IEX, direct quantitation was renounced.<sup>12</sup> This accounted also to GODIC as a result of its alkaline instability. Nevertheless, overall quantitation of mono-valent arginine modification was achieved after acid hydrolysis as imidazolinone. The yield of the bivalent protein modification of GOLD doubled from 1.5  $\pm$  0.06 mmol/mol of Phe in fraction A1 to 3.13  $\pm$  0.08 mmol/mol of Phe in fraction A7 and increased 8-fold between fractions X1 and X9 (from 2.0  $\pm$  0.1 to 16  $\pm$  1 mmol/mol of Phe). The amount of GOLA also increased 8-fold (from 4.8  $\pm$  0.3 mmol/mol of Phe in fraction X1 to 36  $\pm$  3 mmol/mol of Phe in fraction X9) and was more than twice as high as GOLD.

After GPC, it was possible to specifically compare the amounts of AGEs in the monomeric protein species of the above IEX fractions at varying pIs (Figure 3; SDS-PAGE and IEF are shown in Figure SI 5 of the Supporting Information). For glycolaldehyde, quantitation of CML and imidazolinone resulted in a significant increase from monomeric A1 (CML, 63  $\pm$  4 mmol/mol of Phe; imidazolinone, 69  $\pm$  4 mmol/mol of Phe) to monomeric A6 (CML, 192  $\pm$  4 mmol/mol of Phe; imidazolinone, 176  $\pm$  2 mmol/mol of Phe). Thus, the amount of CML and imidazolinone increased with an increasing shift of pI toward the acidic range. HEL showed a slight rise, while GALA and all bivalent protein modifications virtually remained unchanged. For comparison, AGE levels from isolated monomers and dimers of glyoxal and glycolaldehyde IEX fractions basically revealed the same pattern and are shown in Figures SI 6 and Table SI 1 of the Supporting Information. In contrast, Figure 4 shows the AGE levels of glycolaldehyde fraction A5 at a constant pI, comparing monomers to tetramers and oligomers in this specific fraction after separation with GPC. Other than in the isolated monomeric protein species, the cross-linking structures DLP, GOLD, and GOLA showed a clear trend toward higher amounts. On the other hand, CML (170  $\pm$  13 mmol/mol of Phe in monomer versus 122  $\pm$  6 mmol/mol of Phe in oligomer) and imidazolinone (129  $\pm$  9 mmol/mol of Phe in monomer versus 103  $\pm$  5 mmol/mol of Phe in oligomer) decreased slightly. This trend was also verified by glycolaldehyde and glyoxal IEX fractions (Figure SI 7 and Table SI 2 of the Supporting Information).

**Identification of a Novel Glycolaldehyde-Specific Cross-Link.** DLP was detected after enzymatic hydrolysis, demonstrating that this structure is not an artifact generated by

**Table 2.** Comparison of AGEs (mmol/mol of Phenylalanine  $\pm$  Standard Deviation) Formed during Incubations of Glycolaldehyde or Glyoxal in the Presence of RNase A (pH 7.4, 7 Days) after Chromatographic Separation with IEX

fraction	glycolaldehyde		glyoxal	
	A1	A7	X1	X9
GALA	15.1 $\pm$ 0.3	20.7 $\pm$ 0.5	66 $\pm$ 5	74 $\pm$ 7
CML	52.8 $\pm$ 0.9	183 $\pm$ 4 <sup>a</sup>	51 $\pm$ 1	514 $\pm$ 50 <sup>a</sup>
HEL	9.8 $\pm$ 0.1	16.9 $\pm$ 0.1 <sup>a</sup>	9.4 $\pm$ 0.1	15.1 $\pm$ 0.1 <sup>a</sup>
imidazolinone	55 $\pm$ 1	117 $\pm$ 3 <sup>a</sup>	110 $\pm$ 2	370 $\pm$ 30 <sup>a</sup>
GOLD	1.50 $\pm$ 0.06	3.13 $\pm$ 0.08 <sup>a</sup>	2.0 $\pm$ 0.1	16 $\pm$ 1 <sup>a</sup>
GOLA	1.58 $\pm$ 0.01	12.4 $\pm$ 0.3 <sup>a</sup>	4.8 $\pm$ 0.3	36 $\pm$ 3 <sup>a</sup>
DLP	0.58 $\pm$ 0.01	1.59 $\pm$ 0.05	<LOD <sup>b</sup>	<LOD

<sup>a</sup>Significant difference compared to fraction A1 or X1 by the *t* test ( $\alpha = 0.05$ ). <sup>b</sup>LOD = limit of detection.

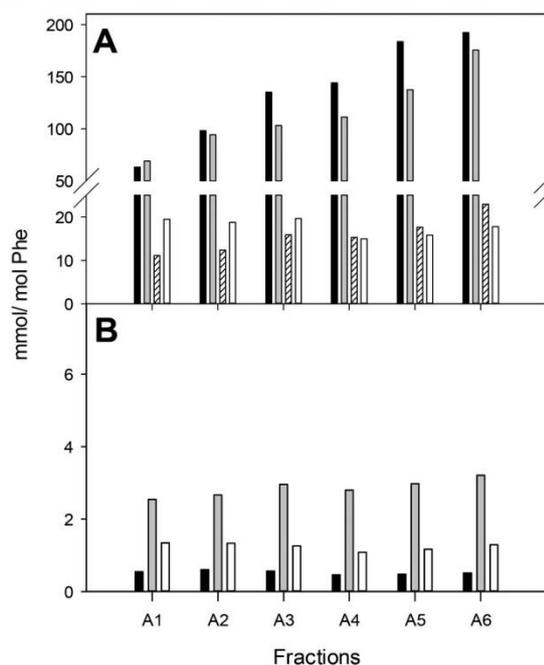


**Figure 3.** Comparison of AGE levels detected in isolated monomers of glycolaldehyde/RNase A incubations after IEX and GPC: (A) closed bars, CML; gray bars, imidazolinone; hatched bars, HEL; and open bars, GALA and (B) closed bars, DLP; gray bars, GOLA; and open bars, GOLD.

the acidic workup procedure. In model incubations of *N*<sup>2</sup>-(*tert*-butoxycarbonyl)-*L*-lysine with glycolaldehyde compared to the presence of both glycolaldehyde and glyceraldehyde, formation of DLP was 6-fold less. Hence, for isolation and purification, incubations were carried out with glyceraldehyde and glycolaldehyde to form quantitatively relevant amounts of DLP. To ensure that DLP formation from glycolaldehyde alone was not an artifact as a result of impurities, glycolaldehyde was analyzed for a possible content of glyceraldehyde. However, glyceraldehyde was not detected. Furthermore, this novel AGE exhibited an ultraviolet (UV) absorbance maximum at 350 nm and fluorescence at 435 nm when excited at 350 nm. Unfortunately, we were not able to isolate appropriate amounts of DLP for NMR. The thus far enriched material was virtually identical to the compound found in the protein incubations (Figure 5). We therefore tentatively assigned the structure based on its similarities with another AGE 1-(5-amino-5-carboxypentyl)-4-(5-amino-5-carboxypentylamino)-3-hydroxy-2,3-dihydro-pyridinium salt (K2P), HR-MS, and collision-induced fragmentation

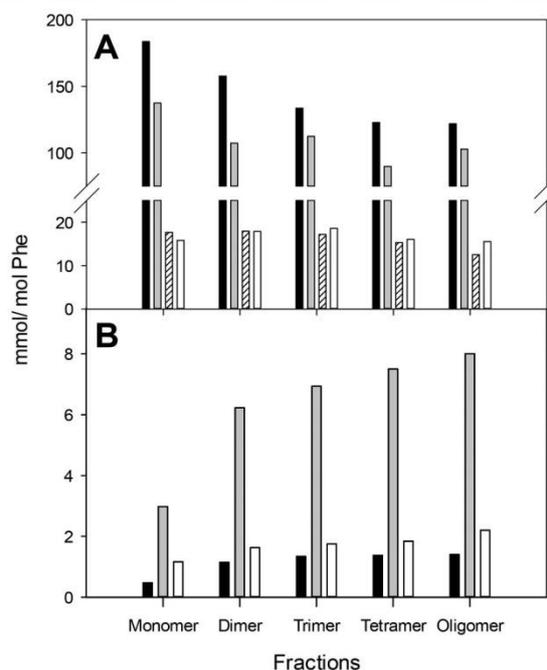


**Figure 4.** Comparison of AGE levels detected in isolated monomer, dimer, trimer, tetramer, and oligomers of fraction A5 of glycolaldehyde/RNase A incubations after IEX and GPC: (A) closed bars, CML; gray bars, imidazolinone; hatched bars, HEL; and open bars, GALA and (B) closed bars, DLP; gray bars, GOLA; and open bars, GOLD.

experiments.<sup>21</sup> As shown in Figure 5, the molecular ion  $[M]^+$  of the pyridinium derivate at *m/z* 353 undergoes multiple fragmentation reactions to *m/z* 308, 224, 179, 130, 95, and 84. Decarboxylation gives the ion at *m/z* 308. The ions at *m/z* 224 and 95 represent the *p*-amino-pyridinium derivate after cleavage of one or two lysine residues, respectively. Elimination of the amino group and cyclization of lysine results in protonated pipelicolic acid at *m/z* 130. Simultaneous loss of water and CO results in the pyrrolinium ion at *m/z* 84. The proposed fragmentation was supported by the elemental composition of the various fragments based on high-resolution mass determination (Figure SI 8 of the Supporting Information).

## DISCUSSION

The present study compares glycosylated RNase A modified by glycolaldehyde and glyoxal, separately. The relevance of glycolaldehyde and glyoxal to modify proteins during the Maillard reaction has been studied previously in model incubations and

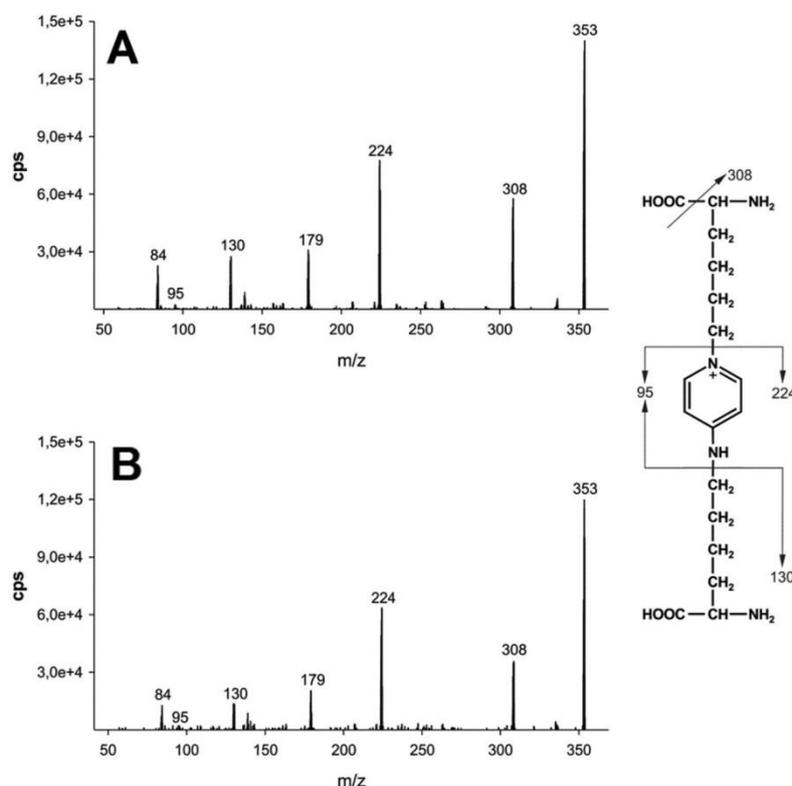


**Figure 5.** Product ion  $MS^2$  of DLP in glycolaldehyde RNase A incubations by CID of  $m/z$  353  $[M]^+$ : (A) authentic reference standard and (B) incubation workup.

*in vivo*.<sup>1,6</sup> However, this is the first time that specific protein species formed by glycolaldehyde or glyoxal were successfully separated by IEX and GPC.

Diverse reaction mechanisms are discussed in the literature to explain the different reaction behaviors of glycolaldehyde and glyoxal. A radical reaction mechanism leading to pyrazine species has been described for glycolaldehyde.<sup>22,23</sup> Nevertheless, both reactive carbonyl compounds form basically the same array of protein modifications, because glycolaldehyde is easily oxidized to glyoxal in the presence of lysine residues.<sup>5</sup> Here, we identified glycolaldehyde as a direct precursor of the novel lysine–lysine cross-link DLP. Thus far, little is known about the formation of such pyridinium salts. Argirov et al. reported the formation of 1-(5-ammonio-5-carboxypentyl)-3-oxido-4-(hydroxymethyl)pyridinium salt (HOP-lysine)<sup>24</sup> as a result of the interaction between lysine, glycolaldehyde, and other carbohydrates. Indeed, on the basis of our preliminary structure elucidation, DLP may represent a potential follow-up structure of K2P after the elimination of water, which was isolated and characterized from human lens protein by Cheng et al.<sup>21</sup> A possible formation pathway of DLP from glycolaldehyde should include an aldol-like cyclization step and the loss of a  $C_1$  unit, like formic acid, as has been suggested for the formation of GOLD.<sup>14</sup>

On the basis of our results obtained for lysine, arginine, and HEL, glycolaldehyde tends to form lysine adducts, whereas arginine clearly represents the major target to be modified by glyoxal. This phenomenon was also observed by Spanneberg et al. using gelatin as a model protein.<sup>13</sup> However, in absolute numbers, we detected a relatively high yield of imidazolinone in glycolaldehyde incubations, which must be due to the

above-discussed oxidation of glycolaldehyde to glyoxal. Other than in gelatin, specifically the presence of cysteine in RNase A may moderate this conversion.<sup>25</sup> Furthermore, oxidation is dependent upon the catalytic action of the  $\epsilon$ -amino moiety of lysine,<sup>6</sup> which may contribute to the potent intermolecular cross-linking potential of glycolaldehyde. Although glycolaldehyde incubations showed higher degrees of polymerization, lower amounts of the bivalent modifications GOLD and GOL were detected in comparison to glyoxal. This suggests that glycolaldehyde-modified protein species are more intermolecularly cross-linked and glyoxal-modified protein species are more intramolecularly cross-linked. Whether inter- or intramolecular lysine–arginine cross-links are formed should depend upon the availability of a lysine residue to a nearby arginine residue. This situation is only given twice in the RNase A molecule.<sup>26,27</sup> In both incubations, we identified GODIC (glycolaldehyde,  $5.6 \pm 0.2$  mmol/mol of Phe, versus glyoxal,  $10.3 \pm 0.3$  mmol/mol of Phe) as the major bivalent cross-link when compared to GOLD (glycolaldehyde,  $1.58 \pm 0.02$  mmol/mol of Phe versus glyoxal,  $2.86 \pm 0.04$  mmol/mol of Phe) and GOL (glycolaldehyde,  $2.7 \pm 0.1$  mmol/mol of Phe versus glyoxal,  $5.6 \pm 0.1$  mmol/mol of Phe). In contrast, Glomb et al. reported GOLD as the major lysine–lysine cross-link structure. However, the ratio of GOLD and GOL strongly depends upon the excess of glyoxal increasing at high concentrations.<sup>14</sup> The increase of bivalent modifications in fraction A5 from monomer to oligomer highlights GOL and GOLD as the quantitatively major structures for intermolecular cross-linking. However, only minor amounts of dimeric and trimeric protein species were observed in glyoxal incubations. On the basis of the data in Table SI 2 of the Supporting

Information, GOLD and GOL A derive specifically from the reaction with glyoxal and, consequently, are of minor relevance in the cross-linking observed in glycolaldehyde incubations. Therefore, the cross-linking potential of glycolaldehyde must be attributed to the formation of aldol condensation products, such as DLP and other yet unknown bivalent AGEs. Initially, glycolaldehyde and glyoxal become reversibly bound to lysine or arginine residues in the protein. However, the considerably faster formation of AGEs by the reaction of glyoxal with arginine when compared to lysine might be the main cause of the differences observed in the reaction behavior of both carbonyls. Furthermore, for a quantitative reaction of glycolaldehyde with arginine, an oxidation step is a prerequisite.<sup>5</sup>

The amount of CML in monomeric protein species correlated with decreasing pI. This is due to the fact that modification in the form of CML significantly changes the pI by direct addition of an extra carboxylic acid group but also by the altered pK<sub>a</sub> of the modified amine group of lysine. The same principle accounts for CMA; however, in this case, resulting from hydrolysis of initially formed dihydroxyimidazolidine. Cotham et al. demonstrated that arginine modification measured as imidazolinone is the primary product formed by the reaction of glyoxal with RNase A.<sup>28</sup> They also showed that Arg 39 and Arg 85 are the favored sites of protein modification. These data are in line with our findings. However, both incubations showed higher amounts of CML in monomeric species from fractions A3 to A6 (glycolaldehyde; Figure 3) and from fractions X3 to X6 (glyoxal; Figure SI 6 of the Supporting Information). The reason for this might be based on the structure of RNase A. There are four arginine residues in the molecule, and only three of them were detected to be modified by glyoxal.<sup>28</sup> In contrast, Dai et al. showed that 6 of 10 lysine residues were modified.<sup>24</sup> In sight of the present data, this suggests that glyoxal initially reacts with arginine residues and then delayed with lysine. This is in line with data observed for the reaction of methylglyoxal with bovine serum albumin.<sup>29</sup> All bivalent modifications in the monomeric protein species are intramolecular cross-linked by definition. They cause the loss of two alkaline amino groups. However, monomeric protein species never showed an increase of bivalent modifications from fractions A1 to A6, because they were quantitatively of minor relevance. This fact supports the hypothesis that decreasing pI of protein species is mainly induced by increasing amounts of monovalent AGEs, including different sites of modification.

In conclusion, we were able to separate glycolaldehyde- and glyoxal-derived protein species of RNase A by IEX and GPC. Quantitation of protein modifications in the various protein species extended the understanding of the physicochemical alteration of proteins by glycation. Furthermore, the identification of the novel glycolaldehyde-specific cross-link DLP led to new insights into the differences of the reaction behavior of glycolaldehyde and glyoxal. A full structure elucidation as well as the formation mechanism will be clarified in a following publication.

## ■ ASSOCIATED CONTENT

### Supporting Information

The Supporting Information is available free of charge on the ACS Publications website at DOI: 10.1021/acs.jafc.8b04023.

Additional information on the fractionation of protein species formed during incubations, quantitation of AGEs, and mass spectrometric data of DLP (PDF)

## ■ AUTHOR INFORMATION

### Corresponding Author

\*Fax: ++049-345-5527341. E-mail: [marcus.glomb@chemie.uni-halle.de](mailto:marcus.glomb@chemie.uni-halle.de).

### ORCID

Alexander Klaus: 0000-0001-9289-5742

Marcus A. Glomb: 0000-0001-8826-0808

### Notes

The authors declare no competing financial interest.

## ■ ACKNOWLEDGMENTS

The authors thank Dr. A. Frolov from the Leibniz Institute of Plant Biochemistry, Halle, Germany, for performing accurate mass determination.

## ■ ABBREVIATIONS USED

AGE, advanced glycation endproduct; CMA, N<sup>7</sup>-carboxymethyl arginine; CML, N<sup>6</sup>-carboxymethyl lysine; DTPA, diethylene-triaminepentaacetic acid; DLP, 1-(5-amino-5-carboxypentyl)-4-(5-amino-5-carboxypentyl-amino)pyridinium salt; GALA, glycolic acid lysine amide, N<sup>6</sup>-glycoloyl lysine; GODIC, glyoxal imidazolinone, 2-ammonio-6-({2-[(4-ammonio-5-oxido-5-oxopentyl)amino]-4,5-dihydro-1H-imidazol-5-ylidene}amino)-hexanoate; GOL A, glyoxal-lysine amide, N<sup>6</sup>-(2-[(5-amino-5-carboxypentyl)amino]-2-oxoethyl)lysine; GOLD, glyoxal-lysine dimer, 1,3-bis(5-amino-5-carboxypentyl)imidazolium salt; HEL, N<sup>6</sup>-(2-hydroxyethyl)lysine; imidazolinone, 5-(2-imino-5-oxo-1-imidazolidinyl)norvaline; K2P, 1-(5-amino-5-carboxypentyl)-4-(5-amino-5-carboxypentylamino)-3-hydroxy-2,3-dihydropyridinium salt; Phe, phenylalanine; RNase A, ribonuclease A from bovine pancreas; IEX, ion-exchange chromatography; GPC, gel permeation chromatography; HFBA, heptafluorobutyric acid; ESI, electrospray ionization; sMRM, scheduled multiple-reaction monitoring; t<sub>R</sub>, retention time; CID, collision-induced dissociation; DP, declustering potential; CE, collision energy; CXP, collision cell exit potential

## ■ REFERENCES

- (1) Glomb, M. A.; Monnier, V. M. Mechanism of protein modification by glyoxal and glycolaldehyde, reactive intermediates of the Maillard reaction. *J. Biol. Chem.* **1995**, *270*, 10017–10026.
- (2) Miyazawa, T.; Nakagawa, K.; Shimasaki, S.; Nagai, R. Lipid glycation and protein glycation in diabetes and atherosclerosis. *Amino Acids* **2012**, *42*, 1163–1170.
- (3) Smith, M. A.; Taneda, S.; Richey, P. L.; Miyata, S.; Yan, S. D.; Stern, D.; Sayre, L. M.; Monnier, V. M.; Perry, G. Advanced Maillard reaction end products are associated with Alzheimer disease pathology. *Proc. Natl. Acad. Sci. U. S. A.* **1994**, *91*, 5710–5714.
- (4) Dinda, A. K.; Tripathy, D. R.; Dasgupta, S. Glycation of Ribonuclease A affects its enzymatic activity and DNA binding ability. *Biochimie* **2015**, *118*, 162–172.
- (5) Klaus, A.; Baldensperger, T.; Fiedler, R.; Girndt, M.; Glomb, M. A. Influence of transketolase-catalyzed reactions on the formation of glycolaldehyde and glyoxal specific posttranslational modifications under physiological conditions. *J. Agric. Food Chem.* **2018**, *66*, 1498–1508.
- (6) Henning, C.; Liehr, K.; Girndt, M.; Ulrich, C.; Glomb, M. A. Analysis and chemistry of novel protein oxidation markers in vivo. *J. Agric. Food Chem.* **2018**, *66*, 4692–4701.
- (7) Henning, C.; Liehr, K.; Girndt, M.; Ulrich, C.; Glomb, M. A. Extending the spectrum of  $\alpha$ -dicarbonyl compounds in vivo. *J. Biol. Chem.* **2014**, *289*, 28676–28688.

- (8) Voigt, M.; Smuda, M.; Pfahler, C.; Glomb, M. A. Oxygen-dependent fragmentation reactions during the degradation of 1-deoxy-D-erythro-hexo-2,3-diulose. *J. Agric. Food Chem.* **2010**, *58*, 5685–5691.
- (9) Anderson, M. M.; Hazen, S. L.; Hsu, F. F.; Heinecke, J. W. Human neutrophils employ the myeloperoxidase-hydrogen peroxide-chloride system to convert hydroxy-amino acids into glycolaldehyde, 2-hydroxypropanal, and acrolein. A mechanism for the generation of highly reactive alpha-hydroxy and alpha,beta-unsaturated aldehydes by phagocytes at sites of inflammation. *J. Clin. Invest.* **1997**, *99*, 424–432.
- (10) Miakar, A.; Spitteller, G. Reinvestigation of lipid peroxidation of linolenic acid. *Biochim. Biophys. Acta, Lipids Lipid Metab.* **1994**, *1214*, 209–220.
- (11) Wells-Knecht, K. J.; Zyzak, D. V.; Litchfield, J. E.; Thorpe, S. R.; Baynes, J. W. Mechanism of autoxidative glycosylation. Identification of glyoxal and arabinose as intermediates in the autoxidative modification of proteins by glucose. *Biochemistry* **1995**, *34*, 3702–3709.
- (12) Glomb, M. A.; Lang, G. Isolation and characterization of glyoxal-arginine modifications. *J. Agric. Food Chem.* **2001**, *49*, 1493–1501.
- (13) Spanneberg, R.; Osswald, F.; Kolesov, I.; Anton, W.; Radusch, H.-J.; Glomb, M. A. Model studies on chemical and textural modifications in gelatin films by reaction with glyoxal and glycolaldehyde. *J. Agric. Food Chem.* **2010**, *58*, 3580–3585.
- (14) Glomb, M. A.; Pfahler, C. Amides are novel protein modifications formed by physiological sugars. *J. Biol. Chem.* **2001**, *276*, 41638–41647.
- (15) Iijima, K.; Murata, M.; Takahara, H.; Irie, S.; Fujimoto, D. Identification of N<sup>ω</sup>-carboxymethylarginine as a novel acid-labile advanced glycation end product in collagen. *Biochem. J.* **2000**, *347*, 23–27.
- (16) Lederer, M. O.; Klaiber, R. G. Cross-linking of proteins by Maillard processes: Characterization and detection of lysine-arginine cross-links derived from glyoxal and methylglyoxal. *Bioorg. Med. Chem.* **1999**, *7*, 2499–2507.
- (17) Klaus, A.; Pfirmann, T.; Glomb, M. A. Transketolase A from *E. coli* significantly suppresses protein glycation by glycolaldehyde and glyoxal in vitro. *J. Agric. Food Chem.* **2017**, *65*, 8196–8202.
- (18) Kang, D.-H.; Gho, Y.-S.; Suh, M.-K.; Kang, C.-H. Highly sensitive and fast protein detection with coomassie brilliant blue in sodium dodecyl sulfate–polyacrylamide gel electrophoresis. *Bull. Korean Chem. Soc.* **2002**, *23*, 1511–1512.
- (19) Smuda, M.; Henning, C.; Raghavan, C. T.; Johar, K.; Vasavada, A. R.; Nagaraj, R. H.; Glomb, M. A. Comprehensive analysis of maillard protein modifications in human lenses: Effect of age and cataract. *Biochemistry* **2015**, *54*, 2500–2507.
- (20) Tanford, C.; Hauenstein, J. D. Hydrogen ion equilibria of ribonuclease I. *J. Am. Chem. Soc.* **1956**, *78*, 5287–5291.
- (21) Cheng, R.; Feng, Q.; Argirov, O. K.; Ortwerth, B. J. Structure elucidation of a novel yellow chromophore from human lens protein. *J. Biol. Chem.* **2004**, *279*, 45441–45449.
- (22) Namiki, M.; Hayashi, T. A new mechanism of the maillard reaction involving sugar fragmentation and free radical formation. In *The Maillard Reaction in Foods and Nutrition*; Waller, G. R., Feather, M. S., Eds.; American Chemical Society (ACS): Washington, D.C., 1983; ACS Symposium Series, Vol. 215, Chapter 2, pp 21–46, DOI: 10.1021/bk-1983-0215.ch002.
- (23) Hofmann, T.; Bors, W.; Stettmaier, K. Studies on radical intermediates in the early stage of the nonenzymatic browning reaction of carbohydrates and amino acids. *J. Agric. Food Chem.* **1999**, *47*, 379–390.
- (24) Argirov, O. K.; Lin, B.; Olesen, P.; Ortwerth, B. J. Isolation and characterization of a new advanced glycation endproduct of dehydroascorbic acid and lysine. *Biochim. Biophys. Acta, Gen. Subj.* **2003**, *1620*, 235–244.
- (25) Schwarzenbolz, U.; Mende, S.; Henle, T. Model studies on protein glycation. Influence of cysteine on the reactivity of arginine and lysine residues toward glyoxal. *Ann. N. Y. Acad. Sci.* **2008**, *1126*, 248–252.
- (26) Dai, Z.; Wang, B.; Sun, G.; Fan, X.; Anderson, V. E.; Monnier, V. M. Identification of glucose-derived cross-linking sites in ribonuclease A. *J. Proteome Res.* **2008**, *7*, 2756–2768.
- (27) Brock, J. W. C.; Hinton, D. J. S.; Cotham, W. E.; Metz, T. O.; Thorpe, S. R.; Baynes, J. W.; Ames, J. M. Proteomic Analysis of the Site Specificity of Glycation and Carboxymethylation of Ribonuclease. *J. Proteome Res.* **2003**, *2*, 506–513.
- (28) Cotham, W. E.; Metz, T. O.; Ferguson, P. L.; Brock, J. W. C.; Hinton, D. J. S.; Thorpe, S. R.; Baynes, J. W.; Ames, J. M. Proteomic analysis of arginine adducts on glyoxal-modified ribonuclease. *Mol. Cell. Proteomics* **2004**, *3*, 1145–1153.
- (29) Lo, T. W.; Westwood, M. E.; McLellan, A. C.; Selwood, T.; Thornalley, P. J. Binding and modification of proteins by methylglyoxal under physiological conditions. A kinetic and mechanistic study with N<sup>ε</sup>-acetylarginine, N<sup>ε</sup>-acetylcysteine, and N<sup>ε</sup>-acetyllysine, and bovine serum albumin. *J. Biol. Chem.* **1994**, *269*, 32299–32305.

## 11 Anhang

### 11.1 Supporting Information zu Journal of Agricultural and Food Chemistry, 2018, 66, 1598-1508

#### Influence of Transketolase-catalyzed Reactions on the Formation of Glycolaldehyde and Glyoxal Specific Posttranslational Modifications under Physiological Conditions

##### Author Names and Affiliations

Alexander Klaus<sup>#</sup>, Tim Baldensperger<sup>#</sup>, Roman Fiedler<sup>+</sup>, Matthias Girndt<sup>+</sup> and Marcus A. Glomb<sup>#</sup>

<sup>#</sup>Institute of Chemistry, Food Chemistry, Martin-Luther-University Halle-Wittenberg, Kurt-Mothes-Str. 2, 06120 Halle/Saale, Germany

<sup>+</sup>Department of Internal Medicine II, Martin-Luther-University Halle-Wittenberg, Ernst-Grube-Str. 40, 06120 Halle/Saale, Germany

##### Corresponding Author

Prof. Marcus A. Glomb

Kurt-Mothes-Strasse 2, D-06120 Halle/Saale, Germany; Telephone: +49-345-5525784; Fax: +49-345-5527341; email: marcus.glomb@chemie.uni-halle.de

## SUPPORTING INFORMATION

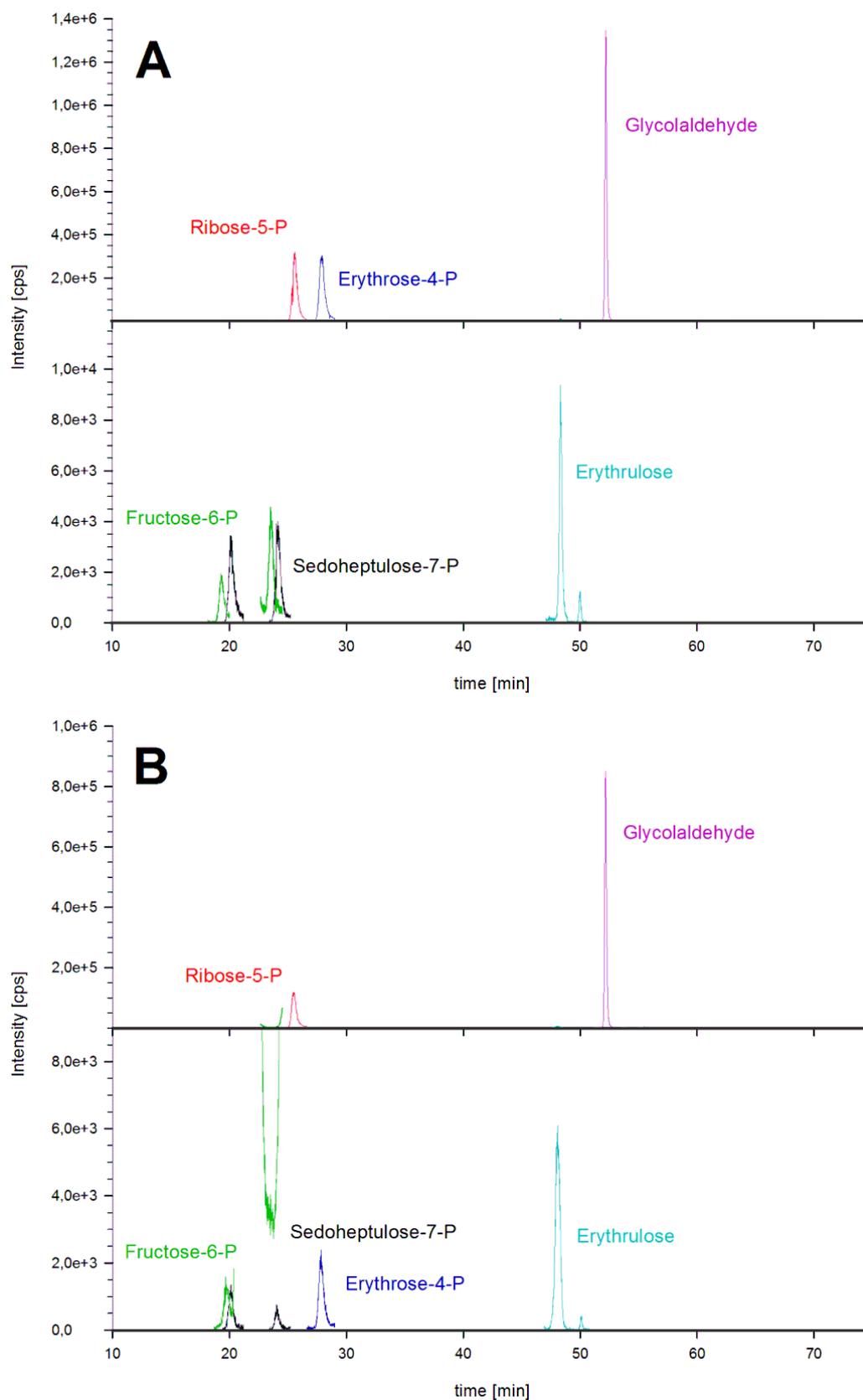


**Figure S1:** LC-MS<sup>2</sup> chromatogram of sugar and sugar phosphate standards (A) and sugar and sugar phosphates detected in human red blood cells (B).

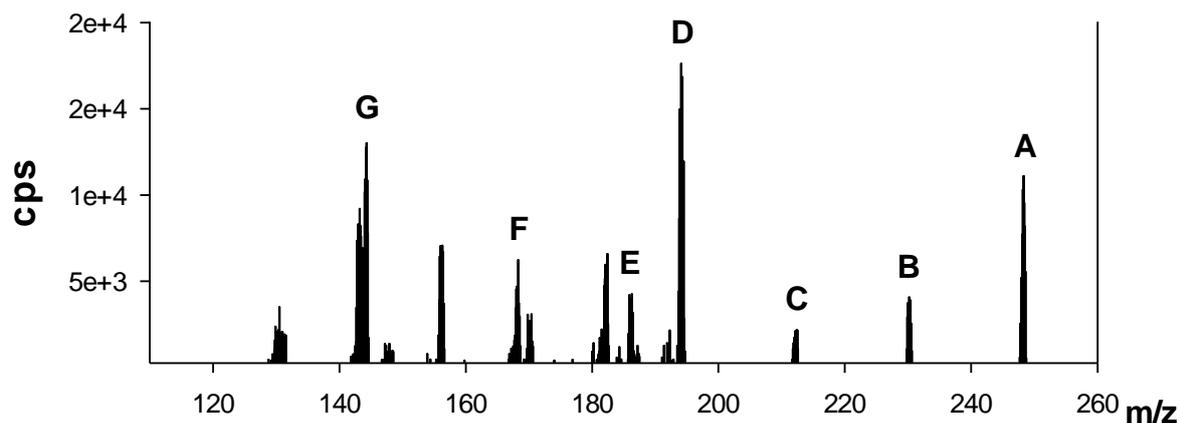


**Figure S2:** Verification of the fragmentation pattern of the erythrulose naphthylamine reference standard by high resolution mass determination: **A**)  $m/z$  248.1287 (found), 248.1281 (calculated for  $C_{14}H_{18}O_3N [M + H]^+$ ); **B**)  $m/z$  230.1181 (found), 230.1176 (calculated for  $C_{14}H_{16}O_2N [M + H]^+$ ); **C**)  $m/z$  212.1075 (found), 212.1070 (calculated for  $C_{14}H_{14}ON [M + H]^+$ ); **D**)  $m/z$  194.0969 (found), 194.0964 (calculated for  $C_{14}H_{12}N [M + H]^+$ ); **E**)  $m/z$  186.0918 (found), 186.0913 (calculated for  $C_{12}H_{12}ON [M + H]^+$ ); **F**)  $m/z$  168.0812 (found), 168.0808 (calculated for  $C_{12}H_{10}N [M + H]^+$ ); **G**)  $m/z$  144.0811 (found), 144.0808 (calculated for  $C_{10}H_{10}N [M + H]^+$ ).

## **11.2 Supporting Information zu Journal of Agricultural and Food Chemistry, 2018, 66, 10835–10843**

Modification and Crosslinking of Proteins by Glycolaldehyde and Glyoxal – a Model System

### **Author Names and Affiliations**

Alexander Klaus, Robert Rau and Marcus A. Glomb

Institute of Chemistry, Food Chemistry, Martin-Luther-University Halle-Wittenberg, Kurt-Mothes-Str. 2, 06120 Halle/Saale, Germany

### **Corresponding Author**

Prof. Marcus A. Glomb

Kurt-Mothes-Strasse 2, D-06120 Halle/Saale, Germany; Telephone: +49-345-5525784; Fax: +49-345-5527341; email: [marcus.glomb@chemie.uni-halle.de](mailto:marcus.glomb@chemie.uni-halle.de)

## SUPPORTING INFORMATION

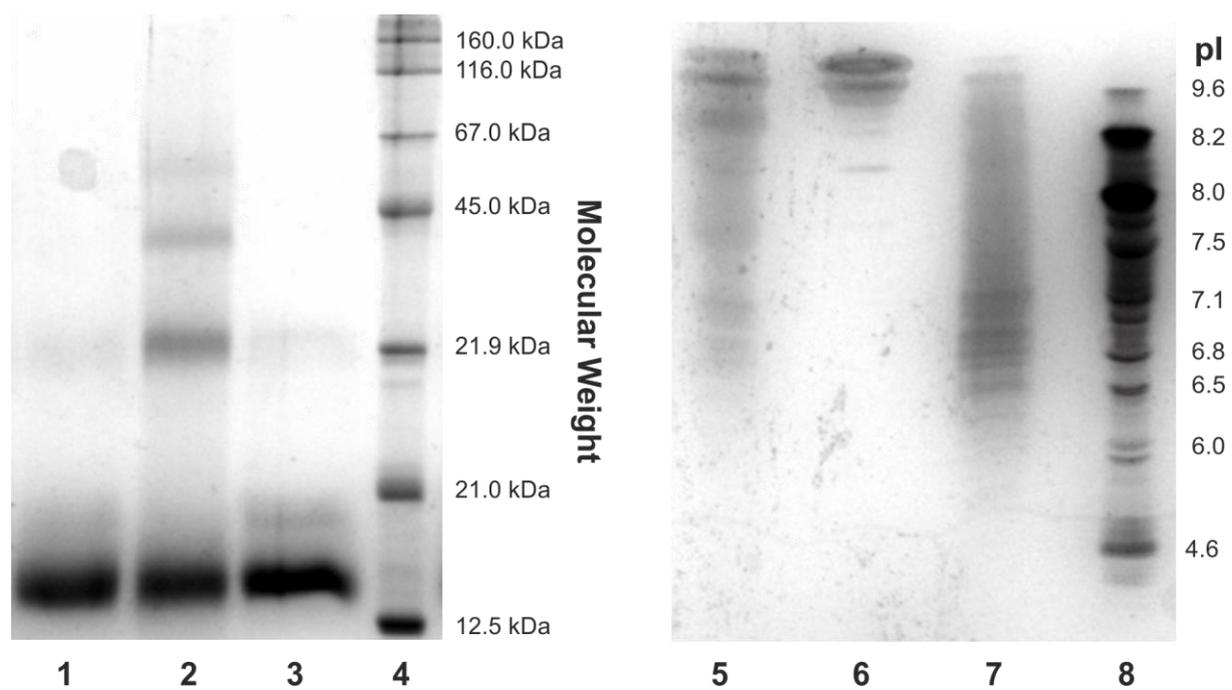


**Figure SI 1:** SDS-PAGE (Samples 1-4) and IEF (Samples 5-8) of the modification of RNase A. Lanes: 1, RNase A standard; 2, glycolaldehyde (total incubation); 3, glyoxal (total incubation); 4, molecular weight standard; 5, glyoxal (total incubation); 6, RNase A standard; 7, glycolaldehyde (total incubation); 8, IEF standard.

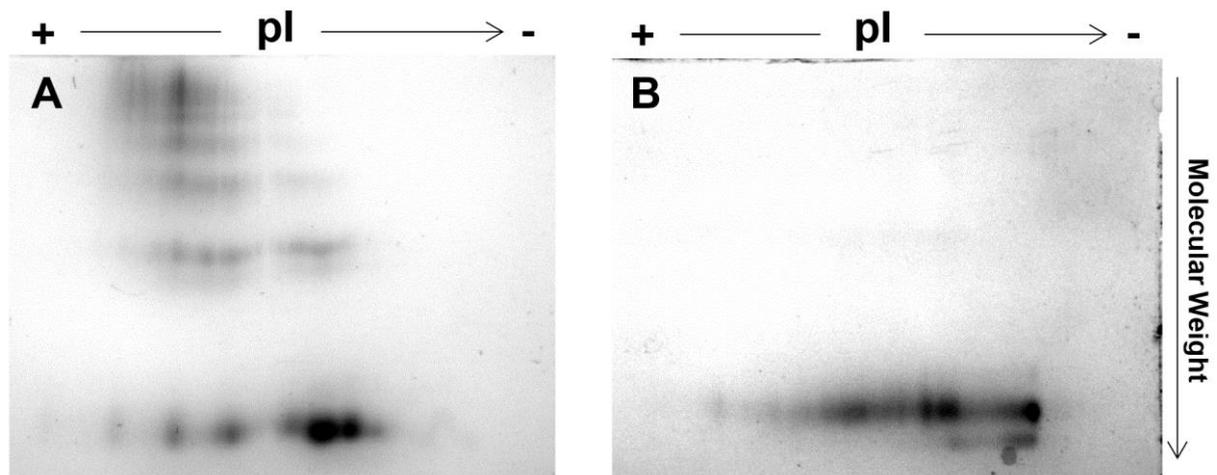


**Figure SI 2:** 2D-PAGE (IPG 3-10, total acrylamide concentration = 15%, cross-linker level = 3.3%) of total glycolaldehyde/RNase A (A) and total glyoxal/RNase A (B) incubations.

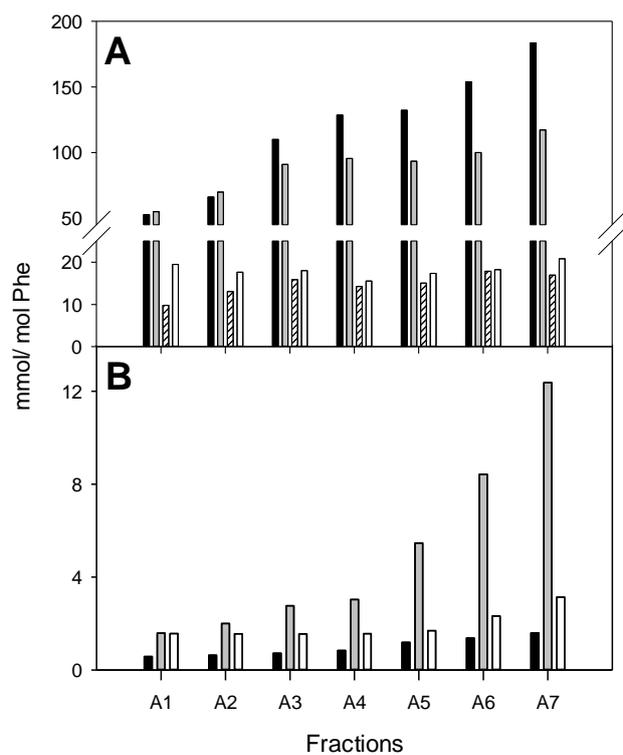


**Figure SI 3:** Comparison of AGE levels detected in isolated fractions of glycolaldehyde/RNase A incubations after ion exchange chromatography: A) closed bars, CML; grey bars, imidazolinone; hatched bars, HEL and open bars, GALA; B) closed bars, DLP; grey bars, GOLLA and open bars, GOLD.

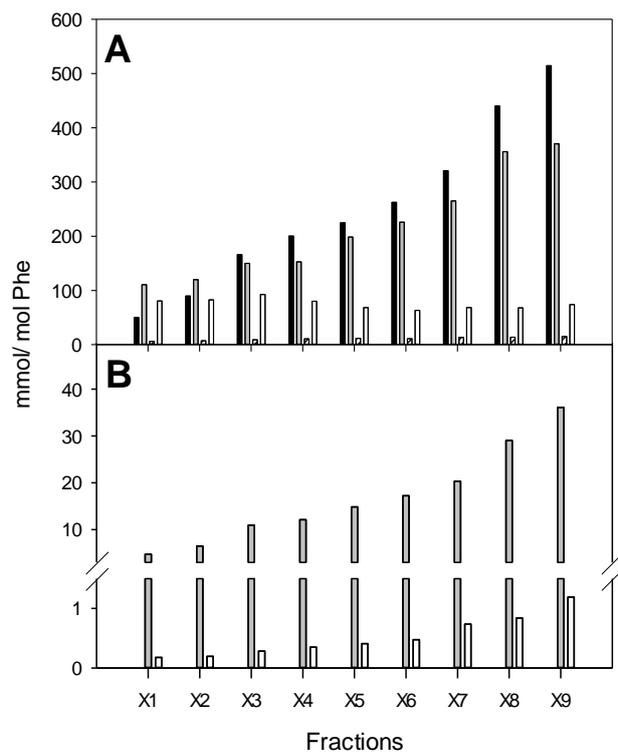


**Figure SI 4:** Comparison of AGE levels detected in isolated fractions of glyoxal/RNase A incubations after ion exchange chromatography: A) closed bars, CML; grey bars, imidazolinone; hatched bars, HEL and open bars, GALA; B) grey bars, GOLA and open bars, GOLD.

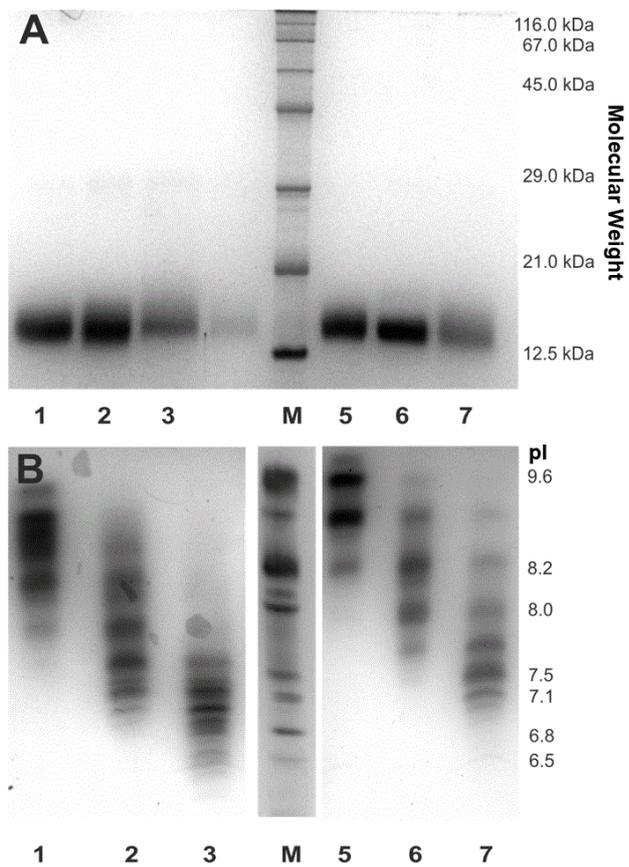


**Figure SI 5:** SDS-PAGE (A) and IEF (B) of isolated monomers from ion exchange fractions by gel permeation chromatography. Lanes: 1, fraction A1; 2, fraction A3; 3, fraction A5; M, molecular weight and IEF standard marker; 5, fraction X1; 6, fraction X3; 7, fraction X5.

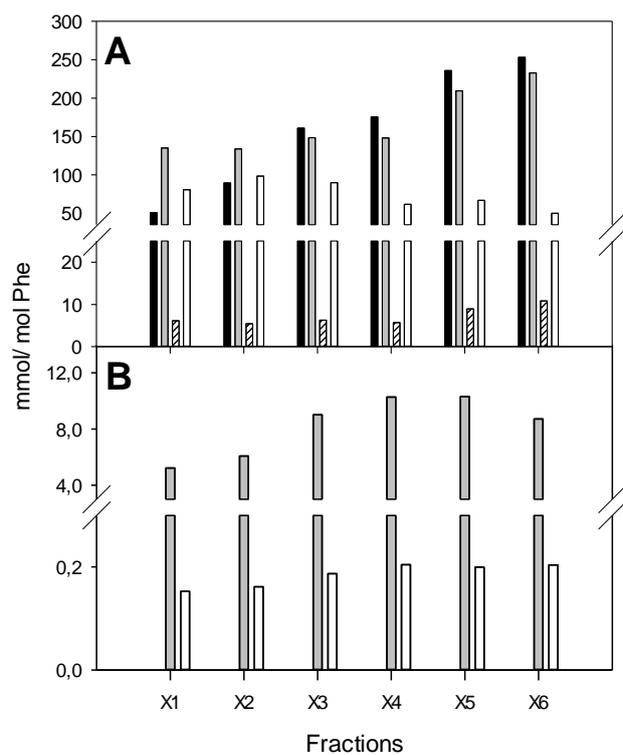


**Figure SI 6:** Comparison of AGE levels detected in isolated monomers of glyoxal/RNase A incubations after ion exchange chromatography and gel permeation chromatography: A) closed bars, CML; grey bars, imidazolinone; hatched bars, HEL and open bars, GALA; B) grey bars, GOLA and open bars, GOLD.

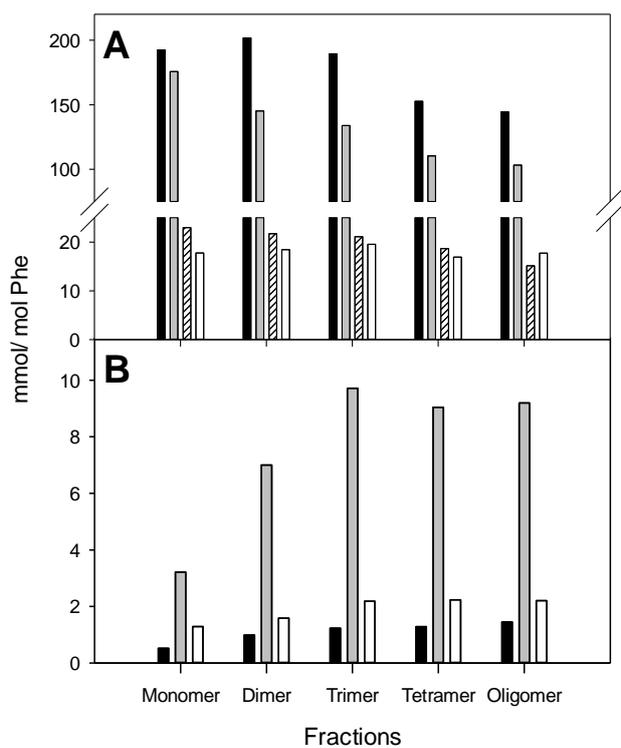


**Figure SI 7:** Comparison of AGE levels detected in isolated monomer, dimer, trimer, tetramer and oligomers of fraction A6 after ion exchange chromatography of glycolaldehyde/RNase A incubation and gel permeation chromatography: A) closed bars, CML; grey bars, imidazolinone; hatched bars, HEL and open bars, GALA; B) closed bars, DLP; grey bars, GOL and open bars, GOLD.

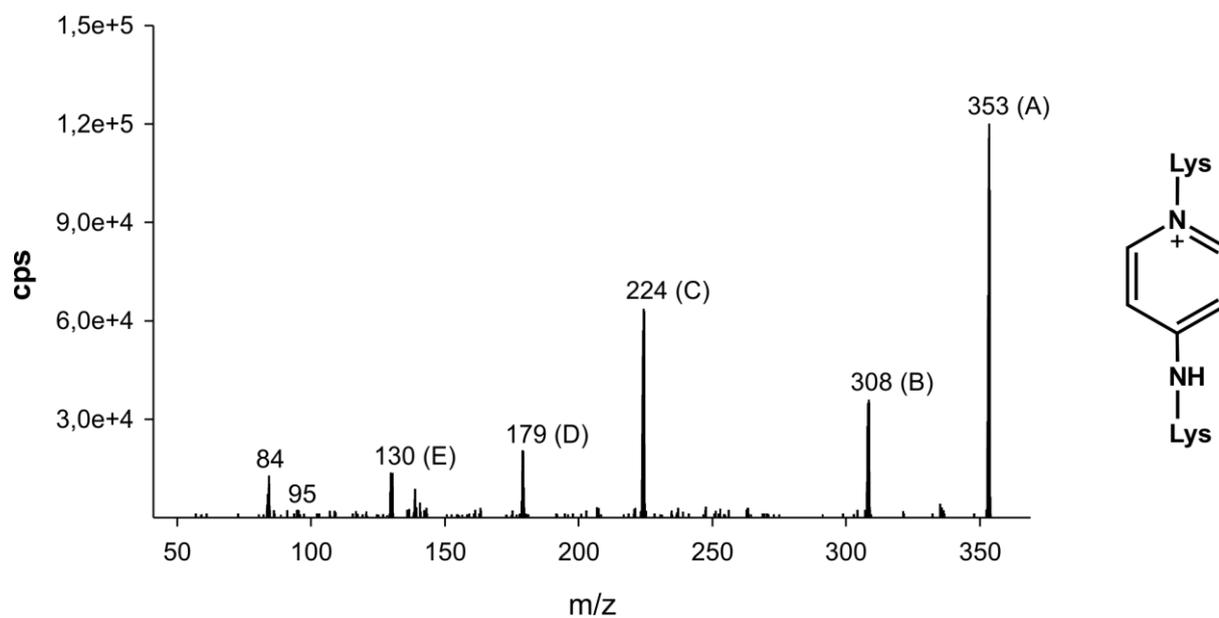


**Figure SI 8:** Verification of the fragmentation pattern of DLP standard by high resolution mass determination: **A)**  $m/z$  353.2182 (found), 353.2183 (calculated for  $C_{17}H_{29}O_4N_4 [M]^+$ ); **B)**  $m/z$  308.1968 (found), 308.1969 (calculated for  $C_{16}H_{26}O_3N_3 [M]^+$ ); **C)**  $m/z$  224.1394 (found), 224.1394 (calculated for  $C_{11}H_{18}O_2N_3 [M]^+$ ); **D)**  $m/z$  179.1179 (found), 179.1179 (calculated for  $C_{10}H_{15}ON_2 [M]^+$ ); **E)**  $m/z$  130.0863 (found), 130.0863 (calculated for  $C_6H_{12}O_2N [M]^+$ ).

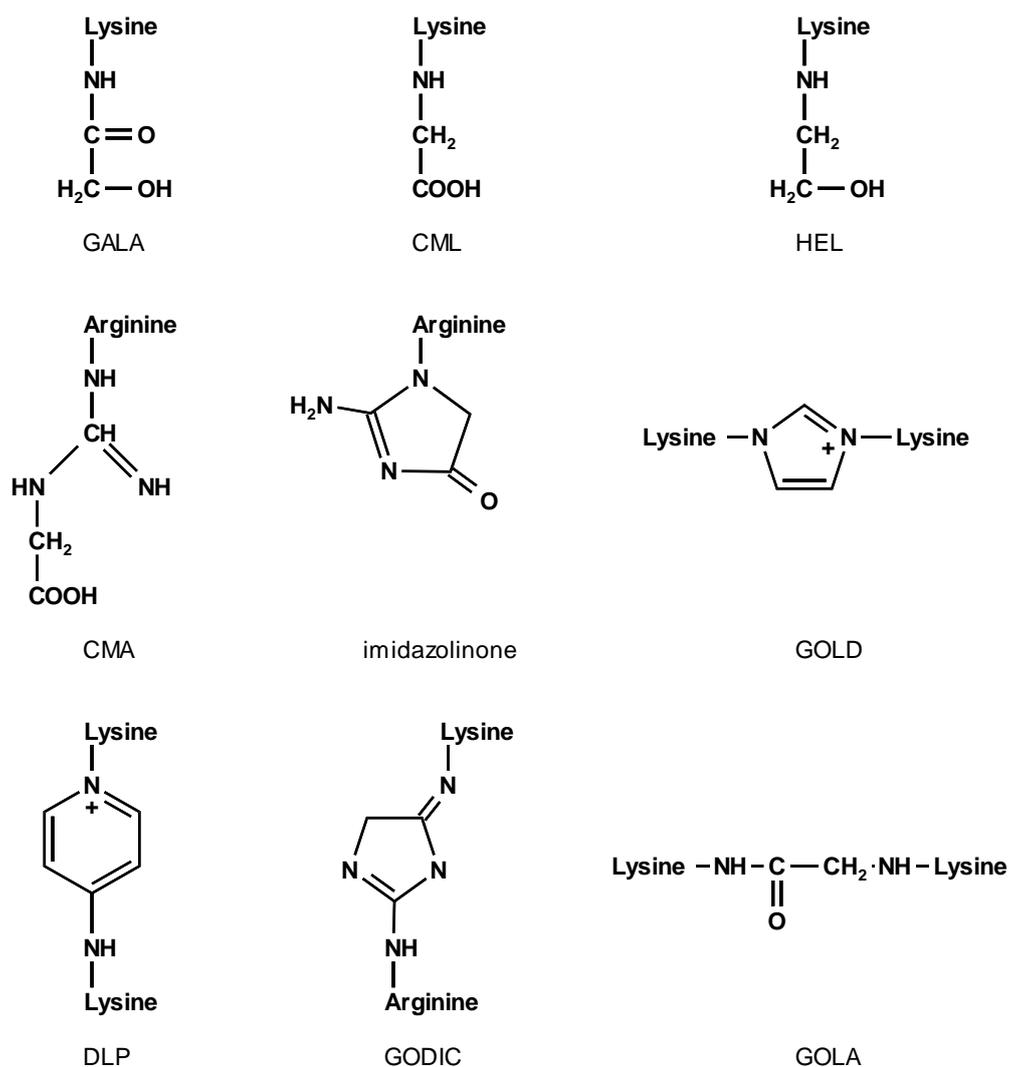


**Figure SI 9:** Overview of all protein modifications detected in the model setup: GALA (glycolic acid lysine amide), CML ( $N^6$ -carboxymethyl lysine), HEL ( $N^6$ -(2-hydroxyethyl) lysine), CMA ( $N^7$ -carboxymethyl arginine), imidazolinone (5-(2-imino-5-oxo-1-imidazolidinyl) norvaline), GOLD (glyoxal-lysine dimer), DLP (1-(5-amino-5-carboxypentyl)-4-(5-amino-5-carboxypentyl-amino)-pyridinium salt), GODIC (glyoxal imidazolinone), GOLA (glyoxal-lysine amide).

**Table SI 1.** Comparison of AGEs (mmol/mol L-phenylalanine  $\pm$  standard deviation) in Dimers formed during incubations of glycolaldehyde or glyoxal in the presence of RNase A (pH 7.4, 7 d) after chromatographic separation with ion exchange chromatography and gel permeation chromatography.

Fraction	Glycolaldehyde (Dimers)				Glyoxal (Dimers)	
	A3	A4	A5	A6	X5	X6
GALA	18.7	17.9	20.2	18.5	73	73
CML	99	137	158	202	187	253
HEL	14	18.6	18	21.7	10.4	10.9
imidazolinone	88	110	108	145	217	344
GOLD	1.6	1.5	1.6	1.6	4.8	4.9
GOLA	5.6	5.5	6.2	7.0	23.5	22.8
DLP	1.04	1.05	1.14	1.0	<LOD <sup>a</sup>	<LOD

<sup>a</sup>LOD: limit of detection

**Table SI 2.** Comparison of AGEs (mmol/mol L-phenylalanine  $\pm$  standard deviation) formed during incubations of glycolaldehyde or glyoxal in the presence of RNase A (pH 7.4, 7 d) after chromatographic separation with ion exchange chromatography (A4 vs X6) and gel permeation chromatography.

	Glycolaldehyde (Fraction A4)			Glyoxal (Fraction X6)		
	Monomer	Dimer	Trimer	Monomer	Dimer	Trimer
GALA	14.9	17	15.7	60	73	88
CML	144	137	112	253	252	144
HEL	15.3	18.5	18.8	10.8	10.9	9.1
GH-3	111	109	116	232	244	257
GOLD	1.08	1.51	1.59	2.8	4.9	15.3
GOLA	2.8	5.5	7.2	8.7	22.7	39.5
DLP	0.46	1.05	1.23	<LOD <sup>a</sup>	<LOD	<LOD

<sup>a</sup>LOD: limit of detection

## 13 Publikationsliste

### Veröffentlichungen

Rakete, S., **Klaus, A.**, Glomb, M. A. Investigations on the Maillard Reaction of Dextrins during Aging of Pilsner Type Beer  
*Journal of Agricultural and Food Chemistry* **2014**, 62, 9876-9884

**Klaus, A.**, Pfirrmann, T., Glomb, M. A. Transketolase A from *E. Coli* Significantly Suppresses Protein Glycation by Glycolaldehyde and Glyoxal *in Vitro*  
*Journal of Agricultural and Food Chemistry* **2017**, 65, 8196-8202

**Klaus, A.**, Baldensperger, T., Fiedler, R., Girndt, M., Glomb, M. A. Influence of Transketolase-Catalyzed Reactions on the Formation of Glycolaldehyde and Glyoxal Specific Posttranslational Modifications under Physiological Conditions  
*Journal of Agricultural and Food Chemistry* **2018**, 66, 1498-1508

**Klaus, A.**, Rau, R., M., Glomb, M. A. Modification and Crosslinking of Proteins by Glycolaldehyde and Glyoxal: A Model System  
*Journal of Agricultural and Food Chemistry* **2018**, 66, 10835–10843

### Tagungsvorträge

Rakete, S., **Klaus, A.**, Glomb, M. A. Bestimmung alterungsrelevanter Dextrinbauprodukte in Bier  
24. Arbeitstagung des Regionalverbands Südost der Lebensmittelchemischen Gesellschaft der GDCh, 25.-26.03.2014, Halle

**Klaus, A.**, Glomb, M. A. Transketolase-katalysierte Reaktionen führen zu posttranslationalen Proteinmodifikationen  
25. Arbeitstagung des Regionalverbands Südost der Lebensmittelchemischen Gesellschaft der GDCh, 26.-27.03.2015, Jena

**Klaus, A.**, Glomb, M. A. Einfluss der Transketolase Reaktion auf die Proteinglykierung  
27. Arbeitstagung des Regionalverbands Südost der Lebensmittelchemischen Gesellschaft der GDCh, 26.-27.03.2017, Halle

Glomb, M. A., **Klaus, A.**; Henning, C. Transketolase suppresses glycolaldehyde/glyoxal mediated formation of advanced glycation endproducts  
254th ACS National Meeting & Exposition, 20.-24.08.2017, Washington, DC, USA

**Klaus, A.**, Rau, R., Blaschke L., Glomb, M. A. Charakterisierung eines Modellsystems zur Proteinfunktionalisierung und -quervernetzung durch reaktive Carbonylverbindungen  
28. Arbeitstagung des Regionalverbands Südost der Lebensmittelchemischen Gesellschaft der GDCh, 22.-23.03.2018, Jena

Glomb, M. A., **Klaus, A.** Transketolase Significantly Mediates the Formation of Advanced Glycation End products under Physiological Conditions.  
13th International Symposium on The Maillard reaction, 10.-13.09.2018, Montreal, CA

**Posterbeiträge**

**Klaus, A.,** Rakete, S., Glomb, M. A. Bestimmung alterungsrelevanter Dextrinabbauprodukte in Bier

43. Deutscher Lebensmittelchemikertag, 22.-24.09.2014, Gießen

**Klaus, A.,** Glomb, M. A. Transketolase vermittelte Bildung posttranslationaler Proteinmodifikationen

44. Deutscher Lebensmittelchemikertag, 14.-16.09.2015, Karlsruhe

**Klaus, A.,** Koch, E., Glomb, M. A. Humane Transketolase unterdrückt die Bildung glycolaldehyd- und glyoxalspezifischer Proteinmodifikationen *in vitro*

46. Deutscher Lebensmittelchemikertag, 25.-27.09.2017, Würzburg

## 14 Lebenslauf

### Persönliche Daten

Alexander Klaus

geboren am 23.03.1989 in Gera

ledig

### Wissenschaftlicher Werdegang

06.2014 – 05.2018      Wissenschaftlicher Mitarbeiter an der Martin-Luther-Universität Halle-Wittenberg, Institut für Chemie – Lebensmittelchemie und Umweltchemie, Arbeitskreis Prof. Dr. M. A. Glomb

### Hochschulausbildung

09.2009 – 05.2014      Studium zum Diplom-Lebensmittelchemiker an der Martin-Luther-Universität Halle-Wittenberg

### Schulische Ausbildung

09.1999 – 08.2008      Abitur am Landkreis-Gymnasium Annaberg-Buchholz

08.2005 – 06.2006      Austauschschüler in Butler, USA

## 15 Eigenständigkeitserklärung

Hiermit erkläre ich an Eides statt, dass ich die eingereichte Dissertation „Einfluss von Glycolaldehyd und Glyoxal auf die Maillard-Reaktion *in vitro* und *in vivo*“ selbstständig und nur unter Verwendung der angegebenen Quellen und Hilfsmittel angefertigt habe. Diese Arbeit wurde bisher an keiner anderen Einrichtung zur Begutachtung vorgelegt.

.....  
Datum, Unterschrift